University of California
Santa Barbara

Confronting Complexity in Marine Population Dynamics and Management

A dissertation submitted in partial satisfaction
of the requirements for the degree

Doctor of Philosophy
in
Environmental Science and Management

by

Owen Ruiya Liu

Committee in charge:

Professor Steven D. Gaines, Chair
Professor Hunter S. Lenihan
Cody S. Szuwalski, Alaska Fisheries Science Center

June 2019

The Dissertation of Owen Ruiya Liu is approved.

Professor Hunter S. Lenihan

Cody S. Szuwalski, Alaska Fisheries Science Center

Professor Steven D. Gaines, Committee Chair

June 2019

Confronting Complexity in Marine Population Dynamics and Management

Owen Ruiya Liu

To Eric Harrington, who first taught me to look out at the ocean, marvel at its beauty, and wonder at its secrets.

Acknowledgements

My work would not have been possible without funding provided by the National Science Foundation Graduate Research Fellowship Program and the Bren School. In addition, thank you to the California Department of Fish and Wildlife for providing data used in part of the dissertation, and to Mike Kenner for the opportunity to help in the research effort at San Nicolas Island. Particular pieces of the dissertation have benefited from specific support or advice from Dr. Hao Ye, Dr. Dan Ovando, Dr. Sarah Teck, Dr. James Thorson, Ying Wang, Elizabeth Hiroyasu, and Alexa Fredston-Hermann. Thank you to my family, who enthusiastically support my every professional endeavor and have proved amazingly skilled at smiling and nodding when I regale them with tidbits of esoteric research. Sabrina and Jacob, thank you for riding out this adventure with me and keeping me inspired by how invested you are in your own work. Erika, thank you for generally keeping me grounded while nonetheless encouraging me to dream. Thank you to the wider Bren School community and my Ph.D. peers for making UCSB such a welcoming academic home for five years. Thank you to the members of Gaines lab for listening and providing feedback at every step of the way; you all are an inspiring and wonderful group of people. And thank you in particular to my past and current office-mates for putting up with me constantly distracting you with whatever idea might pop in to my head. Finally, thank you to my dissertation committee for supporting me intellectually, financially, and technically, and in particular to Steve, who has the uncanny ability to turn my half-baked questions into delicious fully-baked ideas.

Curriculum Vitæ

Owen Ruiya Liu

Education

2019	Ph.D. in Environmental Science and Management (Expected), University of California, Santa Barbara.
2012	M.S. in Earth Systems, Stanford University.
2011	B.S. in Earth Systems, Stanford University.

Professional Appointments

2011-2012	Research Associate, Environmental Defense Fund, Boston, MA

Publications

Kritzer, J. P., and Liu, O. R. (2013). Fishery management strategies for addressing complex spatial structure in marine fish stocks. In S. X. Cadrin, L. A. Kerr, and S. Mariani (Eds.), Stock identification methods: Applications in fisheries science (pp. 29–58). Academic Press.

Liu, O. R., Thomas, L. R., Clemence, M., Fujita, R., Kritzer, J. P., Mcdonald, G., and Szuwalski, C. (2016). An evaluation of harvest control methods for fishery management. Reviews in Fisheries Science and Aquaculture, 24, 244–263. https://doi.org/10.1080/23308249.2016.1161002

Palazzo, J., Liu, O. R., Stillinger, T., Song, R., Wang, Y., Hiroyasu, E. H. T., Zenteno, J., Anderson, S., and Tague, C. (2017). Urban responses to restrictive conservation policy during drought. Water Resources Research, 53, 4459–4475. https://doi.org/10.1002/2016WR020136

Liu, O. R., Kleisner, K. M., Smith, S. L., and Kritzer, J. P. (2018). The use of spatial management tools in rights-based groundfish fisheries. Fish and Fisheries, 1–18. https://doi.org/10.1111/faf.12294

Liu, O. R., Molina, R., Wilson, M., and Halpern, B. S. (2018). Global opportunities for mariculture development to promote human nutrition. PeerJ, e4733. https://doi.org/10.7717/peerj.4733

Abstract

Confronting Complexity in Marine Population Dynamics and Management

by

Owen Ruiya Liu

Species dynamics and interactions in nature often fail to conform to classical ecological models because species interactions can be driven by environmental forcing in complex ways. Appropriate management requires an understanding of how these biotic and abiotic forces jointly drive dynamics, particularly for valuable resources that face the additional pressure of human harvesting. My research uses modern quantitative tools for spatial and time series analysis to help unravel complex ecological dynamics. The first part of the dissertation uses nonlinear time delay embedding to reconstruct and analyze species interactions in a California kelp forest across decades of environmental variability. We show that environmental context greatly alters the strength and direction of species interactions, and therefore equilibrium assumptions about kelp forest community dynamics are likely inadequate for predicting how these systems will respond to environmental change. The second portion of the dissertation investigates a human-wildlife conflict between California sea otters and the southern California red sea urchin fishery at a productive fishing ground. We use Bayesian models that combined fishing and otter predation to reconstruct the past dynamics of the sea urchin fishery and predict the likely effects of future otter population growth. We find that in the past, the urchin fishery rather than otter predation contributed to urchin population decline, but in the near future, continued sea otter population growth will severely reduce sustainable fishery harvest levels. In the final part of the dissertation, I investigate broad spatial patterns in interannual

fluctuations in the distributions of two important harvested species in the eastern Bering Sea: snow crab and one of its primary predators Pacific cod. I show how both species distributions respond to environmental gradients related to temperature and depth, but in distinct and often opposite directions, leading to emergent spatial patterns in expected predation risk. In combination, the projects in my dissertation reveal how long term spatial and time series data can be leveraged through modern quantitative methods to better understand and manage dynamic species distributions and interactions.

Contents

List of Tables

List of Figures

Introduction

Ecologists, conservation biologists, resource users, and managers all depend upon an accurate understanding of species population dynamics. In an era of elevated human impacts on natural systems, understanding the drivers of change in those systems is more important than ever. But populations observed in nature often fail to conform to classical ecological models because ecological processes like competition and predation interact with abiotic forcing in complex, often nonlinear ways to produce chaotic emergent dynamics. Species that interact with humans can display especially complex dynamics, thereby exacerbating human-environment conflicts. My dissertation uses a collection of modern, data-driven statistical modeling tools to confront ecological complexity and better understand and predict the dynamics of species in nature.

The first part of the dissertation uses empirical dynamic modeling (EDM) to reconstruct and analyze species interactions in a California kelp forest across 30 years of environmental variability. As a fundamentally nonlinear approach to multivariate analysis that uses time delay embedding, EDM is flexible in its application to the complex, state-dependent dynamics that characterize many ecosystems. In applying the method to existing monitoring data from subtidal kelp forests, we reveal how environmental context greatly alters the strength and direction of species interactions. In particular, while the dynamics of the foundation species—the giant kelp *Macrocystis pyrifera*—are an im-

portant driver of the dynamics of other, associated species, its interactions and role in the ecosystem are strongly dependent on prevailing environmental conditions. We show how estimated species interactions may vary in strength and direction depending on the current ecosystem state, revealing how environmental fluctuations drive kelp forest community dynamics. The significant context dependency in species interactions found in the study argues for a greater utilization of long term data and empirical dynamic modeling in studies of the dynamics of other ecosystems. More generally, we show that long term ecological monitoring data can be used not just for looking at trends, but for deep ecological inference, and therefore EDM should be used as a complement to controlled ecological experiments to understand species dynamics in real ecosystems.

The second portion of the dissertation investigates a human-wildlife conflict playing out in the same southern California kelp forests. An important keystone predator, the endangered southern sea otter (*Enhydra lutris nereis*), has been recovering and recolonizing its historic range, but is now threatening the existence of a fishery for one of its preferred prey, the red sea urchin (*Mesocentrotus franciscanus*). The goals of the study were to reconstruct past influences of the fishery and otter predation on the sea urchin resource, and predict the likely effects of continued otter population growth on urchin fishery sustainability. I use urchin fishery landings and otter population data to fit Bayesian biomass dynamics models, extending these traditional fisheries models to include multiple representations of otter predation. We show that although predation by otters has had a negative effect on sea urchin populations, this effect has historically been small when compared to the greater pressure put on the resource by the fishers themselves. In the future, though, continued population growth of sea otters will reduce sustainable fishery harvest levels and possibly preclude the urchin fishery altogether from some areas. The quantitative characterization of the fishery-otter conflict can inform future urchin

fishery management actions, and my findings have relevance to the broader literature on recovering natural predators and human-wildlife conflict in managed ecosystems.

In the final part of the dissertation, I tackle another complex species interaction that has significant ramifications for two valuable fisheries in the eastern Bering Sea: snow crab (*Chionoecetes opilio*) and Pacific cod (*Gadus macrocephalus*). Both snow crab and Pacific cod are subject to intense fishing pressure, but their spatial distributions are known to respond to environmental variability in bottom temperature and winter sea ice extent. Moreover, Pacific cod is a known predator of small snow crab, but importance of predation relative to the influence of the environment on spatio-temporal snow crab dynamics is unknown. In the study, we use a dynamic multispecies distribution model to uncover the major drivers of spatial and temporal variation in Pacific cod and snow crab distributions in the Bering Sea and investigate their interaction. Utilizing more than 30 years of spatially-explicit, fishery-independent data on the distribution and abundance of snow crab and cod, we show how both species are likely responding in divergent ways to environmental variability, meaning that their distributions should significantly overlap only under specific environmental conditions. We find further evidence of this in the strong negative correlations between abundances of cod and crab that manifest only in specific, but predictable locations. We propose that in the eastern Bering Sea, environmental variability drives large-scale changes in Pacific cod and snow crab distributions, which in turn lead to greater distributional overlap and presumed predation risk in certain years. Our analyses are relevant to the sustainable management of the snow crab fishery, while the statistical approach is a powerful tool for understanding pattern in complex multispecies dynamics more generally.

Ecologists are entering a new, exciting era in our ability to characterize and predict complex ecosystem dynamics. I show through multiple projects in my dissertation how careful

analysis of long term spatial and time series data with modern statistical techniques can lead to ecological insights. Together, my dissertation projects emphasize the importance of both short and long term environmental variability in driving species distributions and the strength of their interactions. Furthermore, I show how these same analyses can be utilized to manage human-wildlife conflict and harvested resources. Beyond the specific cases examined in my dissertation, the approaches I use have broad applicability to the understanding of species distributions, dynamics, and interactions in any natural or human-dominated ecosystem.

Chapter 1

Environmental Context Dependency in Species Interactions

Abstract

Ecological interactions are not uniform across time. They commonly vary with environmental conditions. Yet, interactions among species are often measured with short-term controlled experiments whose outcome can depend greatly on the particular environmental conditions under which they are performed. Running multiple experiments is one option to address this context challenge, but experimental investigation becomes infeasible over longer time frames. As an alternative, we utilize empirical dynamic modeling applied to a 30-year time series from coastal kelp forests to estimate species interactions across a wide range of environmental conditions. We show that environmental context greatly alters the strength and direction of species interactions. In so doing, we confirm and extend results from previous studies on the utility of empirical dynamic modeling. We identify potentially important but understudied kelp forest dynamics, underscoring

the importance of specifically studying variation in interaction strength rather than mean interaction outcomes. The significant context dependency in species interactions found in this study argues for a greater utilization of long-term data and empirical dynamic modeling in studies of the dynamics of other ecosystems.

Introduction

Interactions between species drive patterns of diversity, stability, resilience, and productivity in nature [1]–[4]. In any ecosystem, the collection of species interactions determines community dynamics. Until recently, most studies viewed these dynamics—e.g., the bleaching and recovery of a coral reef, or the assembly and disassembly of terrestrial plant communities—as processes resulting from static, predictable species interactions. However, the observation that species interactions are not temporally uniform [5]–[8] calls into question assumptions of interaction stability.

Ecologists recognize now that important species interactions may vary over time, but this context dependency remains difficult to measure and describe. Experiments that measure interactions are generally performed at only a few places over a relatively short window of time. They are therefore subject to a specific environmental context that may not encompass the full range of conditions experienced by that ecosystem over longer time scales [9]. The resulting narrow perspective increases the chance that the profound influence of environmental context on the outcome of species interactions ranging from keystone predation[7], to competition[5], [10], [11], to protective symbioses[12]–[14] will remain underappreciated.

Moreover, even when context dependency of species interactions has been examined, studies commonly focus on estimating mean interaction strengths, rather than more com-

prehensive examinations of interaction variance [8]. This focus may be misguided, since interactions that are variable in magnitude and direction—and therefore "weak" when averaged—may actually be some of the most important in driving community dynamics [4]. If key species interactions are variable in this way across environmental gradients, then important species interactions may be dismissed as insignificant observational noise.

It is therefore critical to be able to place interspecific interactions into their appropriate environmental contexts. Controlled experiments can sort out the relative and interactive effects of a few orthogonal environmental drivers at a time; for example, examination of the effects of ocean warming and acidification on algal competition[15]. But as species interaction webs and lists of important environmental variables grow in size, fully factorial experimental designs quickly become unwieldy. Instead, a complementary approach to these difficulties inherent in examination of species interactions in a variable environment is to a) collect ecological observations over a long time period, across a large range of environmental contexts, and b) employ analytical methods that can directly estimate context-dependent species interactions from those observations. Such an approach could help to characterize environmental contingencies in species interactions and explicitly examine interaction variability.

One potential option is to use empirical dynamic modelling (EDM[16]) to estimate a varying species interaction network and establish environmental context dependency in interaction strength and direction. Empirical dynamic modelling uses information from single or multiple time series to empirically model relationships between variables through the reconstruction of dynamic attractors (https://youtu.be/8DikuwwPWsY). The general modelling framework for all EDM methods is readily adaptable to many different sorts of time series variables, including environmental variables manifesting at different scales [17]–[19]. Because the methods are specifically designed for nonlinear dynamic

systems, EDM—in theory—should be able to illuminate context-dependent patterns in species interactions.

Recently-developed EDM methods exist for uncovering dynamic species interactions from time series data [16], but these methods have to date been applied only to simulated and planktonic communities. Their utility to the study of other ecological systems remains untested. Here we extend the exploration of dynamic species interactions using EDM to giant kelp forests in southern California, a diverse and temporally dynamic ecosystem in which many important species interactions are well-documented through decades of experimental and comparative studies [20]–[22]. The study of kelp forests has been foundational to ecological theory, especially regarding the relative influence of top-down and bottom-up structuring forces in ecosystems [23]–[27]. Recently, however, findings from long-term kelp forest research programs have begun to challenge many long-held beliefs about the drivers of kelp forest ecosystem dynamics [28]. In particular, a longer-term perspective has led to a recognition of the importance of environmental context—such as level of physical disturbance or the current state of El Niño conditions—for understanding kelp forest processes [29]–[32]. In this study we analyze long term monitoring data[33] from kelp forests at San Nicolas Island—a small, remote member of the California Channel Islands in the northeast Pacific—to explore the efficacy of EDM in unraveling the context dependence of kelp forest ecosystem dynamics.

To characterize environmental context dependency in kelp forest interactions between species, we take three general steps (see Methods; A full step-by-step description and reproducible code used to produce all analyses and figures are available in this online repository). First, we use empirical dynamic modeling causality tests called convergent cross-mapping [34] to construct a kelp forest species interaction network directly from time series data. In so doing, we test for all unidirectional causal signals between five

common kelp forest species, as well as between five exogenous environmental variables and those species. Second, for each identified causal link between species, we reconstruct the actual species interactions over time, using another EDM tool called multivariate S-maps (sequential locally weighted global linear maps) [16], [35]. Finally, we show how variability in key species interactions can be related back to the environmental context under which they took place.

Our analyses focus on the dynamics of five common southern California kelp forest species, whose interactions are thought to be important in structuring kelp forest ecosystems[20], [22], [36] (Figure 1.1). The giant kelp *Macrocystis pyrifera* is the eponymous foundation species[37], the primary canopy- and habitat-forming kelp along most of the central and southern coast of California [21]. The monitoring data include young *Macrocystis* recruits (sporophytes identified as *Macrocystis* but less than 1 meter tall [33]). We explore *Macrocystis* dynamics and its interactions with two presumptive competitors and two abundant herbivores. The understory kelp species *Laminaria farlowii* and *Pterygophora californica* compete with *Macrocystis* for space, light, and nutrients [38]–[40]. The two herbivores—the purple sea urchin *Strongylocentrotus purpuratus* and the red sea urchin *Mesocentrotus franciscanus*—are thought in many places to control *Macrocystis* density and can sometimes wipe out entire giant kelp forests, leading to the alternative ecosystem state known as an urchin barren [41], [42]. In southern California, *Macrocystis* population dynamics can be driven by nutrient availability and physical disturbance [27], [31]. The availability of nitrate is inversely related to seawater temperature[43] and, over longer time scales, is associated with oscillations in patterns of upwelling and oceanic currents. Accordingly, we include five environmental variables in our analyses to test their relationship to kelp forest species dynamics and interactions: sea surface temperature (SST), physical disturbance (measured by maximum seasonal wave height, SWH),

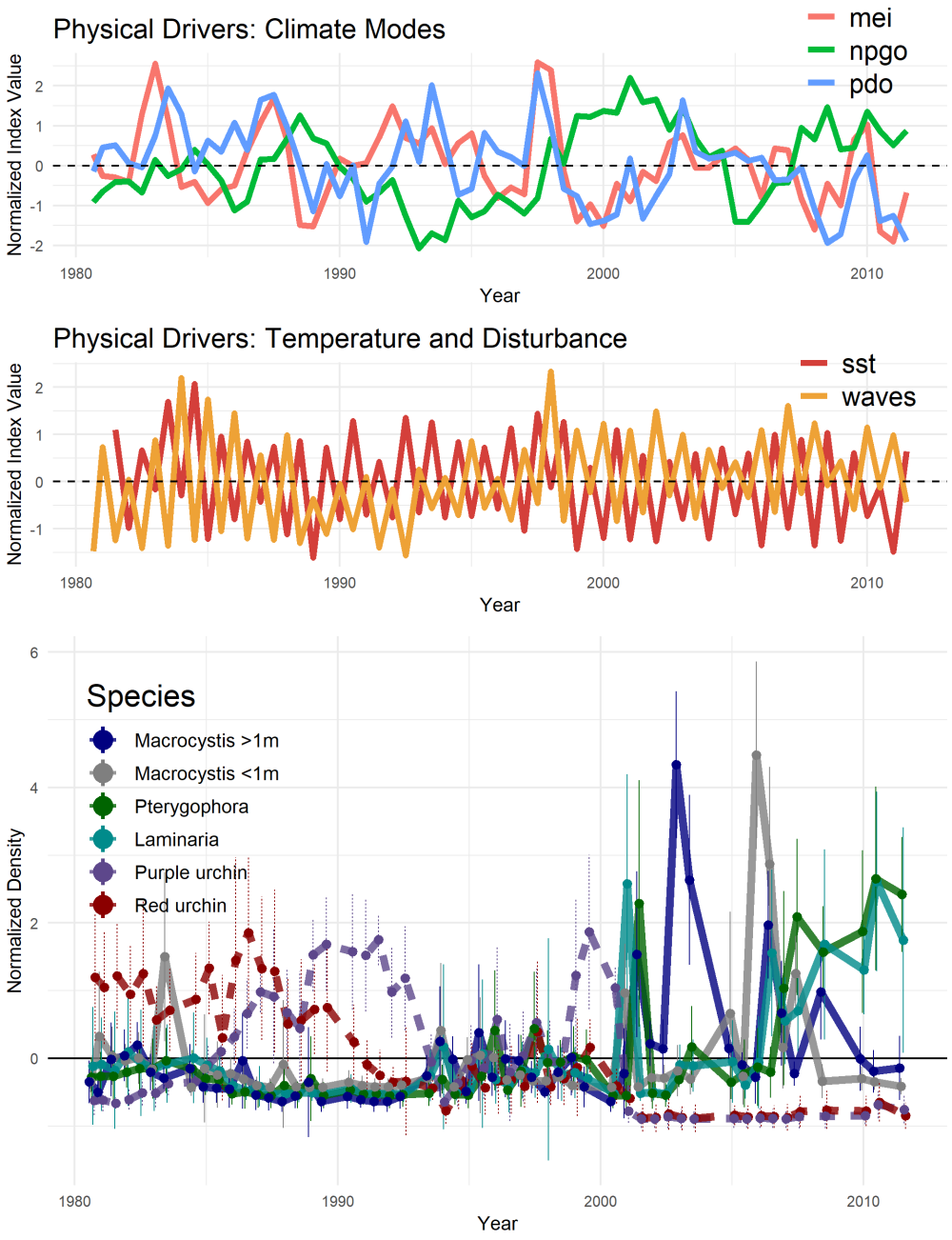

Figure 1.1: Raw data for species and physical drivers included in the study. All variables normalized to zero mean and unit variance

and three indices of low-frequency climate modes: the Multivariate El Niño Index (MEI) [44], the Pacific Decadal Oscillation (PDO) [45], and the North Pacific Gyre Oscillation (NPGO) [46].

Methods

Data standardization

San Nicolas Island is a small, remote island situated about 100 kilometers offshore from southern California. The data in the analysis are from a sampling station on the western end of San Nicolas Island. The benthic monitoring data herein have been collected more or less every six months for more than 35 years by the USGS and its Western Ecological Research Center (USGS-WERC)[33]. The monitoring site consists of 10 permanent transects (see ref. 33 for full monitoring protocols). Data from the 10 transects were combined to produce single long time series, leveraging spatial replication to create denser manifolds, a technique called dewdrop regression[47], [48]. Each species' time series therefore consisted of 630 total observations (63 monitoring periods across 10 replicates).

Physical data included historical sea surface temperature (SST) from NOAA's Optimally Interpolated Sea Surface Temperature (https://www.ncdc.noaa.gov/oisst), the Multivariate El Niño Index (MEI)[44], the Pacific Decadal Oscillation (PDO)[45], and the North Pacific Gyre Oscillation (NPGO)[46]. The actual measures included in analyses for these four indices were the average values for the four months preceding each period in the benthic monitoring data. This metric was chosen to approximate the general environmental conditions under which species interactions were occurring. The measure for maximum seasonal wave height combined modeled wave height data from the USGS Geo-

physical Fluid Dynamics Laboratory (http://cmgwindwave.usgsportals.net/) with updated modeled data from the California Coastal Data Information Program (CDIP MOPv1.1[49]), both based on data from an array of buoys distributed across the Southern California Bight. Significant wave height is here defined as the average maximum daily wave height across the same four months preceding each benthic monitoring period. This is meant to capture any large storm events and provide a general measure of physical disturbance. Unlike the biological data, where there are unique spatial replicates, the physical data have only one value for each of the 63 monitoring periods. Hence, the time series for the physical drivers are identical for each of the 10 spatial replicates.

For attractor reconstruction, all time series were standardized zero mean and unit variance, common practice in empirical dynamic modeling[18].

Convergent Cross Mapping

We used convergent cross mapping (CCM) to test causal relationships between variables[34]. CCM is described in detail elsewhere[18], [34], but is introduced here.

All EDM analyses, including the convergent cross mapping (CCM) and multispecies S-maps algorithms used in this study, are based on extensions of Takens' theorem of nonlinear dynamic systems [35], [50]. Takens showed that a dynamic system could be accurately represented using "shadow attractors", or manifolds, built from time series of observed variables in that system. In basic terms, an attractor or manifold is built from a set of E-length state-space vectors, where E is the number of progressive lags of a single variable (for CCM), or the number of separate variables (for multispecies S-maps) used in the reconstruction. E is called the ***embedding dimension***. Each E-length vector, for example $\mathbf{x_t} =< x_t, x_{t-1}, x_{t-2} >$ is a point on the attractor, and the set of E-length vectors used for the reconstruction is called the ***library***. Takens showed

that these reconstructions are topologically invariant to the "true" (unobserved) dynamic system, with a one-to-one mapping between points on the attractor and points on the true manifold. This powerful theory is what allows EDM to draw inference about nonlinear dynamic systems through attractor reconstruction.

Before variables were included in CCM causality tests, we ensured that each variable could be properly embedded using univariate simplex projection[18] (Figure 1.6). Univariate simplex projection uses attractors built from multiple lags of single time series (e.g. for variable x an attractor with an E of 3 would consist of vectors $\mathbf{x_t} =< x_t, x_{t-1}, x_{t-2} >$). To predict $\mathbf{x_{t+1}}$, the simplex algorithm finds the $E+1$ nearest neighbors of $\mathbf{x_t}$ in the ***library*** of vectors, and the prediction $\widehat{\mathbf{x}}_{\mathbf{t+1}}$ is the average of those nearest neighbors' values at $t+1$, weighted by their Euclidean distance from $\mathbf{x_t}$ at t. This is the essence of simplex projection: a forecast for a given point in state space is surmised from the forward trajectories of observed nearby points. Keep in mind that because of the way attractors are reconstructed, the nearest neighbors are not necessarily nearby in time, but rather close in ecosystem "state" to the predicted point. Applying this method, all variables in the analysis showed significant univariate predictability based on out-of-sample prediction skill (Supplementary Figure 1.6). The best embedding dimension (that is, the number of lags included for each variable that gave optimal predictability) was extracted for each variable. These best Es are an estimate of the dimensionality of the dynamic system experienced by each species.

Extensions of Takens' theory state that if two variables (in our case, species or physical variables) are part of the same dynamic system, their univariate attractors should be topologically invariant from the true attractor, and therefore, should be topologically invariant from one another[17], [19], [34], [48]. This means that there will be a one-to-one mapping ("cross-mapping") between points on the reconstructed attractor of one

variable and the corresponding points on the other variable's attractor. Taking advantage of this property, significant cross-mapping is evidence of causation. In practical terms, if (for example) giant kelp is causally forced by sea urchins, that forcing should leave a signature on the giant kelp time series. CCM tests for causation by using the same simplex algorithm as described above, except that now we use an attractor/manifold built from the time series of one variable (X) to predict contemporaneous values of another variable (Y). If the attractor can accurately predict the dynamics of the second variable, we assert that the second variable has a causal influence on the first. In simple terms, the *causal effect of X on Y is determined by how well Y cross-maps X*[34]. In this way, the inference from cross-mapping is the converse direction of causation. In our example, if sea urchins drive giant kelp, the dynamic information from the urchin time series should be reflected in the kelp dynamics, and therefore we should be able to recover (cross-map) dynamic information about sea urchins using the kelp time series. Moreover, as we use more data in the cross-mapping, the predictive skill should increase. This is because with more data the attractor "fills in" or becomes denser, and consequently predictions made from nearest neighbors become more accurate. This property is called "convergence" (hence "convergent cross mapping") and is an essential criterion for causation and what distinguishes correlation from causation[34]. We assessed convergence by testing whether cross-mapped prediction accuracy (Pearson's ρ between observations and predicted values of the cross-mapped variable) improves with library length (the number of embedded vectors used to construct the attractor). If two variables are spuriously correlated and not causally linked, CCM will not display convergence (concepts more fully explored in refs. 34 and 17).

Following Sugihara et al.[34], each separate CCM test used an attractor built from one variable to predict another. Causation was tested by plotting predictive skill ρ against

library size. The two criteria for CCM to establish causality were first, that cross-map skill using all available data was significantly greater than zero, and second, that predictability was convergent. All species-species and species-environment interactions were tested using CCM (Figures 1.2 and @ref(fig:ccm_all)), and significant interactions among species were retained for use in building multispecies attractors.

Multivariate S-maps

Multivariate attractors follow the same logic as the attractors described above, except that instead of using single variables to reconstruct the attractors, we use contemporaneous values of multiple variables[16]. That is, instead of library vectors or points in state-space taking the form of, for example, $< x_t, x_{t-1}, x_{t-2} >$, they now are formed in true multivariate space, e.g. $< Kelp_t, Urchin_t, Nutrients_t >$. Additionally, instead of making predictions using only nearest neighbors, S-maps (sequential locally weighted global linear maps[35]) uses all library vectors, and exponentially weights them by their distance to the prediction vector before using linear regression to make a forecast; vectors closest to the prediction vector have the greatest weight. Because library vectors are weighted individually in this manner, a separate linear map is created for each predicted vector. This is why the procedure is called "sequentially weighted global linear maps". Conceptually, as the dynamic system moves along the surface of the attractor, S-maps sequentially computes new linear maps to the next point. The varying species interactions (the measure of interest) are the coefficients of these local linear maps.

Mathematically, when making a prediction for a target point $\mathbf{x}^*$, each library vector (point on the attractor) $\mathbf{x_k}$ is given a weight

$$w_k = exp\frac{-\theta \mid\mid \mathbf{x_k} - \mathbf{x}^* \mid\mid}{\bar{d}}$$

where $|| \mathbf{x_k} - \mathbf{x}^* ||$ is the Euclidean distance between the library and target vector, and $\bar{d}$ is the average distance to all library vectors. By controlling the strength of local weighting, the single parameter θ controls the nonlinearity of the model[16], [35].

As described in Results, the multivariate model for each species consisted of all the species that showed significant causation through CCM analysis. An example of a multispecies attractor is shown in Figure 1.10. Additionally, the preferred model for each species was the constructed by finding the value of θ (the amount of nonlinearity) that optimized out-of-sample prediction. Each resulting model estimated 520 interactions, which were then compared to the environmental conditions under which they took place (Figures 1.4 and 1.5). For individual model θ and performance metrics, see Supplementary figures.

Analyses were performed in R[51], especially utilizing the rEDM package (v. 0.7.4[52]). Reproducible code for all analyses available in an online repository.

Results

Applying convergent cross mapping[34] (CCM) to the set of six biological and five physical variables, we find a relatively dense interaction network (Figure 1.2). Out of 90 possible unidirectional links among species and between species and the environmental variables, 41 are significant. Adult *Macrocystis* density is driven by all five environmental variables, with SWH, SST, and the NPGO showing the strongest causal signals. This finding aligns with recent work by others using different methods [31], [53] that showed that these same three variables were the primary controls of giant kelp biomass dynamics across the California coast. More generally, although the included physical variables show significant links to many of the biological variables, the NPGO shows the strongest links to almost all of the biological variables. Our analysis suggests that more attention

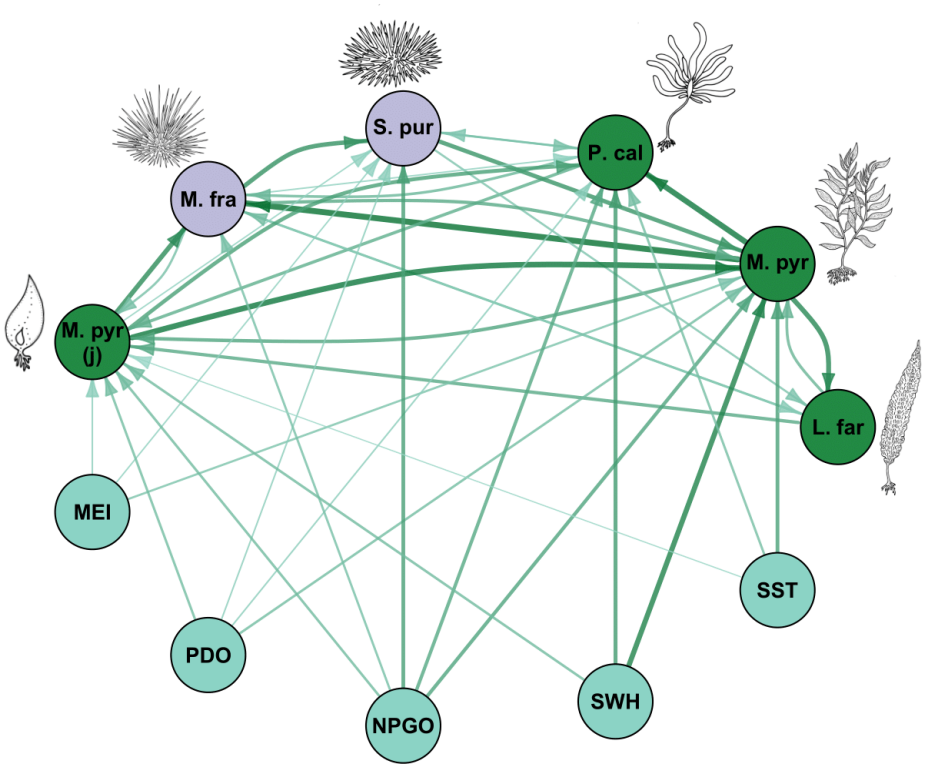

Figure 1.2: Reconstructed interaction web using results of convergent cross mapping. Each arrow represents a significant causal signal, and link width and opacity scale with the strength of causal forcing. Species abbreviations: M. pyr: *Macrocystis pyrifera*; L.far: *Laminaria farlowii*; P.cal: *Pterygophora californica*; M.fra: *Mesocentrotus franciscanus*; S.pur: *Strongylocentrotus purpuratus*. Physical drivers: NPGO: North Pacific Gyre Oscillation; MEI: Multivariate El Niño Index; PDO: Pacific Decadal Oscillation; SST: Sea surface temperature; SWH: Significant wave height.

should be focused on the effects of the NPGO in southern California. Interestingly, in turn, adult *Macrocystis* shows strong causal links to every other biological variable. This is despite the fact that the study site at San Nicolas Island does not have a stable giant kelp forest (see raw time series, Figure 1.1); rather, the site has transitioned from an urchin barren[42] to a *Pterygophora* and *Laminaria*-dominated state to a *Macrocystis* forest at various times throughout the 30-year time series. The implication is that, despite not maintaining dominance in the typical ecological sense of word (large abundance and

biomass), *Macrocystis* remains a key foundation species in this ecosystem, because its dynamics are fundamentally important in driving the dynamics of all the other kelp forest species[21].

CCM analysis confirms that the system studied represents a complex array of significant interactions between algal species and their herbivores. However, CCM alone does not elucidate the direction and magnitude of species interactions. To obtain estimates of the interactions themselves, we use multivariate S-maps[16], [35] (see Methods). S-maps reconstruct dynamic "attractors" by casting the abundances of causally-related species into state space. For a set of causally-related species, a point in multivariate space can be plotted using each species' abundance as an axis. The attractor is then created by tracing this multispecies trajectory forward in time (see example attractor, Figure 1.10). For each point along the attractor, S-maps compute a Jacobian matrix, the elements of which are the estimated partial derivatives between species. These interaction matrix elements are our measure of species interactions. Because Jacobians are computed sequentially for every point along reconstructed attractors, we obtain estimates of interaction strength that vary with ecosystem state.

Dynamic ecosystems are analogous to a landscape of variable topography, where our position on the landscape represents the current ecosystem state. In this analogy, each cardinal direction represents the density of a different species (i.e., axis in state-space), and our movement across the landscape through time represents movement along the multivariate attractor as species densities change. S-maps are simply our reconstructed topographic maps of these ecosystem landscapes. At a given point in time as we move across the landscape, we may be on top of a steep pinnacle, on a flat plain, or in a shallow valley. Regardless, it is the slope of the landscape in each direction (the partial derivative) that defines the local interaction strength between species: a steep upward

slope represents a strong positive interaction between species, while a flat surface is a neutral or weak interaction interaction, and a slight downward slope is a weak negative interaction.

There are two important characteristics of S-maps that deserve mention. First, the S-map estimation procedure, like all EDM methods, is specifically designed for nonlinear systems, and is therefore an appropriate tool for investigating ecosystems exhibiting nonlinear dynamics such as alternative stable states or hysteresis[16]. Secondly, because S-maps utilize reconstructed multispecies attractors, each estimated interaction is fundamentally based on observations of similar past ecosystem states—where each state is represented as a multivariate vector of causally-linked species' densities—rather than a phenomenological extrapolation of the most recent dynamics. For example, instead of asking, "What is our prediction for the strength of herbivory based on last year's observed dynamics," S-maps are concerned with, "What is our best estimate for the strength of herbivory, based on our knowledge of times in the past when the ecosystem was most similar to today?" In the San Nicolas kelp forest, we find a striking prevalence of variables and positive species interactions (Figure 1.3). After grouping species interactions by type, only herbivory (the effect of urchins on algal species) is predominantly negative. Conversely, the effect of the algal species on the urchins has a flatter distribution, with occasional strong negative and strong positive interactions. Likewise, contrary to our expectations, interactions between the algal species and between the urchin species are not always antagonistic. These results suggest that facilitation—direct or indirect—can arise in kelp forests in multiple contexts[54]. For example, since there is evidence here of strong herbivory, then there may be indirect facilitation between algal species because of a shared herbivore[55]: a greater algal density in general could ameliorate the negative effect of herbivory on any one species. This indirect, associative facilitation may

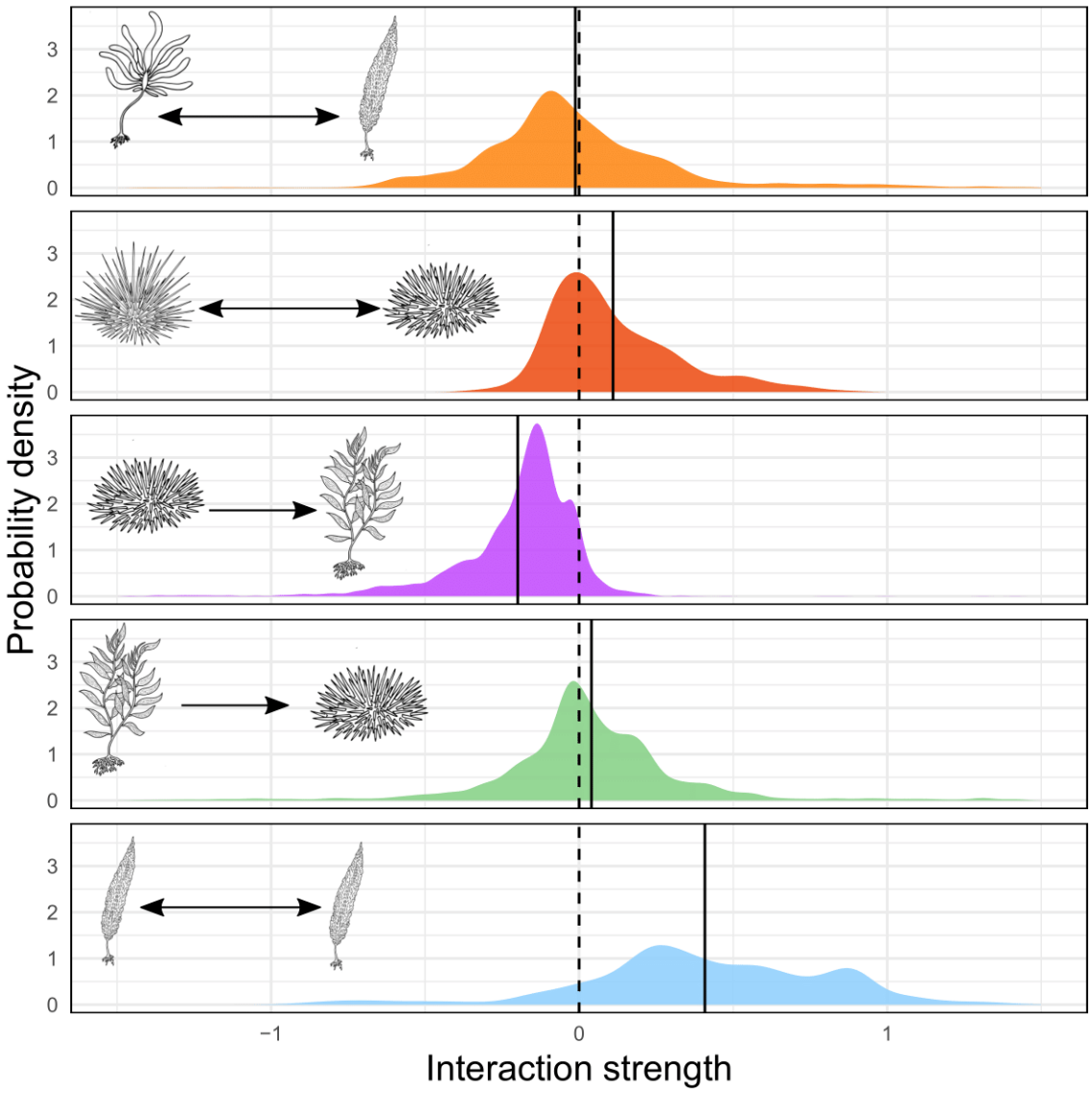

Figure 1.3: Smoothed kernel density histograms of all estimated interactions by type. From top to bottom: Algal competition, urchin competition, herbivory, algae effect on urchins, intraspecies. Solid lines denote means across all estimated interactions of that type.

sometimes outweigh the strength of direct algal competition. Additionally, *Macrocystis* forests can mediate current strength and as a result, can also help retain reproductive propagules of other species[21]. These types of indirect facilitation in kelp forests have received comparatively little attention[56], [57] relative to the strong focus on exploitative competition between these species for light and nutrients[38], [40], but similar effects have been documented in other ecosystems[58]. Our analysis does not contradict the importance of competition in kelp forest ecosystems. Rather it suggests that facilitation, especially indirect facilitation, may be an additional important structuring force [56]. As a case in point, consider the interaction of adult *Macrocystis* and the understory kelp *Pterygophora californica*. *Macrocystis* is often assumed to be the dominant competitor in kelp forests for nutrients and light[38], [40]. However, at this site, *Macrocystis* generally has a neutral to positive effect on *Pterygophora* (Figure 1.4, a result seemingly incongruous with the established competitive hierarchy. However, the study site (a small offshore island) is highly exposed to strong currents and winter storms, partly because it is composed of low-rugosity reefs. These habitat characteristics are known to reduce the ability of *Macrocystis* to be competitively dominant [21], [38]. Our findings strongly suggest that *Macrocystis* competitive dominance is quite rare at this site, or at the very least is outweighed by facilitation in most instances. Facilitation of *Pterygophora* by *Macrocystis* might take the form of associative avoidance of herbivory or facilitation through *Macrocystis*' retention of *Pterygophora* reproductive propagules, as described above[21], [55]. Regardless of the underlying mechanism(s), these results show little evidence for consistent giant kelp dominance and suggest that further attention should be paid to the potential direct and indirect facilitative roles of *Macrocystis*[56].

Organizing the species interaction data by using the oceanographic indices enables us to further unravel the context-dependency in the *Macrocystis*-*Pterygophora* interaction

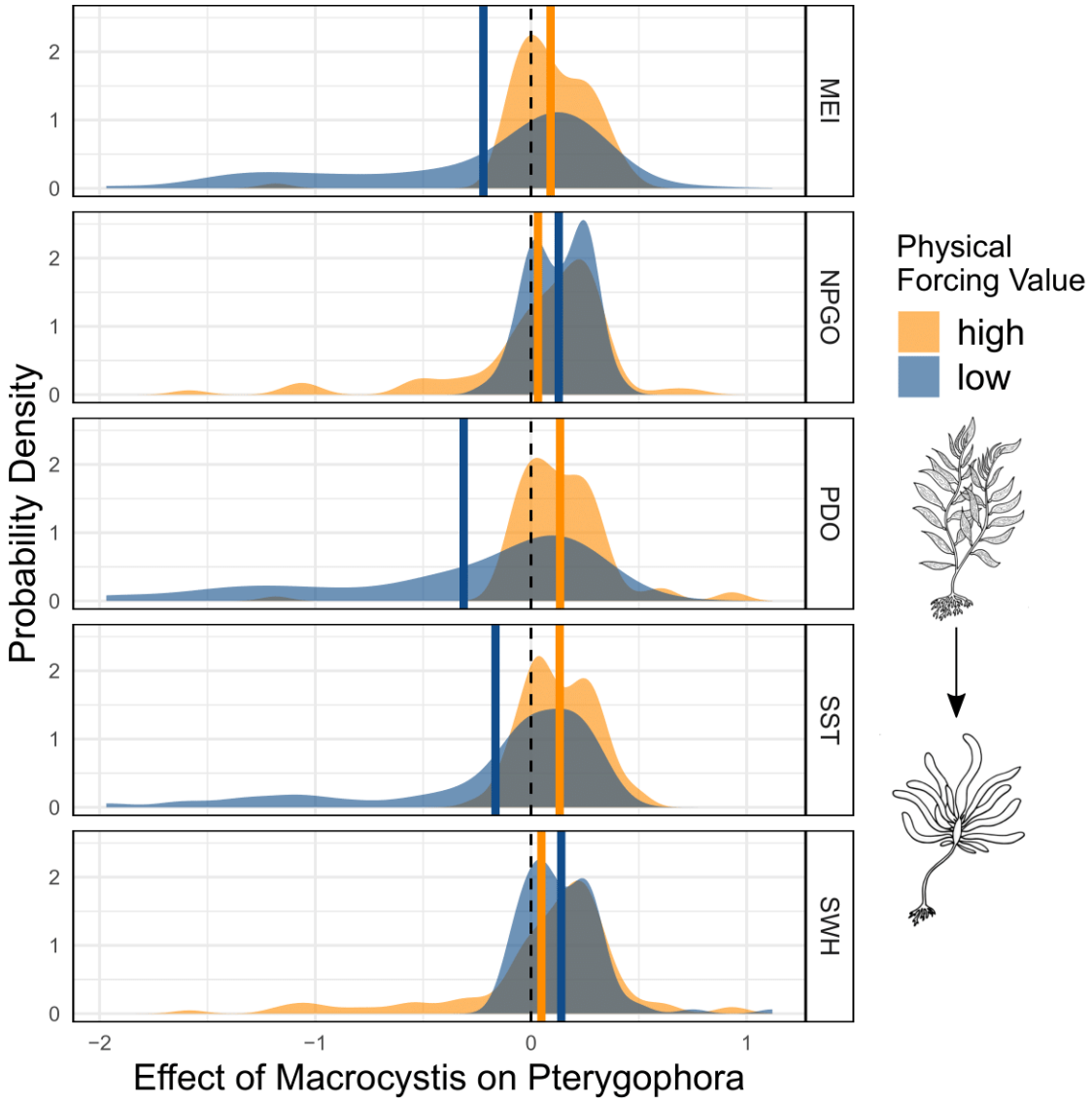

Figure 1.4: Distributions of *Macrocystis* effects on *Pterygophora*, under high (greater than 1) and low (less than -1) values of five normalized environmental indices. Solid lines: mean interactions under each regime.

(Figure 1.4). After splitting the estimated species interactions by those that took place under "low" versus "high" values of the five oceanographic indices (greater than 1 standard deviation below or above the mean conditions in the raw oceanographic data), it immediately becomes clear that strong negative effects of *Macrocystis* on *Pterygophora* only occur under low values of the MEI, PDO, and SST, or high values of the NPGO. These are all climate regimes associated with increased availability of nutrients in southern California[44]–[46]. In southern California, *Macrocystis* is known to be a better competitor under cold-water, nutrient-rich conditions[39], and therefore has a greater chance of flipping its interaction from positive to negative—and asserting interspecies dominance—under low values of the MEI and PDO, and high values of the NPGO (Figure 1.4. Hence, despite the weak mean interaction and common facilitation by *Macrocystis* at this site, the rare negative effects of *Macrocystis* on *Pterygophora* conform to expected patterns across decadal-scale climate shifts[39], [59]. Environmental context alters the strengths of other species interactions as well. Figure 1.5 shows how algal competition and herbivory vary with environmental conditions in the San Nicolas kelp forest. For example, while red urchin *M. franciscanus* herbivory is a strong negative effect (high percentage of significantly negative interactions) under all conditions, the purple urchin, *S. purpuratus*, has a stronger effect in higher-nutrient contexts (low MEI, PDO, and SST). Additionally, *Laminaria farlowii* is a demonstrably better competitor under conditions that are stressful to *Macrocystis*, including low-nutrient, high-temperature, and high-disturbance regimes[39]. Perhaps most clear in Figure 1.5 is, again, the role of *Macrocystis* as both competitor and facilitator. Under El Niño conditions, or strong positive phases of the PDO, *Macrocystis* acts more as a facilitator than a competitor with the other brown algae species, and likewise for low levels of physical disturbance. Only when sufficient nutrients are available under La Niña conditions or cooler sea surface temperatures does *Macrocystis* have predominantly negative effects on the other algae species. The precise

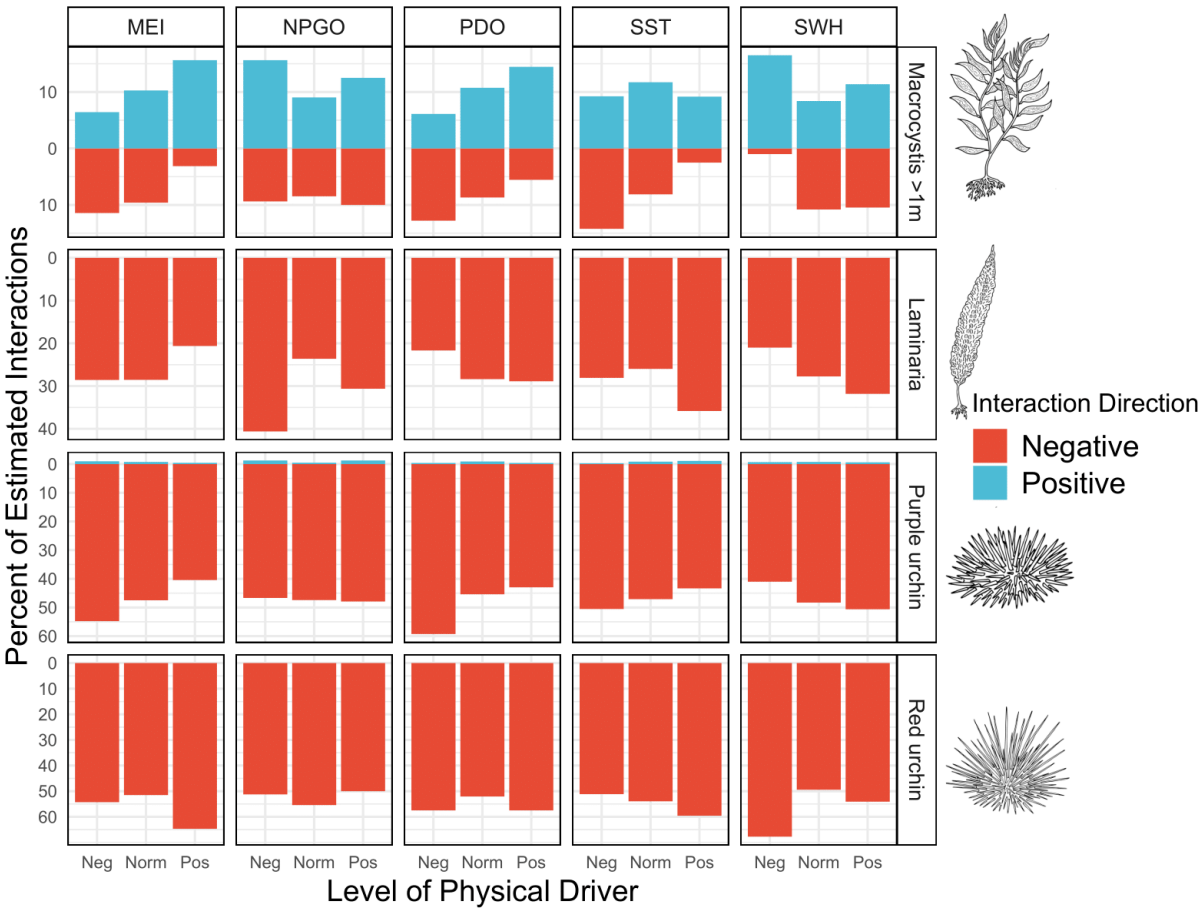

Figure 1.5: Competitive and herbivory effects of selected species under highly negative (Neg: index is less than -1) normal (Norm: index between -1 and +1), and highly positive (Pos: index greater than 1) values of five environmental indices. Each bar represents the percentage of each species' effects that are significantly positive or negative (effects not significantly different than zero not shown). Note varying scale on y-axis. Abbreviations: NPGO: North Pacific Gyre Oscillation; MEI: Multivariate El Niño Index; PDO: Pacific Decadal Oscillation; SST: Sea surface temperature; SWH: Significant wave height.

mechanisms behind the balancing of positive and negative effects of *Macrocystis* cannot be determined directly from these results, but it is clear that the role of this key foundation species shifts with environmental context.

Discussion

Ecosystem dynamics are composed of nonlinear species relationships, played out within shifting environmental contexts. A significant challenge in the study of ecosystem dynamics has been the difficulty in appropriately extrapolating experimental results to real ecosystems, where multiple species-species and species-environment interactions are operating simulateously. We have shown in this study that empirical dynamic modeling can help to tackle this challenge, using time series data to accurately reconstruct nonlinear ecosystem trajectories. Beginning with a published monitoring dataset from a kelp forest ecosystem, EDM methods helped to elucidate causation, build interaction networks, and investigate the influence of large-scale environmental drivers on interaction strength. In this particular ecosystem, our analyses of time series data confirmed decades of experimental work regarding the foundation species *Macrocystis pyrifera*, but also were able to contextualize those classic interactions as to *when* they were important. A classic algal competitive dominance hierarchy[39] is seemingly weak at this site under average conditions, but not absent—under predictable nutrient, temperature, and disturbance regimes, *Macrocystis* can have both competitive and facilitative effects on other species.

An important implication of our study is that if a research goal is to understand the dynamics of entire ecosystems, studying solely the mean outcome of single species interactions may not be adequate. Indirect associations between multiple species and shifting environmental contexts may give rise to rare, critical moments when fleeting strong in-

teractions determine ecosystem shifts. This idea needs further investigation in multiple systems. For example, EDM could be utilized to investigate further the connection between environmental regime shifts and ecosystem tipping points[60]. If widely found in other systems, our general findings imply that context dependency—and its role in mediating varying species interaction strengths—deserves more attention than the identification of context-averaged mean interactions[8]. In a growing number of ecosystems, EDM is helping in this endeavour[16], [61], [62].

EDM does not take the place of experimentation. Rather, we argue that it can help to both contextualize and guide insights from short term experiments. Our analyses are a proof of concept: we started with simple time series from a monitoring dataset in a well-studied but complex ecosystem and showed how previous experimental results play out over a longer time period. The consistency of findings in this well studied system support the potential for this approach to provide credible insights in other ecosystems, where time series data exist but where important interactions may not be nearly as well-established. Where important interactions are known, EDM can help to explore whether environmental context matters in interaction variance. Where ecosystem interactions are not as well known, EDM may be a helpful first step in identification of ecosystem links whose mechanisms can then be further established through other methods.

Supplementary Information

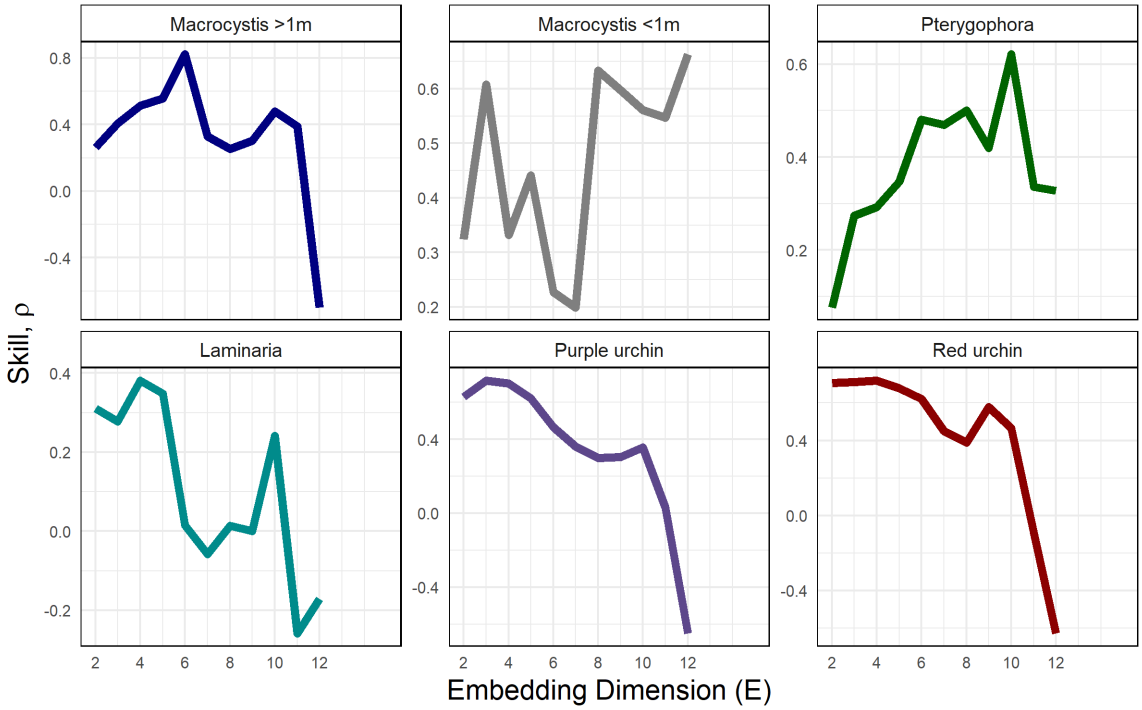

Figure 1.6: Output of simplex forecasting for all species, relating embedding dimension (the number of lags of each variable to use in attractor reconstruction) to forecast skill measured as the Pearson correlation between observations and predictions. The embedding dimension that produced the best forecast skill was used in all further analyses

Table 1.1: Multivariate S-map models for each species. ρ is the predictive skill, MAE is mean absolute error between observations and predictions. All significantly cross-mapped variables were included as predictors.

Modeled Species	Predictors	ρ	MAE
Macrocystis	Macrocystis >1m, Laminaria, Purple urchin, Red urchin, Macrocystis <1m	0.557	0.504
Purple Urchin	Purple urchin, Macrocystis >1m, Pterygophora, Red urchin, Macrocystis <1m	0.734	0.435
Laminaria	Laminaria, Macrocystis >1m, Purple urchin, Red urchin	0.396	0.486
Young Macrocystis	Macrocystis <1m, Laminaria, Macrocystis >1m, Pterygophora, Red urchin	0.439	0.544
Red Urchin	Red urchin, Laminaria, Macrocystis >1m, Pterygophora, Macrocystis <1m	0.756	0.423
Pterygophora	Pterygophora, Macrocystis >1m, Purple urchin, Red urchin, Macrocystis <1m	0.577	0.388

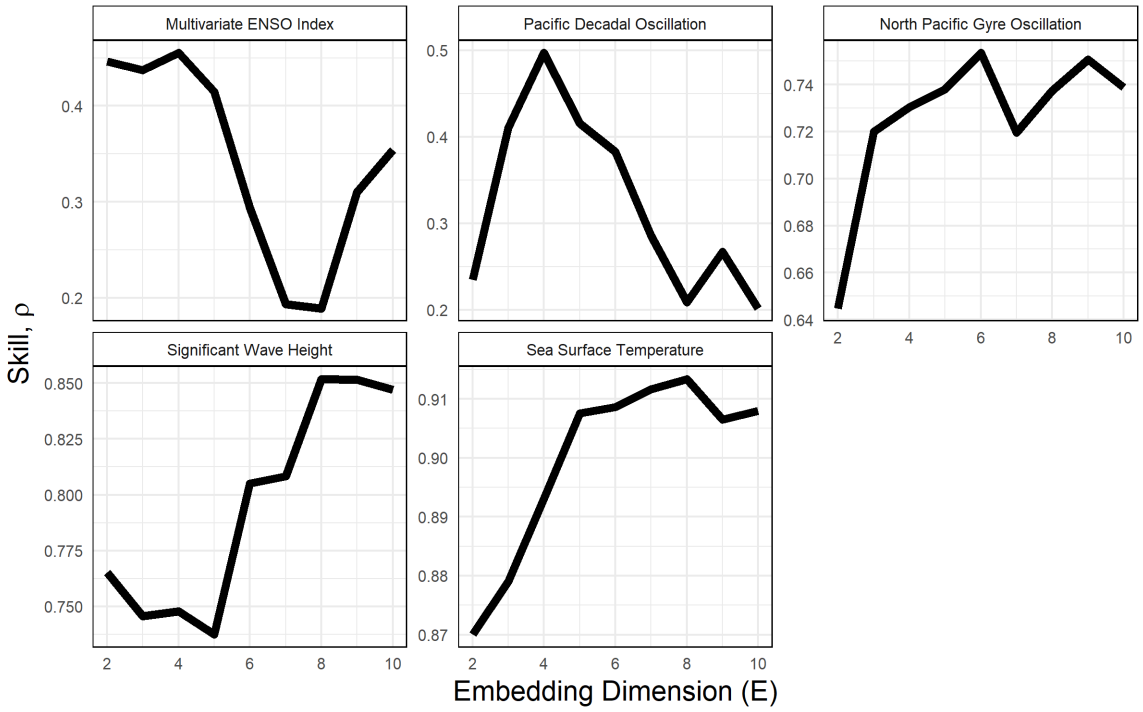

Figure 1.7: Output of simplex forecasting for all physical variables, relating embedding dimension (the number of lags of each variable to use in attractor reconstruction) to forecast skill measured as the Pearson correlation between observations and predictions. The embedding dimension that produced the best forecast skill was used in all further analyses

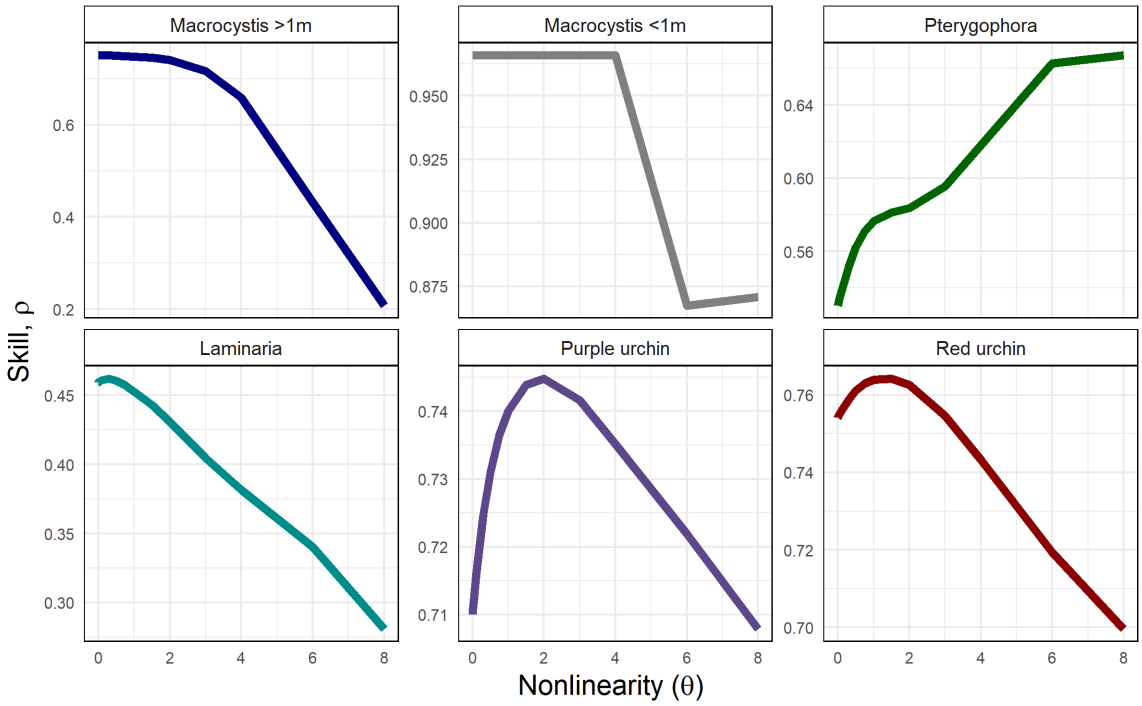

Figure 1.8: Output of univariate S-map forecasting for all species, relating degree of nonlinearity (see Methods) to forecast skill measured as the Pearson correlation between observations and predictions. All species showed increased forecast skill for values of θ greater than zero, suggesting significant state-dependent dynamics. The value of theta that produced the best forecast skill was used in all further analyses

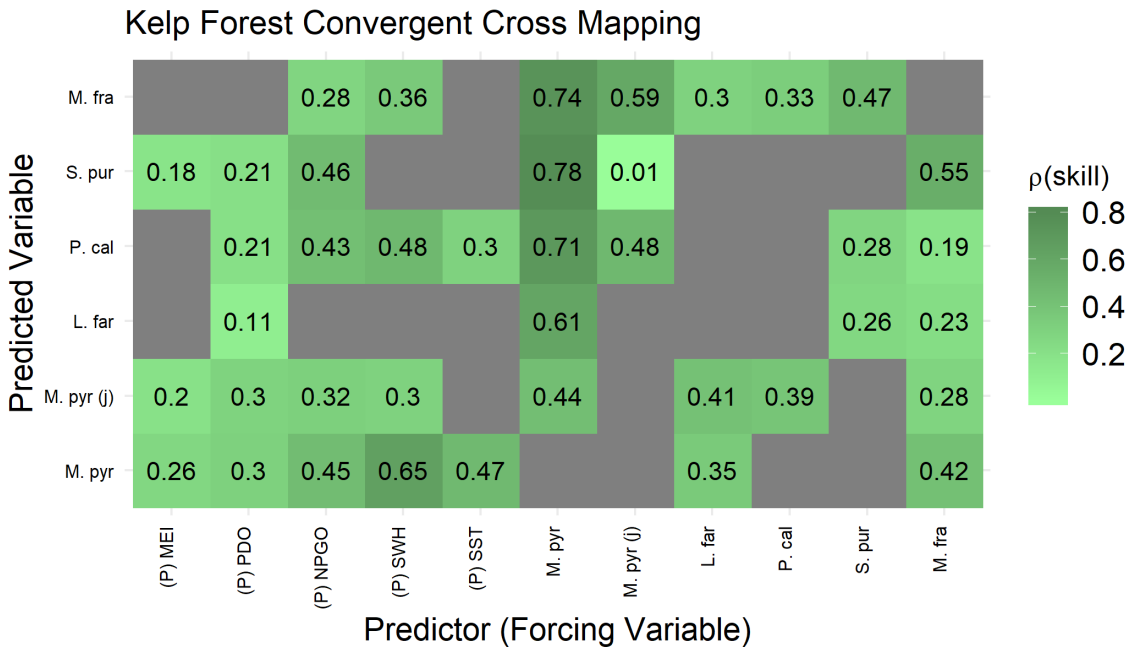

Figure 1.9: The result of applying CCM to all species-species and species-environment interactions. Putative forcing variables are on the x-axis, while predicted variables are on the y-axis. Numbers are the mean predictive skill at library size 500. All non-significant links are grey. Aligns with Figure 2 in the main text. Species abbreviations: M. pyr: *Macrocystis pyrifera*; L.far: *Laminaria farlowii*; P.cal: *Pterygophora californica*; M.fra: *Mesocentrotus franciscanus*; S.pur: *Strongylocentrotus purpuratus*. Physical drivers: NPGO: North Pacific Gyre Oscillation; MEI: Multivariate El Niño Index; PDO: Pacific Decadal Oscillation; SST: Sea surface temperature; SWH: Significant wave height.

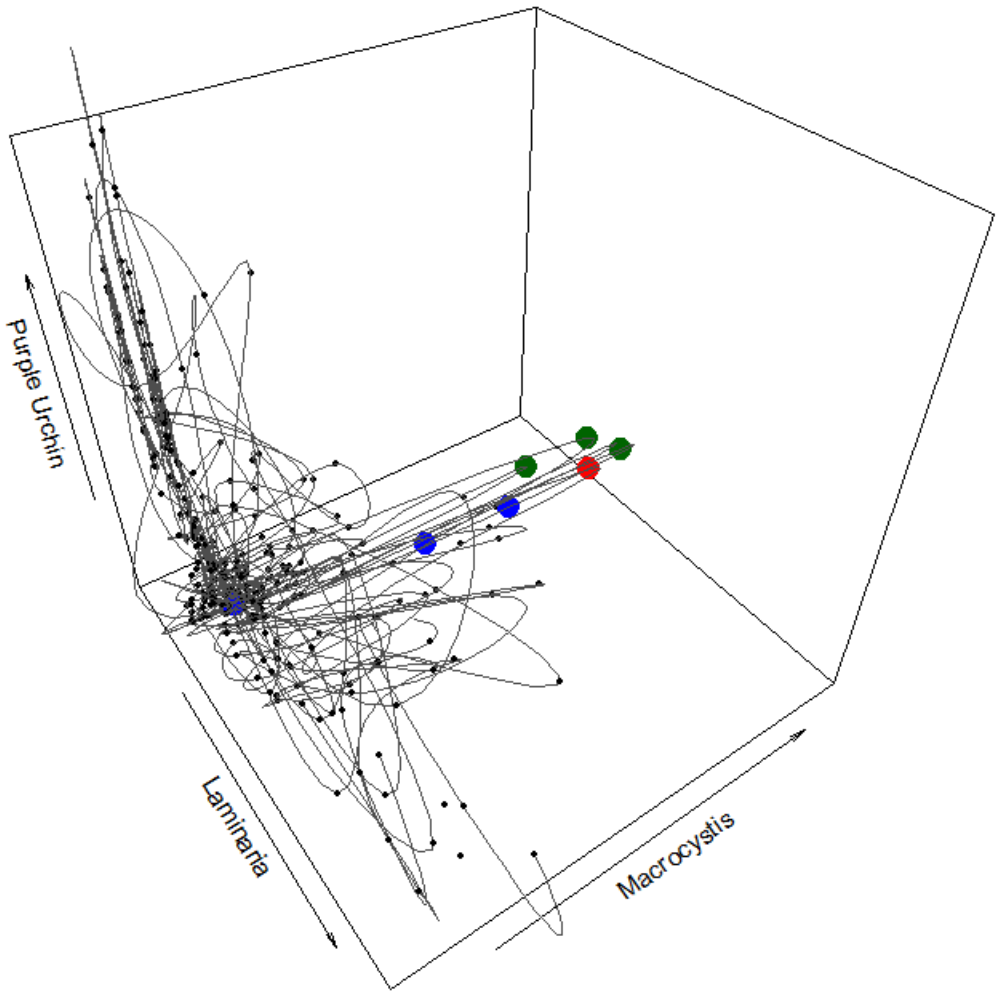

Figure 1.10: An example multivariate attractor using real data from San Nicolas Island. To make predictions for the red point using simplex projection, we take the average of the nearest neighbors (in this case, the 3 green points), projected forward one step in time. For an S-map model, all points in the state space would be used, with each point exponentially weighted by its distance to the target (red) point

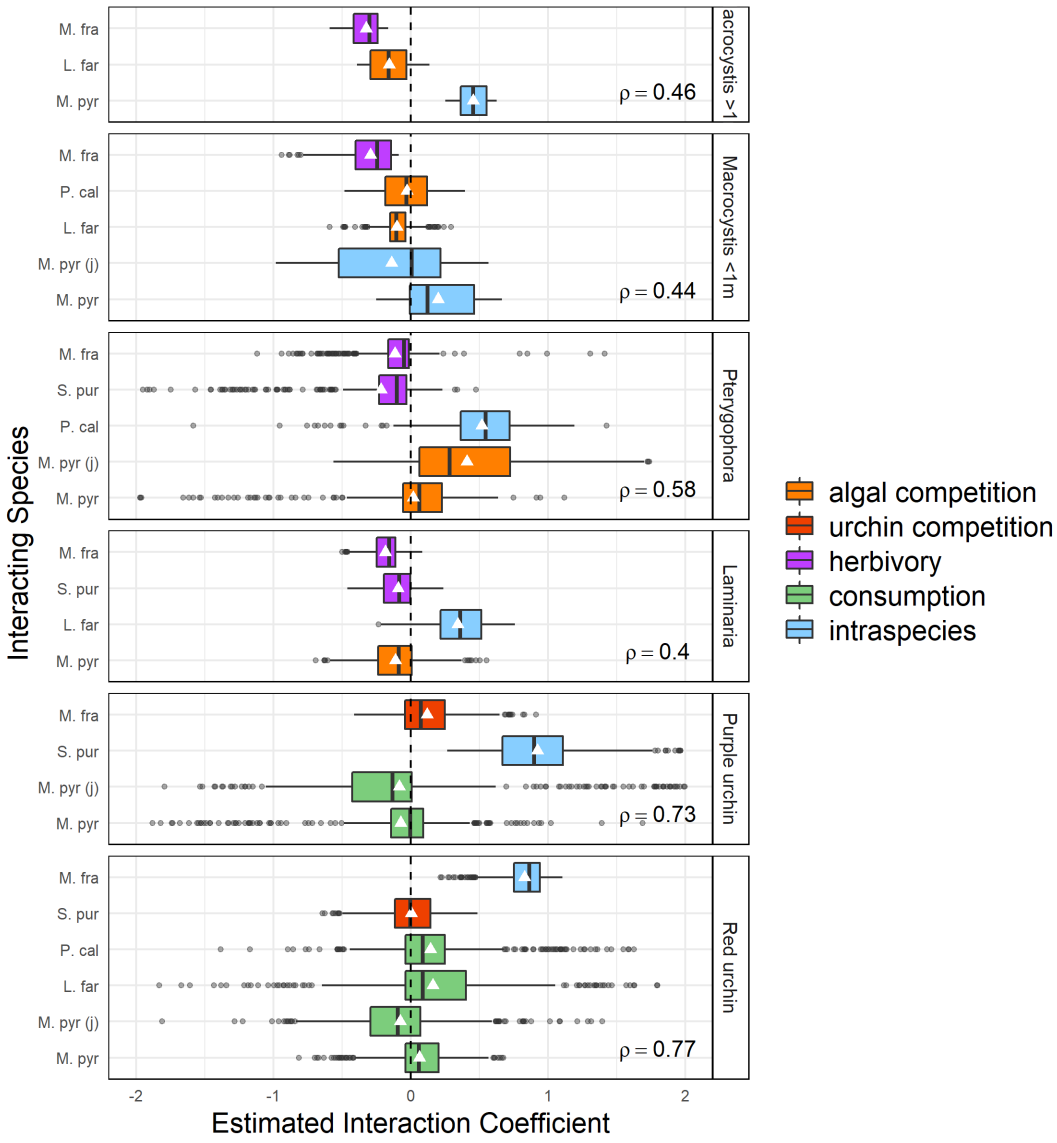

Figure 1.11: Box-and-whisker plots of estimated species interaction strengths from S-map models for the five focal species (panels top to bottom): Macrocystis adults, Macrocystis juveniles, Pterygophora, Laminaria, purple urchin, and red urchin. Each colored box represents the distribution of all estimated interaction coefficients (x-axis) of an interacting or forcing species (left y-axis) on a modeled species (right y-axis) across all data for a given model (white triangles: mean; vertical lines: median; box: interquartile range; whiskers extend to data point at most 1.5*IQR from the box). Each box represents 500-520 estimated interactions. Correlation coefficient between predictions and observations denoted for each model. Color denotes hypothesized interaction type, including interspecific competition (between algae species or between urchin species), herbivory (urchin effect on algae), consumption (algae effect on urchins), and intraspecies interaction (the estimated interaction of a species with itself).

Chapter 2

Recovery of an Endangered Species Threatens a Harvested Resource

Abstract

Many conservation projects have resulted in successful recoveries of previously threatened or endangered natural predators, leading in some cases to competition with humans for harvested prey resources. Informed natural resource management in these situations requires an understanding of the relative effects of human and predator harvesting on the resource. In this study, we investigate one such conflict, between sea otters and the southern California sea urchin fishery. Taking advantage of a natural experiment from San Nicolas Island, where otters were introduced in the late 1980s at a location with an already active sea urchin fishery, we develop and compare Bayesian models that separate the effects of fishery harvesting and sea otter predation on sea urchin biomass. Fitting of multiple models with different functional forms of predation allows us to more accurately represent uncertainty in reconstructed dynamics. We find that the sea urchin fishery, not

sea otter population growth, likely had the most important role in the decline of urchin biomass at the study site. However, as the otter population continues to grow, yield for the fishery may decline to zero within the next 20 years. In the future, continued pursuit of predator recovery in natural systems will lead to difficult decisions between human livelihoods and cultural values. Models like those developed in this study offer a quantitative tool for tackling these tradeoffs.

Introduction

Defaunation is a major global phenomenon in the Anthropocene, and in many ecosystems is most dire for higher trophic level species[63], [64]. The goal of many conservation projects is the recovery of natural predator populations[65], [66]. However, these recovering predators often compete with humans for important prey. In any ecosystem, if human harvesting of prey species developed in the context of a defaunated world, current harvest levels may not be sustainable as natural predators recover[67].

As a result, initial predator conservation successes may lead naturally to management conflict[68], [69]. Often human harvesting of prey will slow, halt, or reverse predator recovery[70], but in other cases natural predators can threaten (or be perceived to threaten) the livelihoods of human harvesters[67], [71], [72]. When such tradeoffs are unavoidable, balancing predator conservation objectives with societal and industry benefits from harvested resources will require difficult choices. The conflict surrounding such decisions can be greatly elevated if they are forced by ongoing conflicts rather than considered in an informed discussion up front. Can we use effective forecasts of predator recovery to anticipate what the expected effect on the shared prey will be? Can human harvesting and healthy predator populations sustainably coexist? Answering these questions is key

to having informed management discussions, and to reducing opposition to prospective conservation efforts when conflicts with human uses are unlikely to occur.

Competition between marine mammals and fisheries is one important category of human-wildlife conflict. In some instances fisheries have caused declines in populations of natural predators. For example, heavy exploitation of important fish species has been an impediment to Steller sea lion (*Eumatopias jubatus*) recovery in large parts of its range[73]. The opposite effect has also occurred: in some cases the perception of a predator's negative effect on fisheries has led to calls for extensive predator culls. From South Africa and the North Sea to eastern Canada and California, culls of marine mammals have been suggested to protect fisheries harvests, even though multiple analyses have suggested that predator culls could actually lead to declines in overall harvests through unanticipated trophic interactions[74]–[76]).

In still other locations, fishery-predator conflicts are just emerging. Sea otters (*Enhydra lutris*) are part of an iconic conservation story, but are also voracious predators on benthic invertebrates[77], [78]. Once ranging from northern Japan all the way across the northern Pacific island chains to Alaska and down to Baja California, the species was hunted nearly to extinction in the 19th century before an international treaty banned hunting in 1911. In California, only one small population of less than 50 individuals remained on the Big Sur coast[79]. Since its protection, however, this southern sea otter (*E. lutris nereis*) has expanded its range both north and south, and now ranges from approximately Pigeon Point near Santa Cruz to just southeast of Point Conception in Santa Barbara County[80].

In the absence of a dominant predator for a century, benthic invertebrates became the basis for multiple productive fisheries in California[81], [82]. Abalone (*Haliotis spp.*) is one informative example[83], [84]. The commercial fishery for abalone in California lasted from the 1920s until approximately 1980, and peaked around 1950 at more than

two million landed tons annually. Abalone is a preferred food for sea otters[78], and otter recolonization of the California coast hastened the decline of the already overexploited abalone fishery. The boom and bust of the abalone fishery was likely a result of interacting effects of overfishing, otter predation, the abalone's slow-growing life history, disease, and increasing prices, all leading to complete collapse of the resource and functional extirpation of abalone in many parts of the California coast[83].

Now, as sea otter populations continue to expand, they are nearing the historically most productive red sea urchin (*Mesocentrotus franciscanus*) fishing grounds in the northern California Channel Islands. The 7 million dollar sea urchin fishery is one of the most valuable in California, and lands approximately 5000 metric tons annually (Fig. 2.1). Although landings have been relatively stable for the last ten years, the fishery is likely fully exploited or overexploited[82]. Concurrently, the state has been struggling to accurately monitor the sea urchin resource and increase its knowledge of the dynamics of the stock[85]. The fishery operates throughout the state, but the majority of landings come from south of Point Conception, in the Southern California Bight region. Sea otters have slowly been extending their range into this region, partially because of an assisted translocation program to San Nicolas Island (one of the California Channel Islands) through the Endangered Species Act, and also through natural southward range expansion along the mainland California coast(Figure 2.2)[80], [86], [87]. Permanent otter breeding colonies do not yet exist in the northern Channel Islands, where much of the sea urchin catch originates, but it may be only a matter of time before otters recolonize those islands[88].

This situation raises a potentially serious management problem. A new source of sea urchin mortality may be introduced as sea otters expand[88], at a time when the resource itself is likely already fully exploited by the fishery. Therefore, understanding the expected effect of sea otters on the urchin resource is key to setting appropriate expecta-

tions or making proactive management decisions for one of California's most important natural resources. The naturally-expanding otter population at San Nicolas Island, which was otter-free for at least a century before the early 1990s, provides a natural experiment through which to test the impact of sea otters on sea urchin fisheries in southern California. Combining these otter population data with landings and effort data from the sea urchin fishery, we parse the relative effects of fishing and natural predators on sea urchin populations using a Bayesian surplus production model modified to include natural predation. We identify the extent of past sea urchin population reduction due to sea otter predation relative to the effect of fishing, and then simulate future harvests under a continuously-growing sea otter population. Finally, we discuss the implications of our approach and results for other systems where recovering predators compete with humans for resources.

Methods

Data Sources

Urchin fishery data

Urchin fishery landings data were obtained from the California Department of Fish and Wildflife. After each fishing trip, urchin divers are required to submit landings receipts which denote landings by weight and where those landings were obtained, referencing a 10' by 10' spatial statistical block (approximately 250 square km). Receipts also contain information on the port where the urchins were landed, the date, and a unique fishing vessel identification number.

In fisheries production models, catch-per-unit-effort (CPUE) is often used as an index of

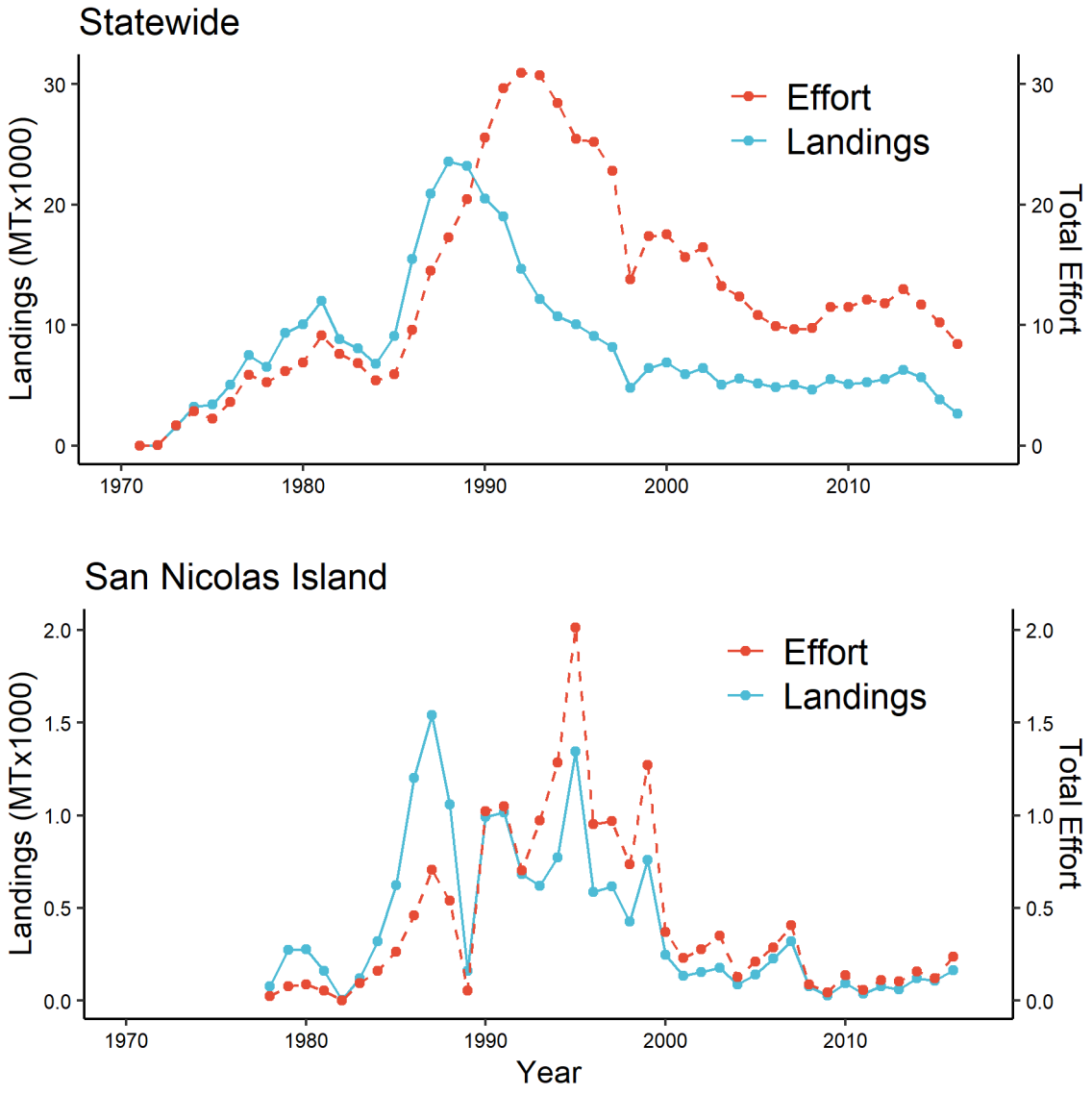

Figure 2.1: California statewide (top) and San Nicolas Island (bottom) sea urchin fishery landings in 1000s of metric tons (solid lines) and effort in 1000s of landings receipts (dashed lines).

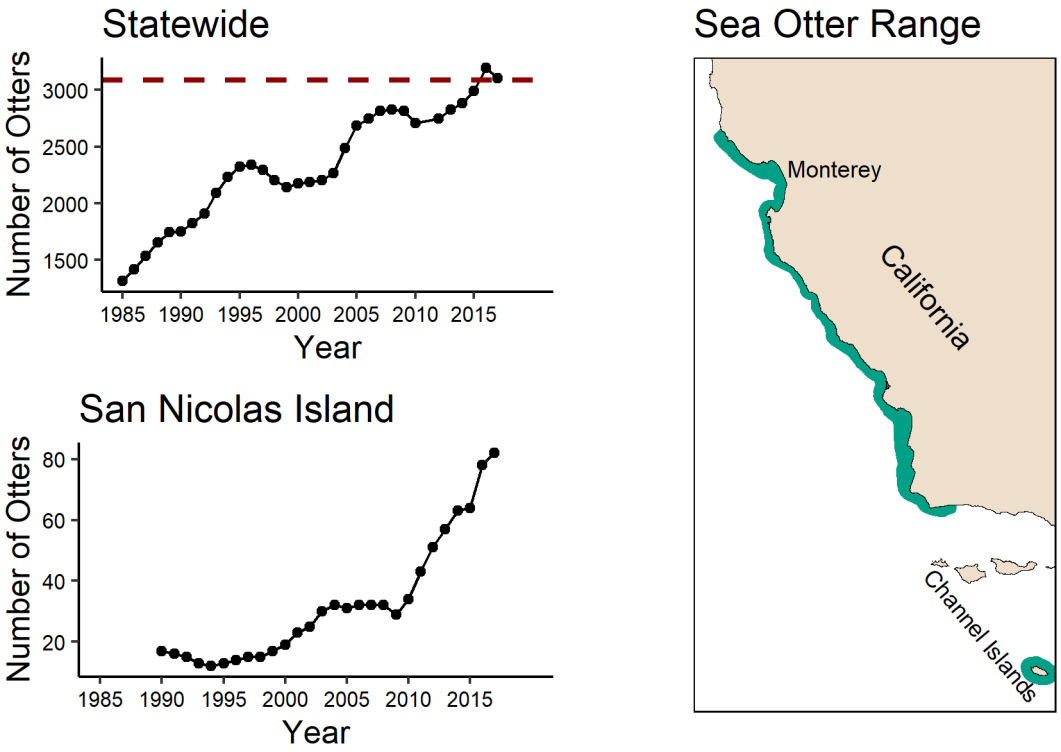

Figure 2.2: (left) Otter population growth along the mainland California coast and at San Nicolas Island. Annual numbers are 3-year running average, while dashed line is the de-listing threshold population size under the Endangered Species Act. (right) Sea otter range in California in 2017. Notice the translocated otter population at San Nicolas Island, lower right.

abundance, in the absence of an independent measure of biomass or population size[89]. We modeled standardized CPUE[89] to use as an index of sea urchin abundance in the population model described below. Standardizing CPUE helps to reduce potential bias in the raw abundance index associated with external factors which may influence catchability of a species. For example, CPUE standardization can help to account for the differences in targeting behavior or skill of different fishing vessels. For the calculation of the CPUE index, urchin landings from the two statistical blocks at San Nicolas Island were aggregated by year, and each individual diver receipt was considered a unit of effort (i.e., one trip by one urchin diver). Then, following Maunder and Punt (2004)[89], the CPUE index was derived from the best fit model among a set of generalized linear models. The preferred model estimated CPUE (landed urchin weight per receipt) as a linear combination of year, fishing port, and fishing vessel (for full description of model selection, see Supplementary Information). We extracted the year fixed effects for the median fishing vessel from the preferred model, and these year effects comprise our standardized CPUE index and our index of sea urchin abundance.

Sea otter population data

The southern sea otter population along the mainland coast is censused annually as part of the official population counts under the Endangered Species Act (methodological details found in refs.[90], [91]). The census measures both sea otter range extent and population size. For this study, total otter population numbers at San Nicolas Island are used to estimate predation effects. Individual sea otters can vary with respect to prey selection and preference[78], [92], but red sea urchins are often a priority diet item when available, including at the San Nicolas study site[93], [94].

Modeling approach

We approached the task of estimating fishery and predator harvest using a Bayesian surplus production model combined with four alternative representations of predation. Our representation of urchin population growth and fishery harvest—common across all models—is described first, followed by an explanation of each different predation model. Urchin mortality due to fishing and sea otter predation are modeled as latent unobserved processes by using our standardized CPUE index to fit a combined fishing and natural predation process model. Each model represents annual changes in biomass B_t of red sea urchins as a function of intrinsic population growth, harvesting, and predation:

$$B_{t+1} = B_t + Growth_t - Harvest_t - Predation_t \tag{2.1}$$

Growth and Harvest

To represent the $Growth_t$ term in equation (2.1), we use the Pella-Tomlinson surplus production model[95]. In the Pella-Tomlinson model, biomass is measured as a function of the previous year's biomass, plus natural growth and mortality, minus fishery removals. The deterministic process equation is

$$B_t = B_{t-1} + \frac{r}{p-1} B_{t-1}\left(1 - \left(\frac{B_{t-1}}{K}\right)^{p-1}\right) - C_t \tag{2.2}$$

where B_t is biomass in year t, r is the instrinsic growth rate of the population, K is the carrying capacity, and C_t is the observed fishery harvest. In the Pella-Tomlinson model, the value of intrinsic productivity r determines how fast the population grows, as well as

the sustainable level of fishing mortality. The additional term p in the Pella-Tomlinson model allows the shape of the resulting yield curve to vary.

This model assumes that r captures natural processes such as birth rate and natural mortality. Additionally, it considers all individuals in the urchin population as reproductively identical, and does not account for age structure. Ignoring age structure has the potential to lead to errors in estimation of reference points[96], [97]. When using a logistic surplus production model like the Pella-Tomlinson to estimate population parameters for a previously unexploited fishery, non-equilibrium processes such as the fishing-down of accumulated biomass can dominate the exploitation history and introduce bias into estimates of reference points. We do not have size or age-structured data for the San Nicolas sea urchin fishery, and so we cannot include age structure in our main analysis.

We link our observed data—the standardized CPUE index—to the growth model using a proportionality constant. Often in fisheries models, we cannot actually observe fish biomass, and instead use an index of abundance such as CPUE to track population changes. The CPUE index I_t is assumed to be directly proportional to total biomass,

$$\hat{I}_t = qB_t \tag{2.3}$$

where the proportionality constant q is known as the catchability coefficient. Combining equations (2.2) and (2.3) allows us to use our CPUE index and observed urchin harvests to estimate year-to-year changes in urchin population size.

We translate the deterministic process model above into a Bayesian framework to allow for the observed data to inform the level of uncertainty in estimated model parameters.

The stochastic versions of equations (2.2) and (2.3) can be written as,

$$log(B_t)|B_{t-1}, K, r, p, \sigma_p^2 = log\Big\{B_{t-1} + \frac{r}{p-1}B_{t-1}\Big(1 - \frac{B_{t-1}}{K}^{p-1}\Big) - C_t\Big\} + \epsilon_t \tag{2.4}$$

$$log(\hat{I}_t)|B_t, q, \sigma_o^2 = log(q) + log(B_t) + \upsilon_t \tag{2.5}$$

In equation (2.4), biomass at $t = 1$ is assumed to be at its carrying capacity (an unfished stock), and the subsequent B_t are modelled as lognormal random variables with process errors $\epsilon_t \sim Normal(0, \sigma_p^2)$. We also observe the CPUE index I_t with observation error $\upsilon_t \sim Normal(0, \sigma_o^2)$.

Sea Otter Predation

All models represent urchin population growth and fishery harvest using equations (2.4) and (2.5), but they differ in how sea otter predation is represented ($Predation_t$ in equation (2.1)). Sea otters have high metabolic rates and consume up to a quarter of their body mass in food per day[98]. To meet this metabolic demand, otters display a wide variety of prey preferences and foraging behaviors, though *M franciscanus* is often a priority prey item because of its relatively high caloric density[78], [92]. Given this diversity in sea otter foraging, the true functional form of sea otter predation dynamics is uncertain. We therefore develop four separate representations of predation to include in models of sea urchin population abundance at San Nicolas Island. The four models all share the Pella-Tomlinson form of urchin population growth and fishery harvesting. Each predation model represents a plausible hypothesis for the functional form of the interactions between *M. franciscanus* and *Enhydra lutris*.The goal of estimating multiple models is to compare inferences derived from the different forms of the predator-prey ecological process. In particular, using multiple models helps in assessing whether the general population and

fishery dynamics, the values of key parameters like the population's intrinsic growth rate, and the relative influence of predator and fishery on the urchin resource are robust to different specifications.

The models generally scale in complexity from Model 1 to Model 4, from an assumption of a constant per capita predation rate to a two-step model that estimates the percent of an individual otter diet comprised of sea urchins, then scales that value to a population-wide consumption rate.

The four predation models are:

1. A linear predation model, where per capita otter consumption is constant, therefore total consumption of sea urchins by otters is a linear function of predator abundance.
2. A predation rate model, analogous to a Lotka-Volterra predator-prey interaction, where predation is proportional to both sea otter abundance and urchin abundance.
3. A predator satiation model, following Hollowed et al. (2000)[99], where the sea otter popultion is modeled as if it were a separate fishing fleet, but with an asymptotic satiation point beyond which total consumption does not increase.
4. A predator functional response model, where known urchin densities are related to the percent of urchins in the sea otter diet, subject to a Holling Type III functional response. Subsequently, per-otter urchin consumption is calculated by multiplying that percent in the diet by the energy requirements of an average adult otter.

Model 1: Linear predation The simplest predation model estimates the effects of otters as linear, ζN_t, where ζ is the per capita effect of annual otter abundance N_t on

urchin biomass, such that a process equation is:

$$B_{t+1} = B_t + Growth_t - Harvest_t - \zeta N_t \tag{2.6}$$

Model 2: Predation rate The predation rate model represents predation as a function of both predator and prey abundance, following the classical predator-prey models of Lotka and Volterra. In this representation, total predation is reduced when prey density declines (unlike in equation (2.6) above). The predation rate is denoted α.

$$B_{t+1} = B_t + Growth_t - Harvest_t - \alpha N_t B_t \tag{2.7}$$

Model 3: Predator satiation Models 3 and 4 represent sea otter predation as a functional response curve. Following a representation of predation mortality from a fishery stock assessment[99], the predator satiation model represents predation as a separate fishery, where the predator has a "catchability" coefficient q_{pred} relating predator abundance to sea urchin consumption. Sea otter predation scales with prey density, similarly to Models 1 and 2. However, the predator can also become satiated, setting a ceiling on the total amount of predation per year.

$$B_{t+1} = B_t + Growth_t - Harvest_t - q_{pred} N_t^{-S(\frac{U_t}{U_{max}} - 1)} \tag{2.8}$$

In equation (2.8), S controls the shape of the satiation curve, and allows for approximation of different Holling-Type curves. A value of S of 0.7 approximates a Holling

Type II functional response. This predation model requires a new data source: U_t and U_{max} correspond to current and maximum prey (urchin) density within the study site. The values of U_t were taken from a subtidal monitoring time series from San Nicolas Island[33], and U_{max} was fitted in the model.

Model 4: Predator functional response The last predation model estimates total annual consumption of otters in a two step process, where D_t is the percent of the otter diet in year t that is composed of urchins.

$$D_t = \frac{F_{max} U_t^H}{N_{half}^H + U_t^H} \tag{2.9}$$

$$B_{t+1} = B_t + Growth_t - Harvest_t - N_t D_{req} D_t \tag{2.10}$$

In equation (2.9), F_{max} is the maximum percent urchins in the diet, and N_{half} is the urchin density at which otter diet percentage is at half of its maximum. H, the Hill exponent, controls the functional response type, where $H = 1$ is a Type II functional response, and $H = 2$ is a Type III functional response. We use a value of 2 for H, to estimate a Type III functional response. In equation (2.10), D_{req} is the annual energy requirement of an average adult otter, in units of urchin biomass. D_{req} is assumed as a constant and is a function of the average weight and caloric energy content of sea urchins[93], [100] and the average metabolic demand of an adult otter[98]. In the estimation of equations (2.9) and (2.10), D_{req} is held constant, while F_{max} and N_{half} are fitted and the U_t are the same data as in equation (2.8).

Fitting and Model Comparison

In the full hierarchical models, we link the observed CPUE index to the unobserved quantities of interest using a lognormal likelihood, treating the otter population and fishery harvests as known. We implemented the model in Stan[101], and fit the model through Hamiltonian Markov Chain Monte Carlo with three chains and 6000 total iterations per chain (2000 warmup and 4000 sampling iterations)[102].

We compare models using the log-likelihood of the observed catch-per-unit-effort index, I, given our estimates of catch-per-unit-effort $\hat{I}_t$ and observation error σ_o^2:

$$log(I_t) \sim Lognormal(log(\hat{I}_t), \sigma_o^2) \tag{2.11}$$

Using the `loo` package in R[103], we compare the models with leave-one-out cross-validation for Bayesian models using Pareto smoothed importance sampling[103]. The measure of predictive fit used to rank the models is the expected log predictive density (equation 4 in Vehtari et al. (2017)[103]):

$$elpd_{loo} = \sum_{t=1}^{n} logp(I_t|I_{-t}) \tag{2.12}$$

where $p(I_t|I_{-t})$ is the leave-one-out predictive density given the data without the ith data point.

Complete fit statistics and posterior parameter estimates for each model are provided in the Supplementary Information.

Maximum Sustainable Yield and Future Simulation

After model fitting, we use draws from the posterior distributions of each model to calculate maximum sustainable yield and project the future dynamics of the urchin population, the urchin fishery, and otter predation. For each posterior draw of p, r, and k from the Monte Carlo simulation, we first calculate maximum sustainable yield in the absence of predation using equation (2.13). Then, using the values of the predation parameters from the same posterior draw, we adjust the calculation of maximum sustainable yield by subtracting the share of the resource that would be taken by predation (equations (2.6) to (2.10)). In this way, the calculation of maximum sustainable yield changes from year to year, accounting for otter predation.

In each simulation, we assume that fishing will continue at the average exploitation rate estimated for the last five years in each draw. Also, we assume continued sea otter population growth. The otter population is assumed to grow at a per-capita growth rate starting at the average rate observed the most recent five years in the data (approximately 12 percent per year), and declining to zero over the time frame of the simulation. Under these assumptions, 33 years is the approximate time the otter population at San Nicolas would take to reach its estimated carrying capacity of just under 500 individuals[88], and so each simulation is run for 33 years. Because each Monte Carlo chain is run with 4000 sampling iterations and three chains, we obtain 12 thousand separate simulations per model, or 48 thousand total simulations.

Results and Discussion

Historical trends in urchin fishery and otter populations

The red sea urchin fishery began on the California coast in the early 1970s, and quickly expanded in response to growing Japanese demand[81]. By the middle of the 1990s, annual statewide harvest had peaked and began to decline (Figure 2.1). The decline was steep, but by the early 2000s statewide harvest stabilized around five thousand metric tons, down from a peak of more than 20 thousand tons. Since 2013, landings have again begun to decline.

The landings from San Nicolas Island follow a similar pattern (Figure 2.1). After the fishery began at the island in the late 1970s, effort and landings expanded quickly, and landings were high but variable from the mid-1980s to mid-1990s, oscillating around a thousand metric tons—a substantial contribution to statewide harvest. However, after 1995 landings declined quickly, from more than 1500 to less than 100 tons.

Sea otters have expanded their range and population size in California during the same time frame (Figure 2.2). Since the modern annual sea otter census[90] began in California in 1985, the sea otter population has more than doubled. The species is now close to its federally-designated population size threshold necessary for delisting under the Endangered Species Act[90]. At San Nicolas Island, the translocated population struggled to establish for several years, but has been growing steadily in the past ten years to more than 80 individuals[90] (Figure 2.2). The population at the island is likely still substantially below its estimated carrying capacity[88]. Given the negative correlation between urchin fishery landings and the sea otter population, a reasonable hypothesis is that otters were the primary cause behind the observed fishery decline. We use combined

population growth and predation models to test this hypothesis.

Effects of fishing mortality and predation on urchin landings

Each of the four models fit the observed catch-per-unit-effort data well, and all models produce similar estimates of common parameters, even though the underlying predation process model was different for each (model selection and fit statistics are provided in the Supplementary Information). The mean posterior estimate for the intrinsic urchin population growth rate r is between 0.2 and 0.3 in all models, and carrying capacity K is approximately 33 thousand tons. Additionally, for all models the estimated Pella-Tomlinson shape parameter p is greater than 2, suggesting that maximum sustainable yield for this population occurs at a population size greater than half of the carrying capacity $\frac{K}{2}$.

We compared models using Bayesian leave-one-out cross-validation[103]. The predator satiation model (Model 3) had the highest log-likelihood, but the standard error of the model likelihood was greater than the difference between models. Therefore, the observed data did not definitively provide evidence for one model over the others (Table S9). Estimated sea urchin population size at San Nicolas follows the declining trend in catch per unit of effort (CPUE, Figures 2.1 and 2.3). The population declined steadily from the beginning of the fishery through the mid 1990s, and has remained at less than a third of estimated carrying capacity since the mid-1990s. The early 1990s was also when the translocated sea otter population was first establishing itself at the island, again raising the question of whether the large observed decline in sea urchin CPUE—and the corresponding estimated decline in urchin abundance—was caused by the arrival of sea otters.

Despite the negative correlation otter and urchin populations, our model estimates sug-

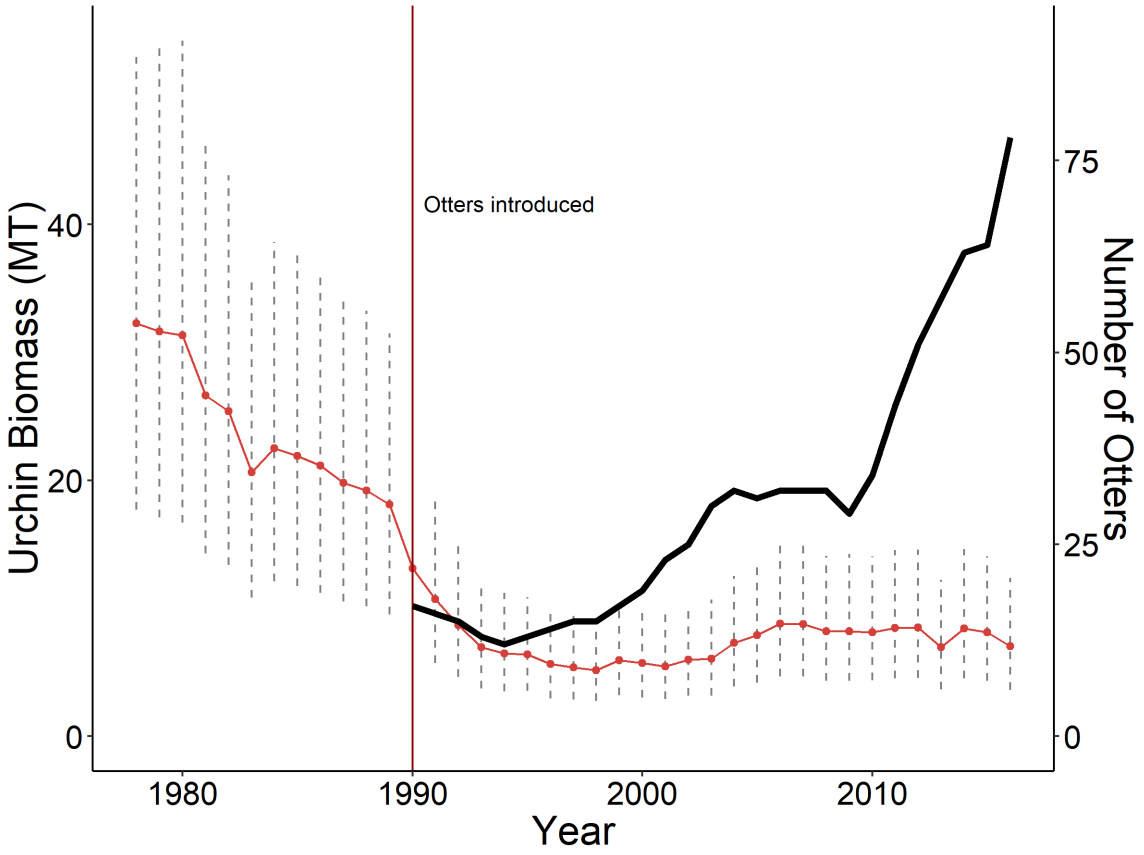

Figure 2.3: Urchin population size over time, San Nicolas Island. Solid lines are mean posterior estimates of biomass in each year from the predator satiation model, although estimates from all models showed a similar trend. Error bars encompass 95 percent credible intervals. Sea otters were translocated to San Nicolas Island in 1990, shown with a vertical bar

gest that human harvesting has had a much larger impact than sea otter predation on sea urchin populations at San Nicolas Island. Using model estimates of total removals of sea urchins by fishers and otters, we estimate annual exploitation rates attributable to each mortality source (Figure 2.4). These exploitation rates show that total pressure on the sea urchin resource has been dominated by fishery-induced mortality for most of the time series. It was not until at least 2001 that the mean estimate of otter exploitation rate exceeded the estimate of fishing mortality, estimated in the predation rate model. Other models suggest an even smaller otter effect, and in the predator satiation model (Model 3), otter exploitation rate never exceeds fishing mortality. In all models, estimated fishing exploitation rate reached a peak in 1995, after which it declined rapidly, coinciding with the observed decline in total urchin harvest (Figure 2.1).

After 2000, models diverge on the estimated effects of sea otters versus fishers, with implications for future projections. In Models 1, 3, and 4, exploitation rate of otters has remained low (less than five percent removal of the total sea urchin stock per year). However, in the predation rate model, the mean posterior estimate of otter exploitation rate is approximately 10 percent per year, with an upper bound as high as 20 percent. The predation rate model also has much higher uncertainty, however, in the estimated otter effect (Figure 2.4). This is likely because total predation in that model (Equation (2.7)) varies as a function of both predator and prey abundance, without a saturating predation response, as is present in the predator satiation and functional response models. Therefore, it is possible the upper bound of otter exploitation in the predation model is an overestimation. Regardless of the model, the total effect of otters relative to the effect of fishers has grown since 2000 as a combined function of otter population growth and fishing effort decline.

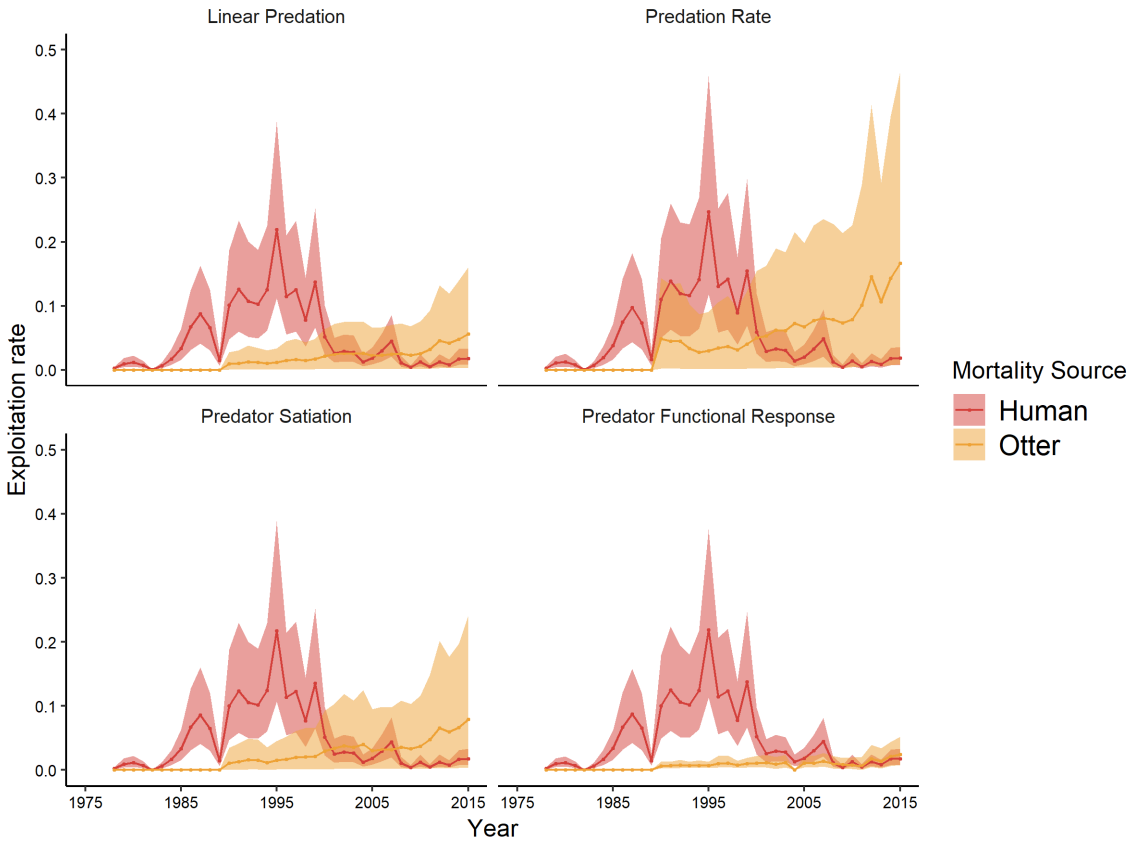

Figure 2.4: Exploitation rate (proportion of the urchin population harvested per year) of human fishers and sea otters at San Nicolas Island estimated by each model. Solid lines are mean posterior estimates of the exploitation rates in each year, while ribbons encompass 95 percent credible intervals.

Future yield

Using posterior model estimates of parameters for the Pella-Tomlinson production model (equation (2.2)), along with additional mortality from sea otter predation, we can estimate maximum sustainable yield for each process model and simulate future harvests under the assumption of an otter population that will continue to grow. For simplicity, in our projections we assume that fishing exploitation rate remains at its estimated mean value from the most recent five years in the data, while the otter population grows logistically towards its estimated carrying capacity at San Nicolas of approximately 500 otters. As the otter population continues to grow, maximum sustainable yield declines in all simulations (Figure 2.5). Annual urchin removals by sea otters have already reached levels at which maximum sustainable yield for fisheries is zero under the predation rate model. Under the predator satiation model, however, the median estimate of maximum sustainable yield is estimated at 800 metric tons, declining slowly with an increased otter population. For the linear predation and predator functional response models, it is estimated that a level of zero sustainable yield will be reached within 20 years. Because of overfishing, though, urchin harvests are already well below the estimates of maximum sustainable yield. This overfishing, combined with continued growth in the population of otters at San Nicolas Island, means that a rebound in the urchin population is unlikely. We can use model estimates to project future harvests starting from current conditions to make short-term predictions (Figure 2.6). In our simulations, we assume that urchin fishing continues at the same exploitation rate as it has for the past five years. As in the calculation of maximum sustainable yield, the projected harvests depend on the chosen predation model. For Models 1, 2, and 3, simulated urchin harvests decline over the next 30 years, with a median projection reaching zero harvest in as little as 16 years (top left panel of Figure 2.6). For the predator satiation model, projected urchin harvests

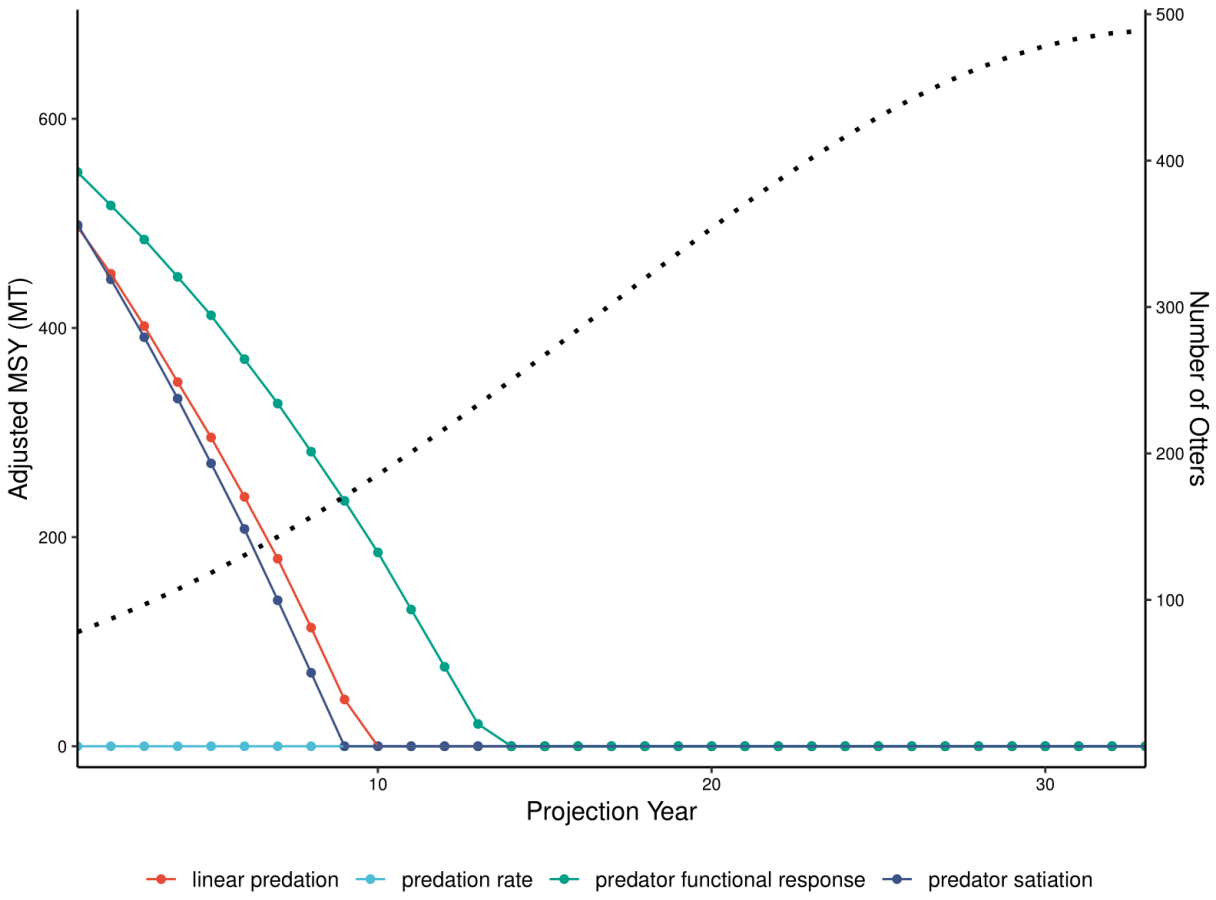

Figure 2.5: Maximum sustainable sea urchin yield under otter population growth for each fitted predation model. Solid lines are median estimates of maximum sustainable yield for each predation model across all simulations, adjusted for estimated sea otter predation. The dotted line is the projected sea otter population size, which is the same across all simulations.

actually increase over the course of the simulation, but with high uncertainty. Overall, our projections suggest a high probability of the disappearance of a sea urchin fishery at San Nicolas Island within the next 20 to 30 years. Estimated annual harvests decline to less than 50 metric tons in half of all simulations within 20 years, and by 30 years in the future, harvests are zero in a quarter of simulations. Our analysis does not account for some additional dynamics that may help to improve future studies. First, we do not include an explicit population growth model for the predator, thereby implicitly assuming that otter population growth is independent of sea urchin abundance. Because sea otters are generalist predators, their abundance is not necessarily closely tied to the abundance of sea urchins *per se*[104]. However, in situations where a predator is known to rely exclusively on a prey that is also targeted by humans, the inclusion of a feedback from prey to predator would be important. Likewise, we do not include an explicit link between the fishers and otters themselves. Sea otters at San Nicolas Island took many years to establish a stable population after their managed translocation, and the reasons for this are still unknown[105]. While it is possible that fishing activity or even direct mortality imposed on the otter population by the urchin fishery affected otter population growth, evidence is lacking on any effects of this type, and therefore that dynamic is excluded from our models.

An additional limitation of our analysis is that it does not account for the age structure of the sea urchin population because we did not have the requisite data for sea urchins at San Nicolas. Not including age structure means that our models do not explicitly account for the transient dynamics associated with "fishing down" the accumulated mature stock of sea urchins[96]. Ignoring age structure can lead to bias in estimates of maximum sustainable yield through mis-estimation of carrying capacity[97], and the direction of that bias is unknown and depends upon the nature of the transient dynamics[96]. Therefore,

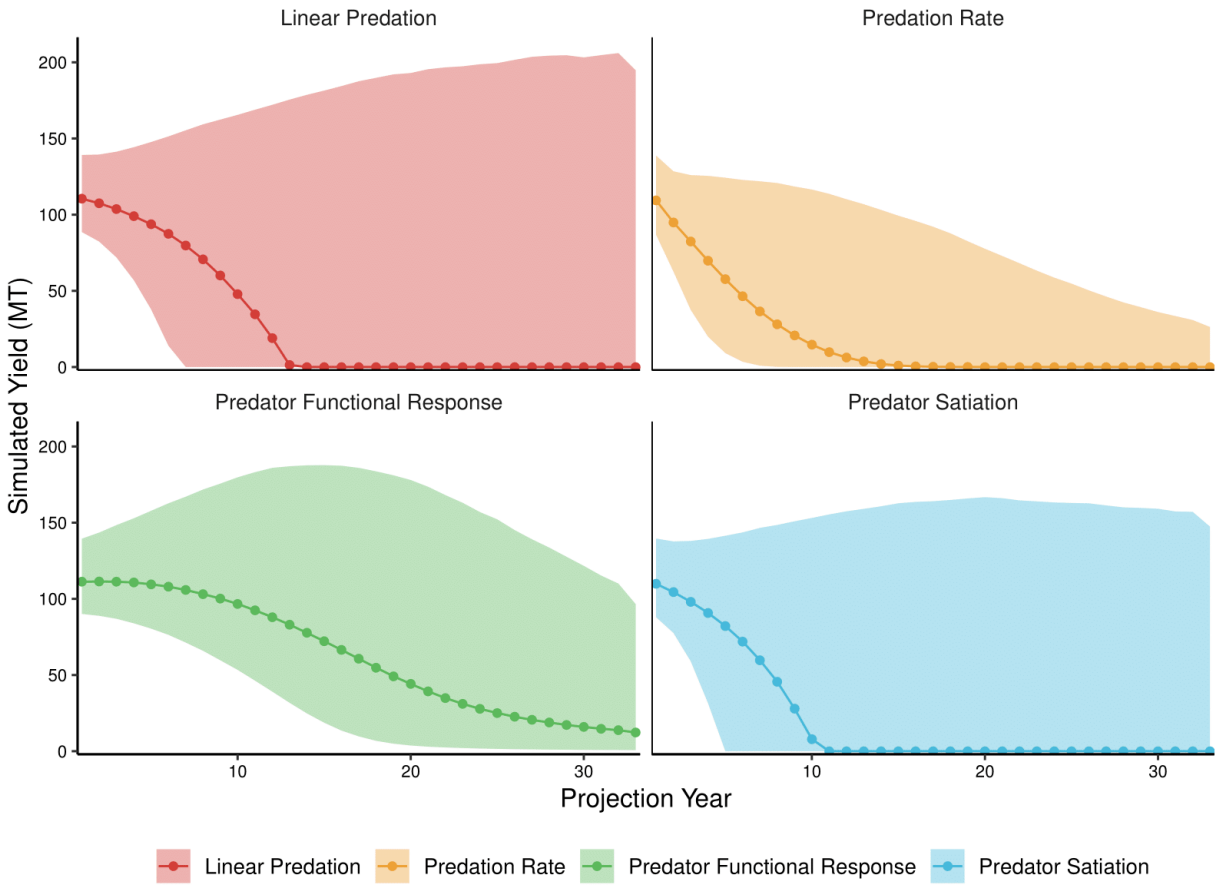

Figure 2.6: Simulated future urchin fishery yield in metric tons for the four models. Simulations are performed using posterior draws of population and predation parameters from each model, with a constant fishery exploitation rate but a growing sea otter population. Solid lines are median estimates of yield from all simulations for a given model, while ribbons denote the 5 percent and 95 percent quantiles of the simulations.

our projections of future and maximum sustainable yield should be considered illustrative of a general pattern rather than a precise estimate of the speed of urchin fishery decline. However, whether our estimate of carrying capacity is high or low does not affect our findings in the historical trend analysis on the relative impacts of fishers and otters at any given point in the past. Nevertheless, in the future it would be informative to perform an analysis like ours with age-structured data.

As predator populations recover from historical pressures, new human-wildlife conflicts like the one analyzed here are emerging. In the marine realm in particular, recovering predators will likely compete with humans for valuable prey[67]. Designing appropriate management of these emerging conflicts will be predicated on our ability to estimate, and ideally forecast, the relative impacts of human and natural predators[106]. Even relatively simple models like those developed in our study can assist in the interpretation of data and the framing of management responses.

We took advantage of a natural experiment—the translocation of California sea otters to an island where they had been absent for more than 100 years—to measure natural predator impact on a valuable fishery. Although the reintroduced otters took many years to establish a stable population at San Nicolas Island[90], their eventual population increase seemed to correspond with a steep decline in the landings and catch efficiency of the red sea urchin fishery. Surprisingly, however, our models strongly agree that the sea urchin population and fishery decline were primarily caused by human overharvesting, not predation. We were able to come to this conclusion only through the use of models that combined dynamic representations of human and predator exploitation of the resource, allowing the data to inform the relative evidence for and against the alternative hypotheses, with associated uncertainty.

Our approach allowed us to use data from the past to inform thinking about the future of

human-wildlife conflict in our study area, and has wider relevance to other systems where recovering predators may exacerbate human-wildlife conflicts surrounding harvested resources[107]. The fitting of multiple model representations of predation in a Bayesian framework allowed us to utilize multiple, disparate types of data, and gain additional insight through their comparison. For example, our linear predation and predation rate models were fit using only catch per unit effort, harvest, and otter population data—standard data types available for many types of natural resource problems. Alternatively, the predator satiation model utilized an additional, independent urchin density time series, and the predator functional response model made use of known relationships between urchin caloric energy content and sea otter metabolic demand to produce a "bottom-up" estimate of urchin consumption. By tying all of these representations of predation to their effect on sea urchin population size, and thereby to the availability of the resource to fishers, we were able to reconstruct the exploitation history of the red urchin at San Nicolas Island. This fitting of multiple models provides more confidence in overall conclusions than one model alone, while concurrently allowing for a more nuanced look at the uncertainties inherent in our understanding of the system (e.g., in the divergent trajectories of our harvest simulations). We recommend that other researchers and managers take a similar, multi-model comparison approach when approaching human-wildlife conflicts with high uncertainty.

Predator recovery projects involve contending with the predator's effect on natural resources (prey) that may be of economic or intrinsic value to humans[67]. The type of conflict described in our analysis is not unique. For example, in the greater Yellowstone ecosystem, recovering populations of gray wolves threaten both livestock and populations of recreationally-hunted elk. An explosive management issue is whether and how to conduct lethal control (culling) of the wolf population[71], a conversation which should be

fundamentally informed by knowledge of the historical—and predicted future—relative effects of humans and natural predators on the resources of value. One analysis of historical Yellowstone data found, as in our sea otter case, that human harvesting and severe climate impacts likely had a much larger impact on elk populations than wolves[108]. Apportioning impact like this to one mortality source over another is often a primary topic in policy discussions, because it is used as evidence for or against active management of predator populations[71].

Understanding past dynamics also offers a baseline to help us set expectations for the future, and could help predict the effects of proposed management actions. In our analysis, we were able to use the fitted model parameters to explore what effect the continued growth of the sea otter population will have on sustainable urchin fishery yields. According to their Species Recovery Plan under the Endangered Species Act, sea otters are still substantially below their estimated carrying capacity at San Nicolas Island[105]. We estimate a decline in sea urchin yields with an increasing otter population, but the slope of that decline varies substantially depending on the predation model used. This finding is relevant for other predator recoveries because multiple plausible but divergent models provide natural resource managers with bounds on the range of potential futures. Predicting when and how extensively predator recovery may negatively impact future sustainable harvests is a primary endeavor of many recovery programs, but making incorrect predictions may have undesirable consequences. For example, in the East China Sea, management focused solely on the recovery of large predatory fish may cause declines in prey species that are the basis of some of the most productive fisheries in the world[69]. In other cases, though, explicit predator removal can also cause declines in prey. In the Benguela ecosystem of southern Africa, a cull of recovering fur seals was strongly considered to protect an important fishery. However, careful food web analy-

sis suggested that the proposed cull would likely do more harm than good, and might actually cause a decline in the catch of the target species because of indirect trophic interactions[75], [109]. In a terrestrial example, lethal culling of coyotes in the western United States likely causes a negative indirect effect on the greater sage-grouse, the species the cull is purportedly intended to benefit[110]. This type of unintended consequence is not uncommon: in 113 predator removal experiments reviewed by Sih et al.[111], prey density declined after predator removal in 54 of them. Ultimately, effective prediction and management of complex predator-prey systems requires models like ours that combine human harvesting with ecological processes[68].

If we value both healthy predator populations and the livelihoods of natural resource harvesters, then we must establish whether they can coexist. Our projections of future maximum sustainable yield and fishery harvests suggest that if the sea otter population continues to grow at San Nicolas Island, an urchin fishery will no longer be viable in the near future. But from another perspective, otters and urchin fishers have coexisted at the island since 1990. Extensions of our work could further explore the long-term implications of alternative predator management actions for the urchin fishery, such as culling (currently illegal under the Endangered Species Act) or the managed spatial separation of otters and fisheries. Regardless of the actual actions taken, managers must proactively plan for the consequences of an overexploited fishery now facing an increasing additional mortality source from a recovering predator. However, management decisions should also consider other effects of predators beyond their direct impacts on prey resources, including overall ecosystem health. Sea otters, as a keystone species, promote the creation and resilience of healthy kelp forest ecosystems. Wolves and other terrestrial predators are known to preferentially select older and diseased ungulates, helping to maintain herd health[112]. Amid a push towards a greater emphasis on holistic, ecosystem-based

management, these broader implications of predator recovery should be considered.

The Anthropocene has ushered in elevated human pressures on harvested natural resources and the natural predators that depend on them. At the same time, a growing conservation ethic and appreciation of the ecological importance of predators means that decision-makers must contend with difficult tradeoffs and complex dynamics in trying to balance predator recovery with human livelihoods and economic values. Models like those presented in this study offer a way to leverage known ecological relationships and commonly available data to confront these tradeoffs in human-wildlife conflicts in a quantitatively-robust way.

Supplementary Information

Model Structure

Urchin mortality due to fishing and sea otter predation were modeled as latent unobserved processes by fitting a standardized CPUE index to a combined fishing and natural predation process model. Each model represents change in biomass B_t of urchins over time as a function of intrinsic growth, harvesting, and predation:

$$B_{t+1} = B_t + Growth_t - Harvest_t - Predation_t$$

For all models, $Growth_t - Harvest_t$ is modeled with the Pella-Tomlinson model (Equation 2 in the main text):

$$B_t = B_{t-1} + \frac{r}{p-1} B_{t-1}\Big(1 - \Big(\frac{B_{t-1}}{K}\Big)^{p-1}\Big) - C_t$$

SUPPLEMENTARY INFORMATION

In a classic logistic growth model without p (sometimes known as the Schaefer or Graham-Schaefer model in fisheries applications), the *maximum sustainable yield*—the biomass that can be consistently withdrawn from the stock year over year—occurs at a stock size equal to half the carrying capacity, $\frac{K}{2}$. In the Pella-Tomlinson model, the biomass level producing the maximum sustainable yield (B_{MSY}) can occur at any fraction of k (equations (2.13) and (2.14)), dependent on the fitted parameter p. When $p = 2$, the model reduces to the simple logistic growth model. When $p > 2$, maximum sustainable yield occurs at a stock size greater than half the carrying capacity, and when $p < 2$, maximum sustainable yield occurs at a stock size less than half the carrying capacity.

$$MSY = rk(\left(\frac{1}{p}\right)^{1+\frac{1}{p-1}} \tag{2.13}$$

$$B_{MSY} = k\left(\frac{1}{p}\right)^{\frac{1}{p-1}} \tag{2.14}$$

In the fitting of the Pella-Tomlinson models, harvest C_t is treated as known (observed urchin harvest) and r, p, and K are fitted. Biomass B_t is linked to the observed catch-per-unit-effort data I_t via a fitted catchability coefficient q:

$$\hat{I}_t = qB_t$$

The four models differed in their representation of $Predation$, described below.

Model Data and Parameter Descriptions

Note: otter daily caloric demand is defined as 15.7 MJ per day (98). To put the value into units of red urchin biomass, this number was divided by the average caloric energy content of a medium-to-large urchin (60-100 mm test diameter) of 142.8 kJ (93) to get a

Table 2.1: Data used in model fitting

Data	Description	Source
C_t	Harvest of red sea urchins in year t	California Department of Fish and Wildlife
I_t	Standardized CPUE index	Standardized from California Department of Fish and Wildlife
N_t	Otter population at San Nicolas Island in year t	USGS Western Ecological Research Center
U_t	Red sea urchin density at San Nicolas Island in year t (predator satiation and functional response models)	Kenner et al.(2013)
D_{req}	Annual caloric demand of an adult sea otter if 100 percent of the diet were urchins* (predator functional response model)	Yeates et al.(2007), Bentall et al.(2005), Shears et al.(2012)

maximum number of urchins eaten per day, then multiplied by the average total weight of that same urchin (60-100 mm diameter) of 231g (100). Finally, the caloric demand was scaled up from a daily to an annual value in metric tons.

Table 2.2: Quantities estimated as combinations of the fitted parameters

Quantity	Description	Equation in main text
B_t	Biomass of red sea urchins at San Nicolas Island in year t	2,4
$\hat{I}_t$	Estimated CPUE index of abundance in year t	3,5
D_t	Percent urchins in the sea otter diet in year t	9

Table 2.3: Parameters of the Pella Tomlinson surplus production model, common to all four models developed in the text

Parameter	Definition	Prior
K	Carrying capacity of red sea urchins at San Nicolas Island	$Normal(10max(Ct), 10max(Ct))$
r	Intrinsic population growth rate	$Normal$(0.4,0.2)
p	Pella-Tomlinson shape parameter	$Normal$(2,4)
$Log(q)$	Log of catchability coefficient (scaling factor relating 'true' biomass to the index of abundance	$Uniform$(-15,-1)
σ_p	Biological process error	$InvGamma$(2,1)
σ_o	Observation error in the CPUE index	$InvGamma$(2,1)

Table 2.4: Parameters specific to each of the four predation models

Model	Parameter	Definition	Prior/Value
Linear predation	ζ	Consumption of red sea urchins per otter	$Normal$(5,5)
Predation rate	α	Lotka-Volterra type predator prey interaction term	$Uniform$(1,10)
Predator satiation	q_{pred}	Sea otter catchability coefficient	$Normal$(5,5)
	S	Shape of predator satiation curve	$Normal$(0.7,0.7)
	U_{max}	Maximum prey density	9 (constant)
Predator functional response	F_{max}	Maximum percent sea urchins in otter diet	$Normal$(0.5,2)
	N_{half}	Urchin density at which otter diet percentage is at half of its maximum	$Uniform$(0,9)

Choice of Prior Parameter Distributions

Bayesian models can be sensitive to the choice of prior distributions. The priors used in our models reflect the degree of knowledge for each model parameter, and although many parameters were fit starting from extremely broad or "uninformative" prior distributions, other priors were based on findings from previous research. For many (but not all) of the parameters estimated, the posterior distributions departed significantly from these priors, suggesting that our data contain sufficient information for reasonable estimation of parameters. Here we briefly discuss the choices behind prior distributions for model parameters.

For the Pella-Tomlinson model, a minimally informative prior was chosen for carrying capacity (a normal distribution with mean and standard deviation equal to ten times the maximum recorded sea urchin catch), since we had no prior information on K. For the intrinsic growth rate r, we used a prior distribution based on another study of a red sea urchin population in Baja California[113]. The Pella-Tomlinson shape parameter p was normally distributed around the value (2) that would result in the simple logistic model, but with a large standard deviation since the shape of the sea urchin yield curve is not well-known. The catchability coefficient q was unknown and therefore its prior was an uniformative uniform distribution. The inverse gamma priors for process and observation error were also minimally informative.

Each separate predation model required priors for model-specific parameters. In Model 1, the normal prior distribution for ζ was broad, with its mean at the maximum annual estimated biomass of large urchins consumed by an adult male otter if 50 percent of the diet were composed of urchins (using the same calculation for caloric demand used in Model 4). In Model 2, the predation rate constant was unknown and was therefore fit

starting from a uniform prior distribution. For Model 3, q_pred is analogous to ζ and so the same reasoning was used for its prior. S describes the shape of the predator functional response curve, and its prior was normally distributed around a value of 0.7, which would produce a Holling Type II curve[99]. Finally, for Model 4, the maximum percent in the sea otter diet composed of sea urchins (F_max) was based on observed data from two sea otter foraging studies[93], [94], while the density at which the diet percentage was at half of its maximum (N_half) used a uniform prior distribution varying between zero and the maximum density ever observed at San Nicolas Island.

Key Model Parameter Fit Statistics

Each of the models below represents sea otter predation in a different way. We show each predation equation, followed by model fit statistics and posterior parameter distributions. Every model is fit in Stan[101] through Hamiltonian Markov Chain Monte Carlo[102]. Each model is fit with 3 chains of 4000 iterations each.

The model parameter tables below show mean, standard deviation, and the 2.5%, 50%,and 97.5% quantiles of the estimated posterior distribution for each key parameter in each model. Rhat and n_eff are Bayesian fit statistics. n_eff indicates the effective sample size for a given parameter, which is the number of independent draws from the posterior. The Rhat statistic is the Gelman and Rubin potential scale reduction statistic[114], and helps in determining whether the n_eff effective sample size is too low for reliable inference about a parameter. Across chains, Rhat measures whether the separate chains have reached a stable posterior distribution, despite being seeded at different initial values. Rhat should be less than 1.1[114].

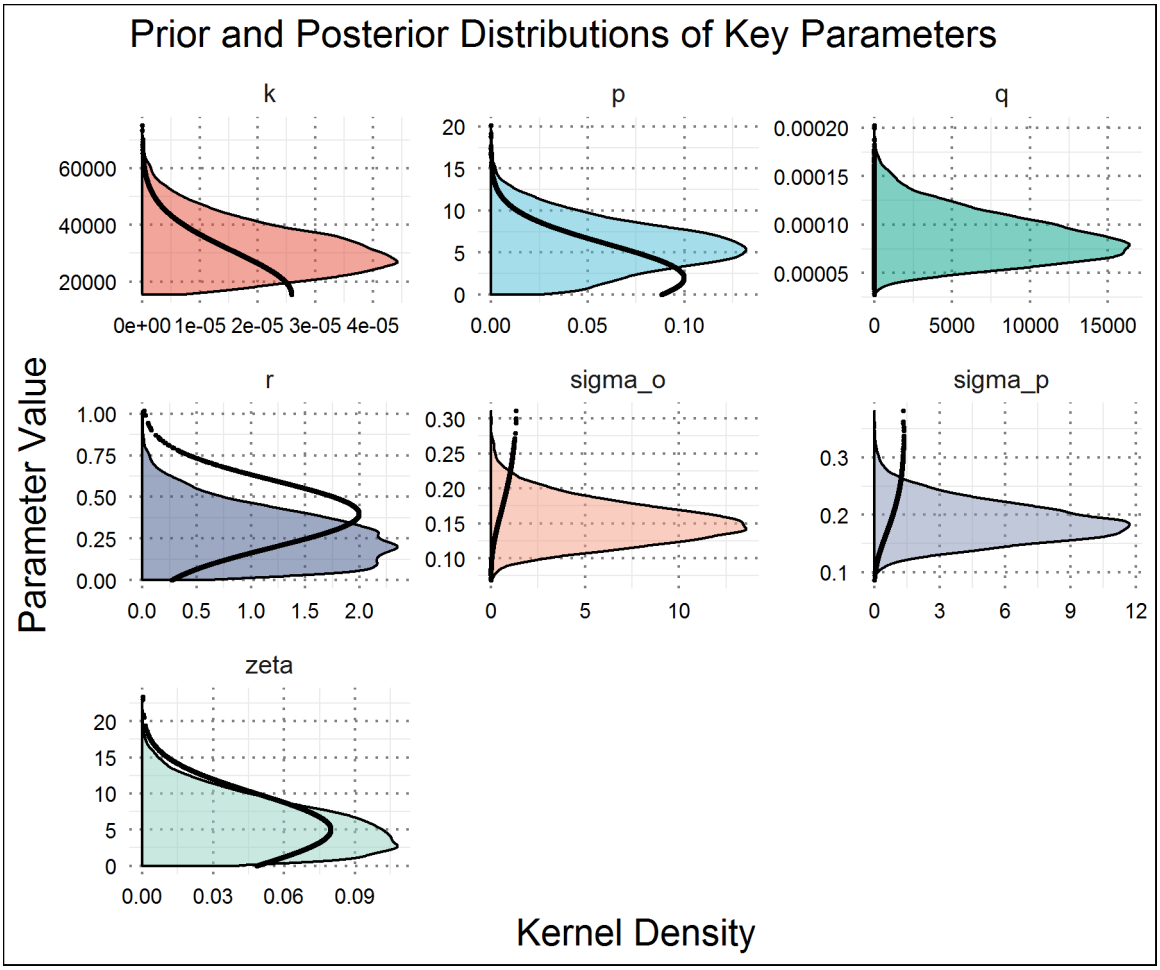

Figure 2.7: Model 1 prior and posterior parameter distributions. Prior distributions are shown in black lines, posterior distributions as the colored curves for each parameter.

Model 1: Linear Predation

$$B_{t+1} = B_t + Growth_t - Harvest_t - \zeta N_t$$

Model 2: Predation Rate

$$B_{t+1} = B_t + Growth_t - Harvest_t - \alpha N_t B_t$$

Table 2.5: Parameter fits for the linear predation model.

Parameter	Rhat	n_eff	mean	sd	2.5%	50%	97.5%
r	1.001	4424	0.261	0.158	0.027	0.244	0.609
K	1.001	4550	31647	9262	17214	30404	52830
q	1.002	2911	0.000	0.000	0.000	0.000	0.000
p	1.001	5381	5.748	2.988	0.496	5.599	12.028
ζ	1.000	6578	5.529	3.552	0.357	5.054	13.474

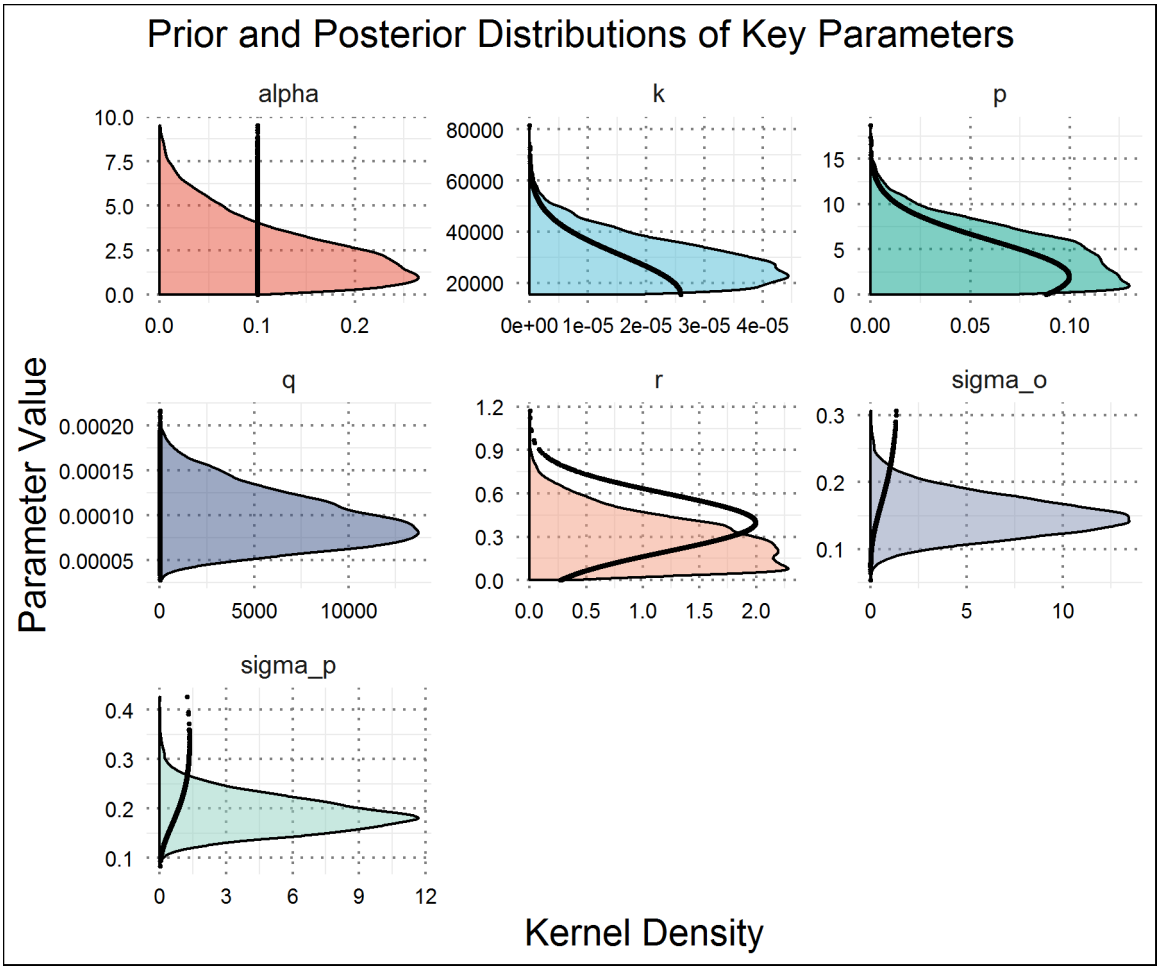

Figure 2.8: Model 2 prior and posterior parameter distributions. Prior distributions are shown in black lines, posterior distributions as the colored curves for each parameter.

Table 2.6: Parameter fits for the predation rate model.

Parameter	Rhat	n_eff	mean	sd	2.5%	50%	97.5%
r	1.000	3967	0.272	0.166	0.037	0.251	0.642
K	1.001	5354	28886	9134	16147	27509	49685
q	1.001	3935	0.000	0.000	0.000	0.000	0.000
p	1.001	3386	4.341	2.955	0.174	3.996	10.866
α	1.000	4335	2.363	1.692	0.127	2.039	6.404

Model 3: Predator Satiation

$$B_{t+1} = B_t + Growth_t - Harvest_t - q_{pred} N_t exp(-S(\frac{U_t}{U_{max}} - 1))$$

Note: U_{max} is set at 9 urchins per square meter, the 0.95 quantile of all observed urchin densities at San Nicolas Island (Kenner et al.2013).

Table 2.7: Parameter fits for the predator satiation model.

Parameter	Rhat	n_eff	mean	sd	2.5%	50%	97.5%
r	1.000	4241	0.265	0.161	0.026	0.247	0.615
K	1.000	3570	32275	9258	17690	31103	53071
q	1.000	2400	0.000	0.000	0.000	0.000	0.000
p	1.000	4307	5.512	2.943	0.464	5.395	11.687
q_{pred}	1.000	5409	4.450	3.226	0.207	3.805	12.149
S	1.000	8544	0.708	0.465	0.043	0.644	1.743

Model 4: Predator Functional Response

$$D_t = \frac{F_{max} U_t^H}{N_{half}^H + U_t^H}$$

$$B_{t+1} = B_t + Growth_t - Harvest_t - N_t D_{req} D_t$$

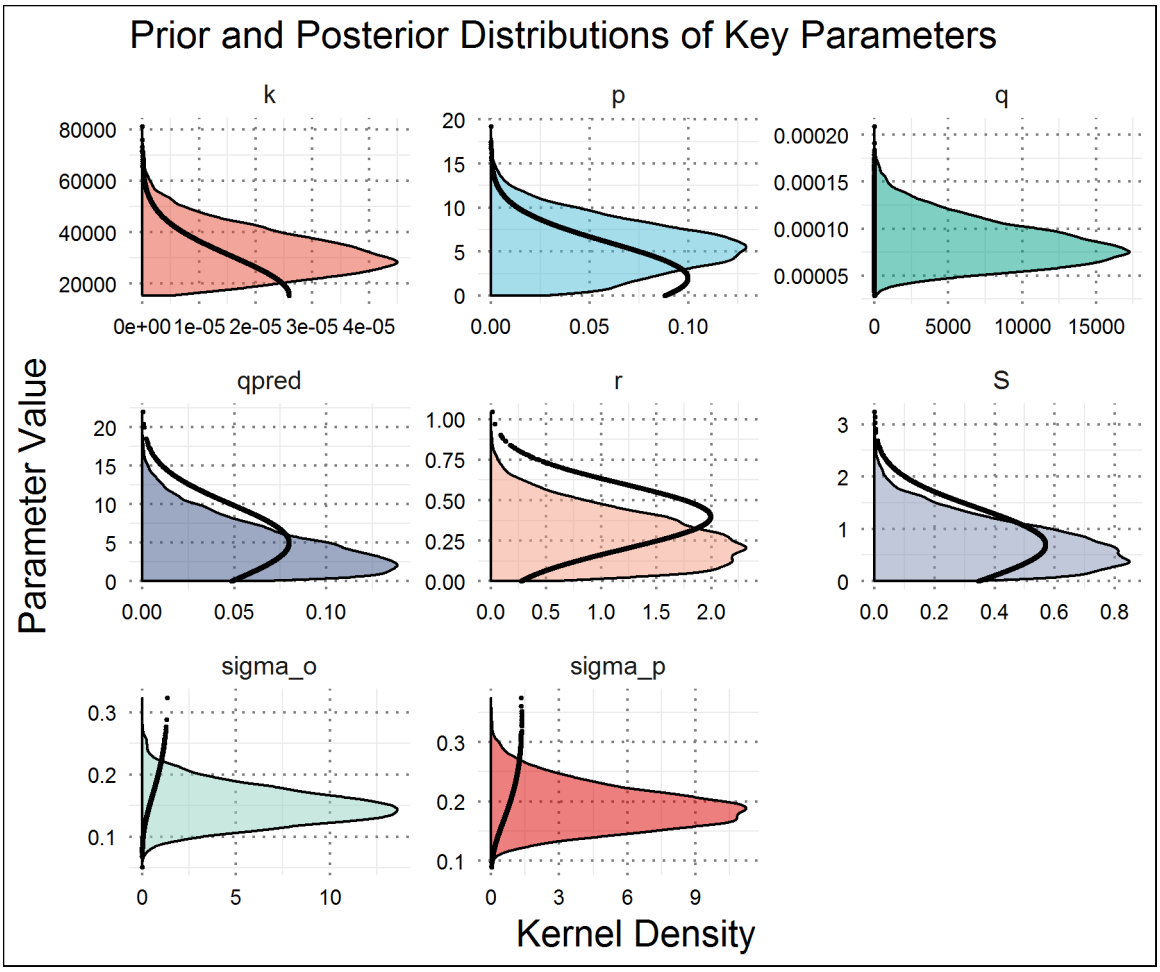

Figure 2.9: Model 3 prior and posterior parameter distributions. Prior distributions are shown in black lines, posterior distributions as the colored curves for each parameter.

Table 2.8: Parameter fits for the predator functional response model.

Parameter	Rhat	n_eff	mean	sd	2.5%	50%	97.5%
r	1.001	5716	0.250	0.156	0.019	0.233	0.587
K	1.000	6689	31646	8751	18192	30519	51752
q	1.001	4624	0.000	0.000	0.000	0.000	0.000
p	1.001	5895	6.042	2.926	0.669	5.949	12.123
F_{max}	1.003	1606	0.466	0.355	0.244	0.384	1.333
N_{half}	1.002	2073	0.959	0.981	0.131	0.707	3.817

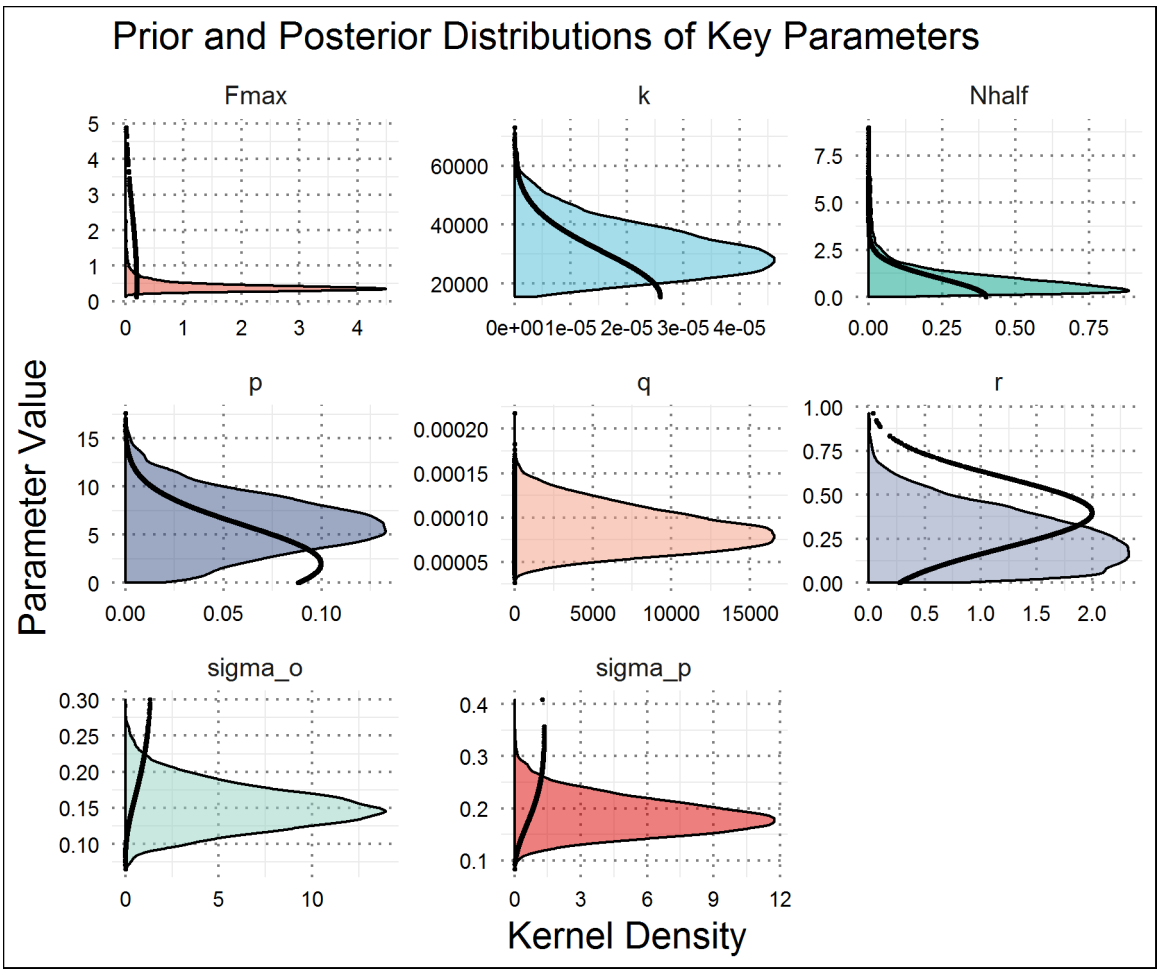

Figure 2.10: Model 4 prior and posterior parameter distributions. Prior distributions are shown in black lines, posterior distributions as the colored curves for each parameter.

Model Comparison Using Leave-one-out Log-likelihoods

We compare models using the log-likelihood of the observed catch-per-unit-effort index, I, given our estimates of catch-per-unit-effort $\hat{I}_t$ and observation error σ_o^2:

$$log(I_t) \sim Lognormal(log(\hat{I}_t), \sigma_o^2)$$

Using the `loo` package in R, we compare the models with leave-one-out cross-validation for Bayesian models using Pareto smoothed importance sampling[103]. The measure of predictive fit used to rank the models is from equation 4 in Vehtari et al. (2017)[103], called the "expected log predictive density":

$$elpd_{loo} = \sum_{t=1}^{n} logp(I_t|I_{-t})$$

where $p(I_t|I_{-t})$ is the leave-one-out predictive density given the data without the ith data point. In the table, elpd is the expected log predictive density and SE elpd is

Table 2.9: Model comparison using leave-one-out log-likelihoods of CPUE estimates

Model	elpd	SE elpd	Difference
Predator Satiation	9.158	3.709	0.000
Predation Rate	8.933	3.774	-0.225
Predator Functional Response	8.636	3.699	-0.522
Linear Predation	8.328	3.675	-0.830

the standard error of expected log predictive density. According to log likelihoods, the difference in model likelihoods is smaller than the scale of the standard error, signaling no strong support (in the likelihood context) for one model over the others.

Note: the lack of strong support for one model over any others was true as well for WAIC

(widely applicable information criterion) computed from the pointwise log-likelihood. One of the reasons for this is that the models do not differ immensely in their complexity (i.e., no one model has a much greater number of parameters than any other).

Chapter 3

Environmental Variability Drives Predation Risk: A Bering Sea Example

Abstract

Species interactions and environmental variability can impede effective ecosystem-based fishery management. Even in some of the most studied and valuable fisheries in the world, stock collapses or recovery failures have been attributed to some combinations of unanticipated species interactions and environmental changes. One important example of these complex dynamics is in the eastern Bering Sea, where Pacific cod (*Gadus macrocephalus*) are known predators of snow crab (*Chionoecetes opilio*). In this study, we use a multispecies, size-specific dynamic distribution model to uncover the major drivers of spatial and temporal variation in Pacific cod and snow crab distributions in the Bering Sea. We perform a spatial dynamic factor analysis, finding that average distributions of cod and

crab follow interpretable spatial patterns associated with bottom temperature and depth. But, their distributions across the eastern Bering Sea have also oscillated markedly from 1982 to the present, and the two species ordinate on the dominant spatio-temporal factors in divergent ways. This finding indicates that Pacific cod and snow crab populations respond differently to environmental fluctuations. Using modeled spatial abundance, we find that cod and crab distribution shifts in specific regions are significantly correlated with temperature anomalies. Moreover, there are strong, consistent negative correlations between abundances of the two species in some locations. We propose that in the eastern Bering Sea, environmental variability drives large-scale changes in Pacific cod and snow crab distributions, which in turn leads to variability in the overlap of their distributions and altered predation risk across years. Given the influence of temperature variability in this system, climate change will undoubtedly alter species distributions and interactions in this system. Models like those utilized here provide one way to understand and predict how complex spatio-temporal dynamics in marine systems may shift in the future.

Introduction

The goal of ecosystem-based fisheries management (EBFM) is to promote sustainable marine ecosystems and fisheries through consideration of interactions between humans and both biotic and abiotic elements of the natural environment. Although EBFM has been actively pursued for decades[115], [116], implementation has been a difficult goal to achieve[117]. One of the reasons for the slow adoption of EBFM is the technical difficulty inherent in trying to simultaneously account for the influences of species interactions and varying environmental conditions on species' abundances and distributions across space[118].

INTRODUCTION

Some fishery collapses or lack of recoveries have been attributed to a failure to account for species interactions[119], [120]. Importantly, omitting species interactions like predation from models of population dynamics may lead to an underestimation of uncertainty and perhaps to overly optimistic or risky management advice[99]. At the same time, environmental drivers act on these interacting species, influencing phenology, patterns of species movements, recruitment of new individuals into differen locations, and by extension, overall productivity[121], [122]. When environmental change drives greater spatial overlap between predators and prey, interactions will intensify and the relative influence of predation will strengthen[123]. In this way, environmental variability can determine patterns of species interactions.

Given that fishing pressure alone cannot explain widespread declines from historic abundances in many harvested species, many studies have attempted to attribute causation to species interactions or environmental change in addition to fishing pressure[124], [125]. One such fishery is the snow crab (*Chionoecetes opilio*) fishery in the eastern Bering Sea (EBS). The fishery for snow crab is one of the most valuable crustacean fisheries in the world, but has experienced marked fluctuations in stock size over the course of its exploitation history[126]. Production in the snow crab fishery peaked in the 1991, but landings declined by more than an order of magnitude from that point until to the early 2000s. In spite of conservative, scientifically-informed management measures since, the stock has remained at low levels relative to the past, and in 2016 the stock was estimated at its lowest point in the history of the fishery[127].

A number of hypotheses have been suggested to explain the fluctuations in the snow crab population in the EBS, including oceanographic and climate forcing[126], [128], [129]. Juvenile snow crab settlement has been correlated to the annual spatial extent of the "cold pool" across the middle portion of the shelf, an area with near-bottom

temperatures $< 2°C$ which is created by severe stratification of the water column as ice melts across a large portion of the Bering Sea in the spring[130], [131]. After warmer winters, the cold pool extent is reduced to the northwest, while after colder winters it can extend across a wide area of the shelf to the southeast. Moreover, after warm years as the snow crab population contracts to the northwest, the stock can have trouble recolonizing the southern portion of the shelf. Orensanz et al. (2004)[129] postulated that this is due to the fact that prevailing currents in the region flow in a northwesterly direction, preventing larvae from being advected "upstream" to other portions of the shelf, even after environmental conditions have returned to normal[132].

Predation by fish predators on juvenile snow crab may be another important driver of their spatial population dynamics[129], [133], [134]. Previous research suggests that the southern boundary of snow crab distribution in the Bering Sea is mediated by Pacific cod (*Gadus macrocephalus*) predation. Pacific cod in some years consume enormous amounts of juvenile snow crab, just as Atlantic cod predate on snow crab in eastern Canada[133], [135]. This effect of cod predation on snow crab mortality is size dependent for both species[134]; that is, the size of snow crab consumed by cod is dependent on both crab size and cod size. It has been suggested that this predation effect can interact with and exacerbate the cold pool effect on juvenile snow crab settlement[129]. Pacific cod distribution also responds to environmental variability. In warmer years the centroid of adult cod distribution moves to the northwest[128], although juvenile cod distribution is relatively stable across the EBS[136]. When snow crab distribution retracts to the northwest in warmer years, the expanded cod distribution may be an additional factor preventing the reexpansion of the snow crab stock towards the southeast.

In this study, we investigate the spatial distributions of snow crab and Pacific cod using spatial dynamic factor analysis applied to size-structured annual trawl survey data.

We examine the time period from the early 1980s to the present (2016), a time period characterized by large fluctuations in both crab and cod abundance. The hypothesis is that cod and crab will both respond to fluctuations in patterns relating to environmental drivers, specifically bottom temperature and depth. In addition, after constructing a spatio-temporal model of crab and cod distributions, we test whether cod abundance is significantly correlated with crab abundance in the EBS, which would indicate a potential predation effect. Given the previous research on Pacific cod diet, we expect that cod abundance will be significantly negatively associated with the abundance of small snow crab, but that this effect will depend on interannual changes in environmental conditions.

Data and Methods

Trawl survey data

To investigate the spatio-temporal patterns in Pacific cod and snow crab distributions, we use a joint dynamic species distribution model(JDSDM)[137]. JDSDMs estimate "factors" representing latent spatial and spatio-temporal patterns in observed data. We fit the model to fishery-independent bottom trawl survey data from the Gulf of Alaska. The survey, conducted each summer, enumerates all species caught in each of approximately 375 tows across a 20 by 20 nautical mile grid, providing an annual census of the Bering Sea demersal fish and invertebrate communities (full survey details can be found at https://www.fisheries.noaa.gov/resource/document/groundfish-bottom-trawl-survey-protocols). Along with the number and weight of species caught, the survey also records near-bottom temperature, depth, and area swept by the trawl. For both cod and crab, all individuals are sexed and measured by

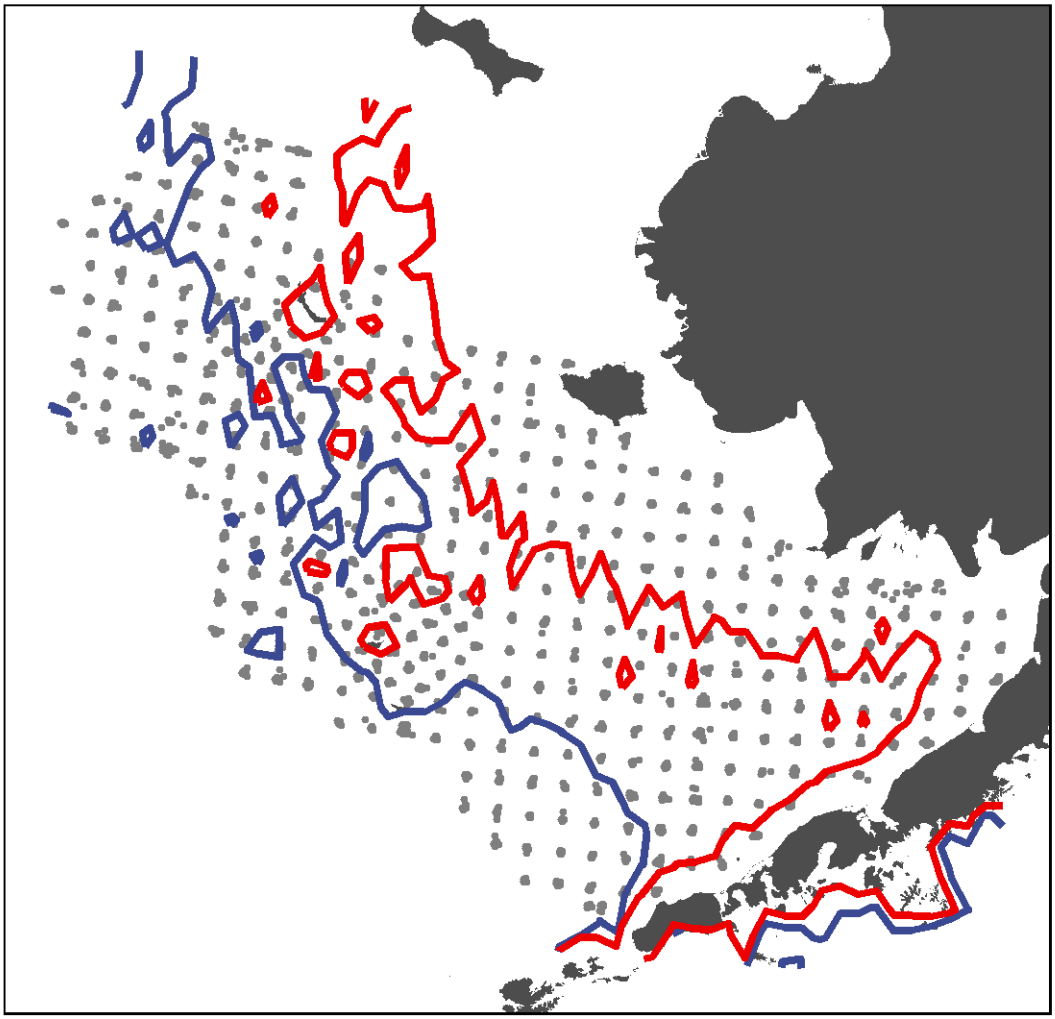

Figure 3.1: The study area in the eastern Bering Sea. Locations of trawl survey data points used to train the spatial dynamic factor analysis model are shown in gray. Bathymetric lines indicate the 50 and 100m depth contours, which broadly delineate the coastal, middle, and outer domains of the Bering Sea referred to in the text.

fork length (FL) for cod or carapace width (CW) for crabs. Additionally, the survey denotes crab maturity stage, enabling us to distinguish between immature and mature crabs.

From the survey data, we extract all observations of snow crab and cod, then sort them into size bins. For snow crab, we defined two classes: immature snow crab and mature female snow crab. Mature males were not included in the analysis as we were focused primarily on factors affecting the spawning stock of snow crab. We defined immature crabs as crabs of both sexes that were smaller than 58 mm CW and sexually immature. The 58 mm cutoff is based on a diet study that found that 95% of all crabs found in Pacific cod stomachs are smaller than 58mm. We define mature female crabs as any mature females, regardless of egg-carrying status or size. Size at maturity for snow crab varies with latitude and year, although in most regions and years, primipara (first-time female spawners) are larger than 50 mm CW[132].

For Pacific cod, we enumerate total abundance at each survey station for cod within three size classes. As with snow crab, our size classes were based on previous studies of cod predation, which found that cod containing snow crab in their stomachs were typically between 200 and 800 mm FL[133], [134]. We define small cod as those <200 mm FL, medium cod as between 200 and 800 mm, and large cod as larger than 800 mm. Therefore, with our definitions, we would expect a predation interaction between medium cod and immature snow crab. Size frequency distributions for all classes used in the model are shown in the Supplementary Information. In the following, we refer to the two crab and three cod categories in the data as "classes".

Temperature and depth are included as environmental covariates in the model described below. To ensure the environmental covariates matched the observed data as closely as possible, we extracted near-bottom temperature and depth directly from the survey itself,

and then used inverse-distance weighting to interpolate values between survey points.

Joint dynamic species distribution model

We implement the JDSDM through the publically available Vector Autoregressive Spatiotemporal R package `VAST`. VAST uses a delta-generalised linear mixed modeling method and takes into account spatio-temporal correlations among species (or size classes of one species, as in our model). A full description of the modeling framework can be found elsewhere[137], [138], but we describe the key equations here.

The JDSDM is a dimension-reduction technique that models response variables as a multivariate process where the predicted abundance of a class at a location is represented as the combination of two linear predictors: encounter rate (i.e., presence/absence of a class at a given location), and positive catch rate (i.e., the prediction of abundance given the presence of a class in a location). VAST estimates fixed and random effects for the two linear predictors that are each a function of an intercept, a spatial effect, a temporal effect, and any density covariates. In our model, bottom temperature and depth were used as density covariates. More specifically, the first linear predictor represents encounter rate for sample i as,

$$p_1(i) = \beta_1(c_i, t_i) + \sum_{f=1}^{n_{\omega 1}} L_{\omega 1}(c_i, f)\omega_1(s_i, f) + \sum_{f=1}^{n_{\epsilon 1}} L_{\epsilon}(c_i, f)\epsilon_1(s_i, f, t_i) + \sum_{p=1}^{n_p} \gamma_1(c_i, t_i, p)X(s_i, t_i, p) \tag{3.1}$$

where p_i is the linear predictor for encounter rate, $\beta_1(c_i, t_i)$ is the intercept term in year t for class c, the terms starting with L_ω and L_ϵ are the spatial and spatio-temporal factor models, respectively, and X is the matrix of density covariates defined for each location s, time t and covariate p that have linear effects γ on the predictor. In the factor model terms, $L\omega$ and L_ϵ are loading matrices relating the classes to each of f factors, and $\omega(s, f)$

and $\epsilon(s, f, t)$ are vectors of random effects representing latent spatial and spatio-temporal variation at each location. VAST models average spatial variation ω as being constant across years, while spatio-temporal variation ϵ varies among years. The second linear predictor, representing positive abundance, has an analogous formulation.

We use a log-link to transform both linear predictors to predict the observed data (see 138 for all model equations):

$$r_1(i) = 1 - exp(-a_i \times exp(p_1(i)))r_2(i) = \frac{a_i \times exp(p_1(i))}{r_1(i) \times exp(p_2(i))} \tag{3.2}$$

where a_i is the area associated with sample i in the survey. Positive abundance is modeled with a gamma distribution.

An important feature of VAST is that it accounts for spatial autocorrelation, or the fact that values nearby in space tend to be more similar than locations further away. Each spatial (ω) and spatio-temporal (ϵ) factor in both linear predictors is represented as Gaussian random fields, where the covariance between nearby locations is approximated with a Matern correlation function[139] through the R-INLA software[140]. The correlation function follows geometric anisotropy, where the rate of decline in correlation between locations can be different in different directions (i.e., correlation can decline more rapidly in the east-west than the north-south direction).

Parameter estimation for VAST is accomplished through Laplace approximation of the marginal likelihood for fixed effects while integrating across the random effects using the Template Model Builder software[141]. The model requires the estimation of 87 fixed effects and 25752 random effects. For this study, we are primarily interested in the spatial and spatio-temporal factors, and how the five classes in our study relate to those factors, represented by the factor loadings matrices. We estimated three spatial and

three spatio-temporal factors for both linear predictors, while including temperature and depth as covariates. As derived quantities, VAST can also calculate each class' spatial abundance-weighted center of gravity and effective area occupied within the EBS, as well as an overall (non-spatial) index of abundance. We use these derived quantities to further explore the spatial and temporal dynamics of snow crab and cod.

Results

Dominant spatial and spatio-temporal patterns

The estimated spatial and spatio-temporal factors represent latent (unobserved) spatial variables or patterns that underlie the observed spatial trends in species abundances. The intuition is that the collection of time series—in our case, the time series of cod and crab abundances at each survey station across years—can be represented in a reduced number of dimensions through the identification of common spatial patterns. These patterns are called latent factors and can be thought of as representing unmeasured environmental drivers of processes that drive a degree of synchronization of the time series. Each individual time series can then be represented as a linear combination of the factors, which is precisely what is shown in equation (3.1). The goal of the analysis is to identify this reduced set of spatial patterns in the data in order to explore how the patterns relate to known environmental drivers.

We estimate three factors for spatial and spatio-temporal variation in the five classes (two snow crab and three Pacific cod classes). To visualize the factors, we estimate all spatial values within 100 distinct spatial regions across the EBS, analytically chosen to minimize the average distance between those locations and the available data. There are

clear, interpretable patterns apparent in the average spatial variation of cod and crab. These patterns manifest in both the northeast-to-southwest dimension (the longer axis), and the cross-shelf or shorter axis of the EBS. Figure 3.2 shows the spatial distribution of the first two factors describing presence/absence and positive abundance. The first factors for both encounter rate and positive abundance (panels a and c of Figure 3.2) have negative values in the southeast towards Bristol Bay, increasing to positive values with greater depth and latitude. The second factors for encounter rate and positive abundance show slightly different patterns. For encounter rate, positive values clearly delineate the mid-depth band of the EBS. It is strongly and significantly associated with lower temperatures (Pearson's ρ -0.51), picking up the signal of the EBS cold pool. The second factor for positive abundance shows a transverse pattern across the shelf from northeast to southwest, and is also significantly associated with temperature (ρ 0.47). Figure 3.2 shows the main static patterns in size-structured cod and crab distributions in the EBS, but we can also investigate the major patterns in species distributions over time through the estimation of spatio-temporal factors, i.e. the $\epsilon(s, f, t)$ terms in equation (3.1). These latent spatio-temporal factors are important in describing interannual variation in species distributions, but display complex temporal patterns. For example, consider Figure 3.3 that shows the values of the first spatio-temporal factor for positive abundance (i.e., abundance given the presence of a class at a location). In many years, much of the factor is near zero, with occasional strong spatial signals in specific areas of the EBS. For example, in 1983 and 1999, the factor displays strong negative values in the Bristol Bay and southeastern coastal areas, while in 1985 and 2012 there are strong positive values in the northern coastal portion of the study area.

The variation apparent in Figure 3.3 is not clearly associated with near-bottom temperature anomalies across the study period. The average spatial values of the factor in each

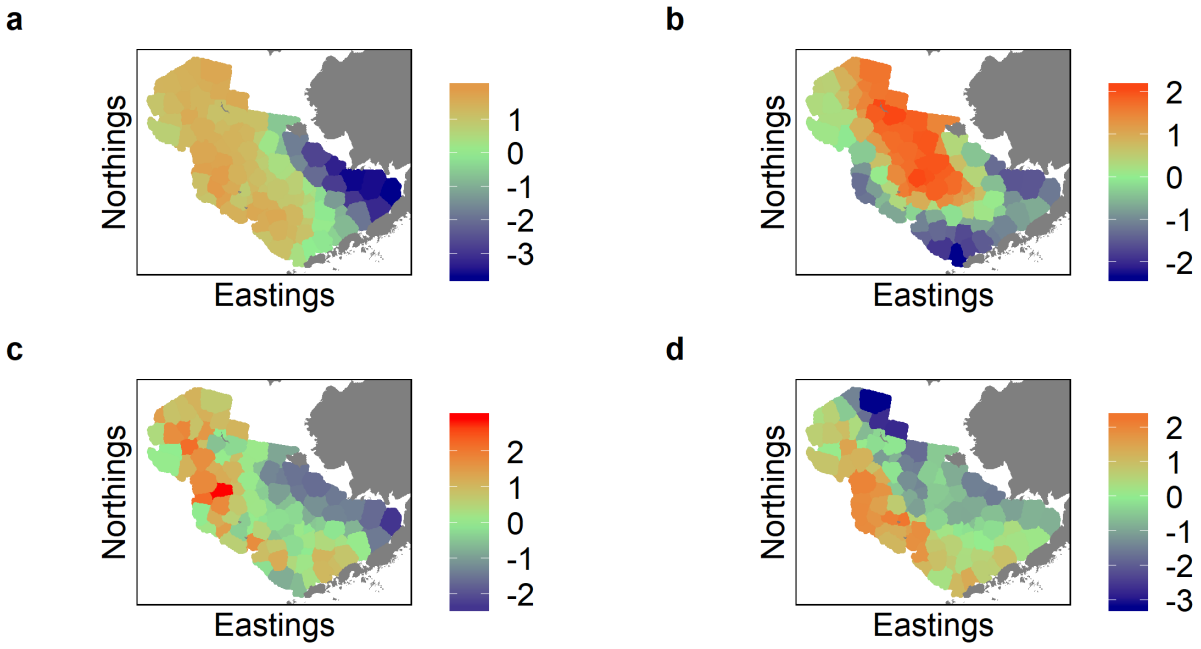

Figure 3.2: The first two spatial factors describing encounter rate (presence or absence, panels a and b) and positive abundance (panels c and d) of snow crab and Pacific cod in the EBS. Panels a and c are the first factor of encounter rate and positive abundance, respectively, and panels b and d are the second factors. Warmer colors represent positive values of the factor, while cool colors represent negative values.

location across years are not signficantly correlated with average temperature anomaly (p>0.05), and while in certain years the relatoinship between the factor and temperature is significant, some of these correlations are positive and others are negative. It is likely, therefore, that the spatio-temporal factors represent the combined influence of a number of temporally-varying environmental and predation processes and are therefore difficult to interpret through any single environmental variable. Maps of all three factors for all four linear predictors are shown in the Supplementary Information.

Species associations with spatial and spatio-temporal factors

Figures 3.2 and 3.3 show some of the major patterns in cod and crab distributions across the EBS, but to explore how each species associates with these patterns, we investigate the factor loading matrices L_ω and L_ϵ. Figure 3.4 shows the loadings of each species on to the three factors for each linear predictor. The first two factors for average spatial variation explain 85.1% and 88.2%, respectively of the between-class variance in encounter rates and positive abundance (the left two columns of Figure 3.4). Snow crab and cod show opposite relationships to the first spatial factor for both encounter rate and positive abundance. Snow crab, and mature females in particular, are strongly positively associated with the first factor, while small cod are negatively associated and medium and large cod have smaller loadings. The encounter probabilities of snow crab and small cod are positively associated with the second factor for average spatial variation in encounter probability, while all classes except immature crabs are positively associated with the second factor for variation in positive abundance.

The right two columns of Figure 3.4 show how the presence and abundance of each class is related to annually-varying factors. Together, the first and second factors describing spatio-temporal variation in encounter rates explained 84.8% of between-species

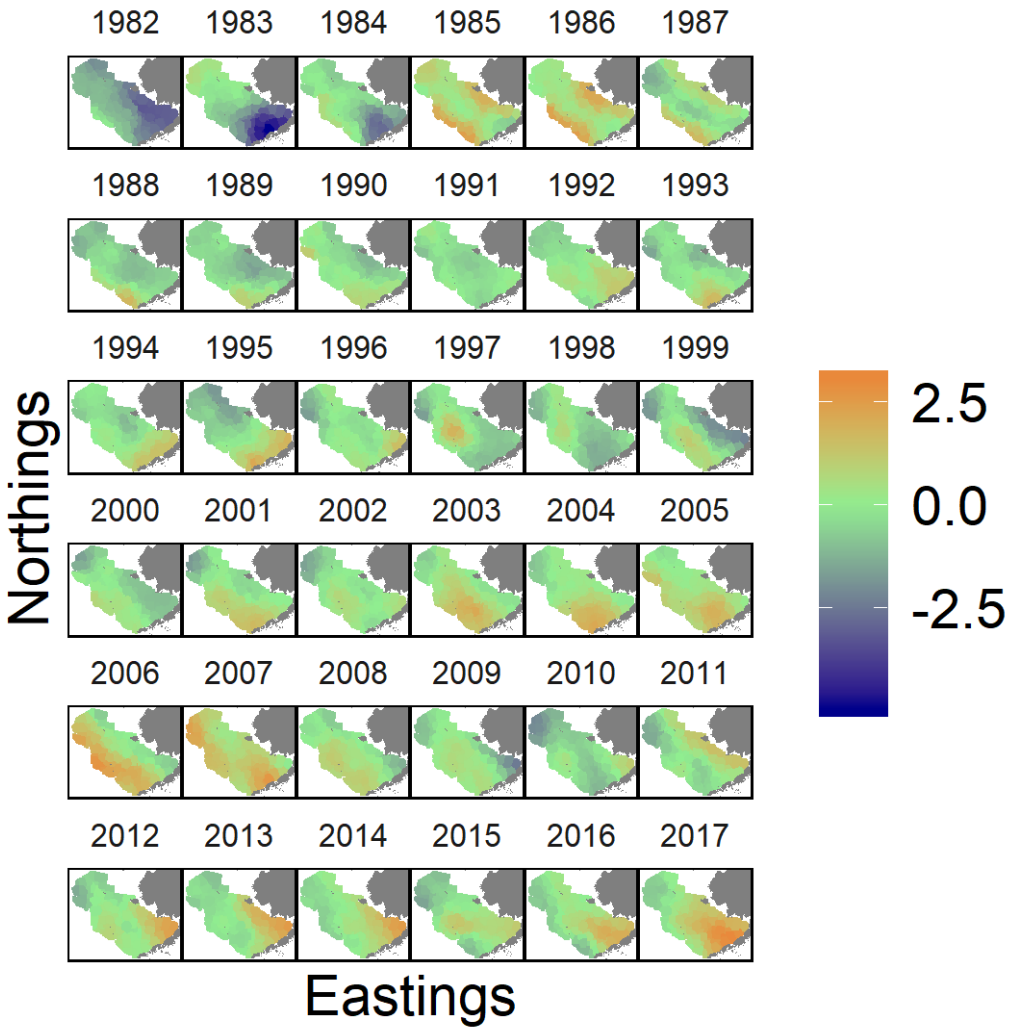

Figure 3.3: Values of the first spatio-temporal factor for encounter probability in each year in the study. Warmer colors represent positive values of the factor, while cooler colors represent negative values.

variance. The first factor shows clear differences between species, where snow crab are negatively associated and Pacific cod positively associated. Conversely, crab and large cod are positively associated with the second factor, while small cod is negatively associated. Finally, the first factor describing spatio-temporal variation in positive abundance primarily represents the distributions of the two crab classes. The second factor for spatio-temporal variation in positive abundance separates the two crab classes, where the positive abundance of immature crabs is negatively associated and the abundance of spawners positively associated. The third factor in all four linear predictors show more positive associations across all classes, but explains a much smaller proportion of overall variance in cod and crab distributions. However, the third factor seems to be where much of the variance in the distribution of medium-sized cod is contained—the highest loading of medium cod on to any factor is for the third factor of spatio-temporal variation in positive abundance. Figure 3.4 suggests that for the most part, crab and cod associate in divergent ways to the spatial and spatio-temporal patterns described above. The separation between species is more clearly evident when plotted in two-dimensional space. For instance, Figure 3.5 shows the first two factors describing spatio-temporal variation in the positive abundance of all five classes in the study. Clearly, the two species are distinguished along the first factor, while the second factor segregates immature from mature crabs. Medium and large cod have little relationship to either factor, but small cod is associated positively with both factors. Comparing factor loadings (Figures 3.4 and 3.5) to factor maps (Figures 3.2 and 3.3) gives a view of the major patterns across species' distributions. For example, the average encounter probability for immature snow crab is described well by the first factor (panel (a) in Figure 3.2), showing that on average, immature crabs are more likely to be found towards the northern section of the EBS, and much less likely to occur in the Bristol Bay region. At the same time, we know from Figures 3.4 and 3.5 that distributional change over time in the same class is

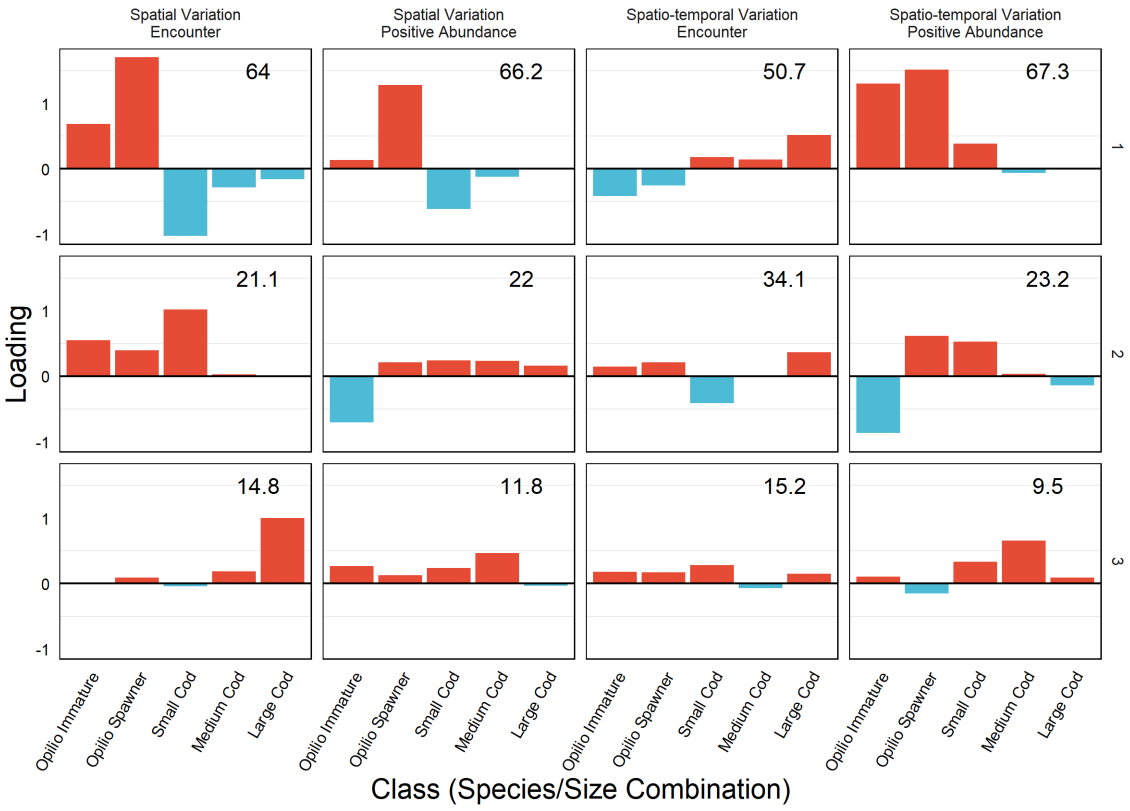

Figure 3.4: Factor loadings for each class (bars), linear predictor (columns) and factor (rows), where positive loadings are shown in red and negative loadings in blue. Numbers in the upper right corner indicate the overall between-class variance explained by each factor. The five classes are small immature snow crab (Opilio Immature), spawner snow crab (Opilio Spawner), and small (<200mm FL), medium (between 200 and 400mm), and large (>800mm) Pacific cod.

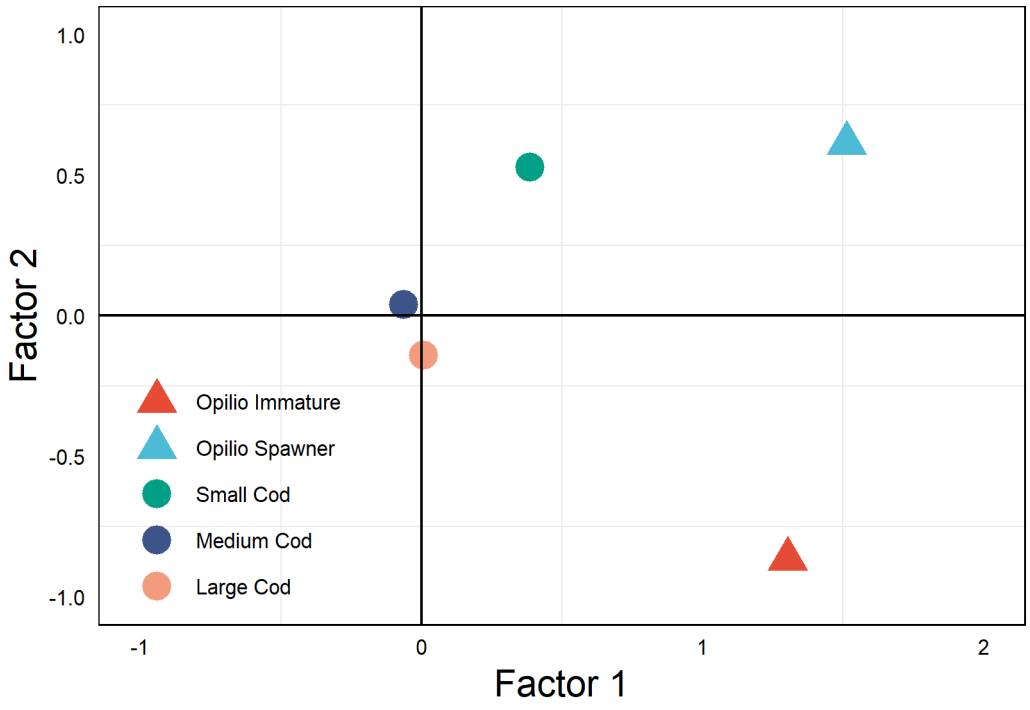

Figure 3.5: Loadings of all classes on to the first two factors for spatio-temporal variation in positive abundance. Triangles indicate snow crab classes and circles indicate cod classes.

well-described by the first spatio-temporal factor for positive abundance, which is seen in Figure 3.12. The map of this factor clearly represents the major changes in juvenile snow crab stock. Especially apparent is the depressed abundance throughout the southern and middle regions of the EBS from the mid-1990s until at least 2005. Moreover, these spatial and spatio-temporal patterns are more similar within than across species, showing that these two species likely to not track each other's distributions, but rather are each independently responding to environmental changes, which subsequently leads to greater or lesser overlap in specific years and locations.

Species center-of-gravity

Together, the factors describing the variations in distribution of cod and crab across the EBS result in predictions of their abundances across space. Predicted total abundance in any location is simply the product of encounter rate and positive abundance and is produced as a derived quantity in our analysis. Along the same lines, we can derive measures of the abundance-weighted center of gravity of each class to explore how that center has varied over time, as well as an overall non-spatial index of stock abundance. Although we can map species distributions across space and time (see predicted abundance plot for immature snow crab in the Supplementary Information), the important general trends in species distributions are apparent in their centers-of-gravity. In Figure 3.6, it is clear that in general, the bulk of snow crab abundance is centered towards the north and west, while small cod occur in the south and east (Bristol Bay). The center of larger-sized abundances of both species occur towards further to the south and west than their smaller counterparts, more towards the middle and outer portions of the EBS shelf. There have also been major changes in these species and size-specific centers of gravity over time. In particular, the north-south fluctuations in the snow crab distribution are

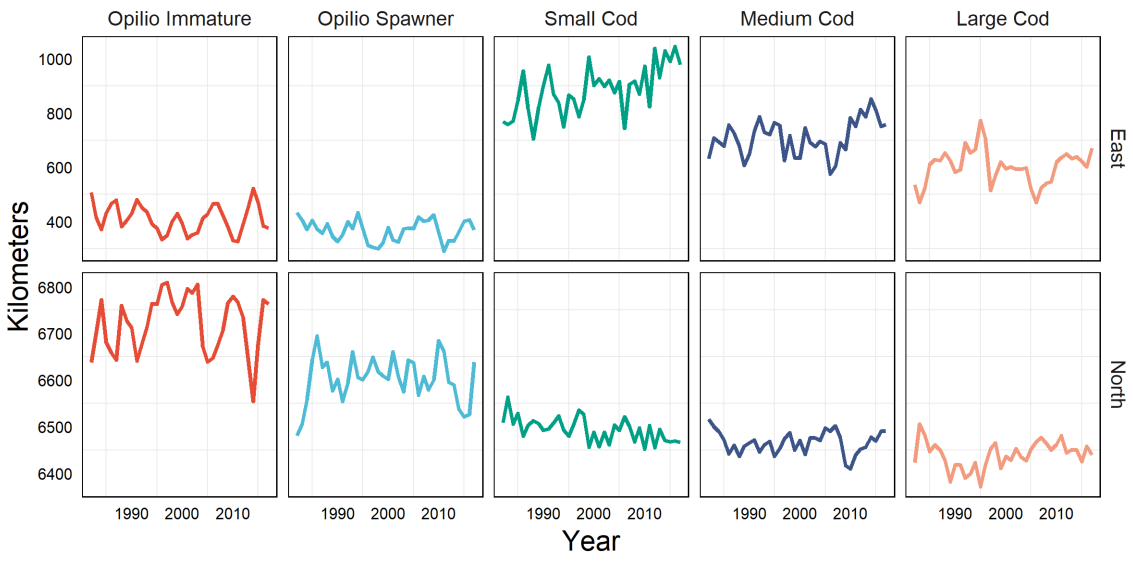

Figure 3.6: Eastward (top row) and northward (bottom row) components of abundance-weighted center of gravity for each class (columns) across the study period.

clearly evident, with a rapid northward shift in the juvenile distribution of approximately 150 km from the mid-1990s to the mid-2000s. This could be due to strong crab recruitment pulses pulling the center of gravity northward, but this is also the period of severely depressed landings in the snow crab fishery. In more recent years, a strong shift in cod distribution is apparent, with the distribution of small cod retreating to the south and east over time. Since the mid-2000s, the distributions of medium and large cod have also shifted east and towards the inner or coastal domain of the EBS.

Relationships between abundance and temperature

Lastly, we can use the derived abundances of each class to explore significant relationships among species abundances and between species abundances and environmental variables. We find no strong correlations—positive or negative—between overall abundances of classes, when we combine data across all locations (Figure 3.7a). This is

contrary to our hypothesis that immature snow crab and medium-sized cod abundances should be negatively correlated. In fact, they show a significant positive, if small, correlation, suggesting that cod may be tracking crab abundance. However, when we separate correlation estimates across space, a clearer picture begins to emerge. Figure 3.7b shows the correlation between medium cod and immature crab abundance, calculated across years but separately for each spatial location. Medium cod and immature crab abundance are strongly negatively correlated in Bristol Bay and in the coastal domain of the EBS (throughout much of the core distribution area of cod), but not significantly correlated in the rest of the study area except for small pockets in the middle and far northwest domains of the study area. Although the negative correlation between the two species is strongest in Bristol Bay, this is an area where snow crab almost never occur in the survey, so the pattern in Bristol Bay may be due more to inhospitable environmental conditions than cod predation. However, the negative correlation between medium cod and immature crab abundance along the edge of the middle domain suggests that predation may be an important factor driving snow crab dynamics in that area. But we know from the factor analysis that both species are responding to other environmental cues as well, which may alter predation risk for snow crab in different years. Figure 3.7c provides further evidence that immature crab distribution responds to temperature. In a broad region of the southeast shelf, immature snow crab abundance is strongly negatively correlated with annual temperature anomalies; in other words, when temperatures are warmer in these areas, crab abundance seems to decline, due either to distributional change or direct mortality. Significant negative correlations between immature crab abundance and temperature anomalies are also found in select other areas of the study area, one area notably around St. Matthew Island, the remote island towards the north of the EBS. Medium cod distribution has an even more striking spatial relationship with temperature anomalies (Figure 3.7d). Abundance of medium-sized cod is strongly positively related

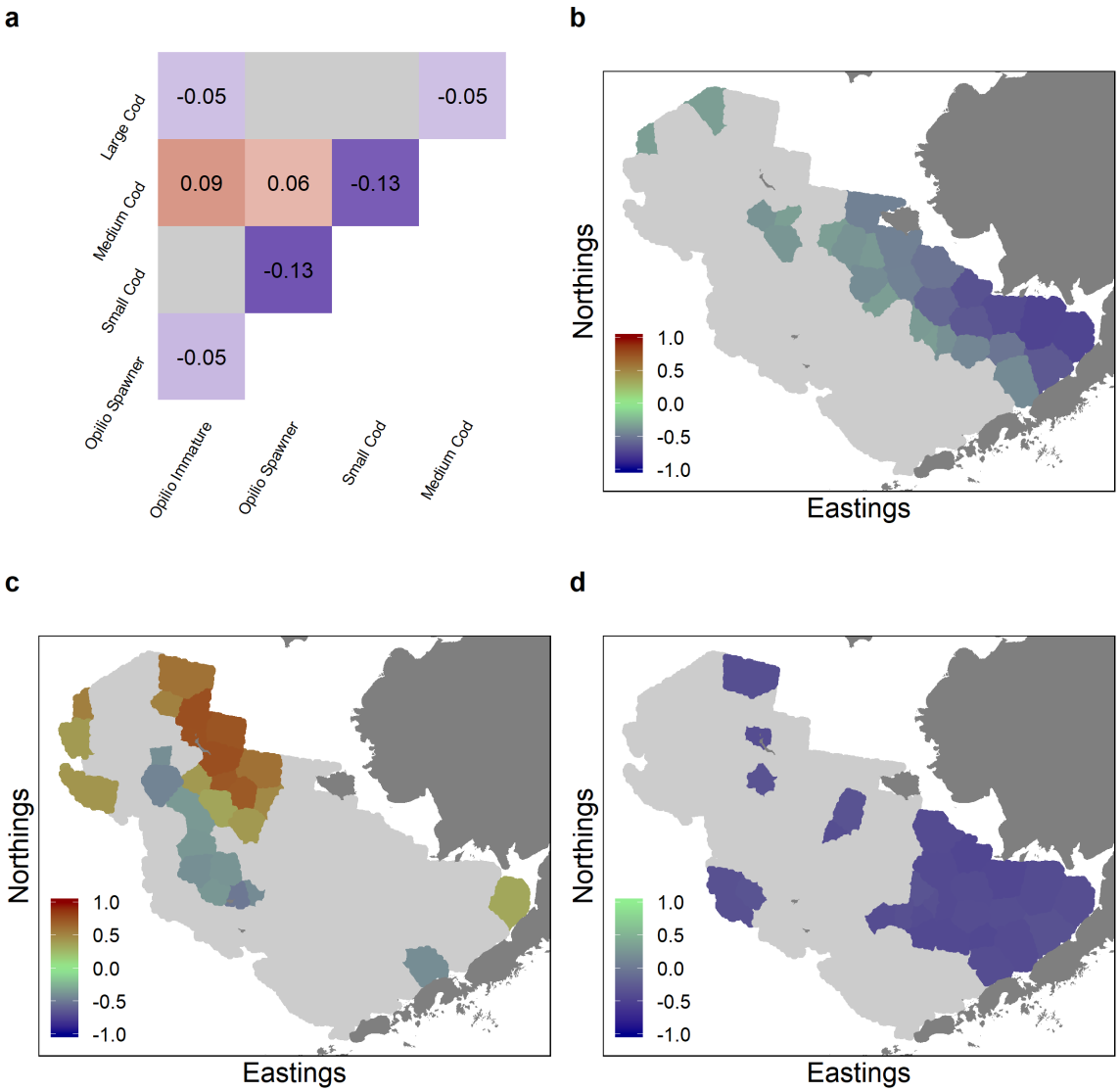

Figure 3.7: Correlations between species abundances and between abundances and temperature anomalies. In all panels, cool colors indicate negative correlations, while warm colors indicate positive correlations and gray indicates non-significant correlation. (a)Correlations in predicted abundances of all species across all locations. (b)Spatial correlations between predicted abundances of medium-sized cod and immature snow crab. (c)Spatial correlations between immature snow crab and annual near-bottom temperature anomalies. (d)Spatial correlations between medium-sized cod and annual near-bottom temperature anomalies.

with years of elevated temperatures in the far north region of the EBS, most strongly right around St. Matthew Island. Conversely, cod abundance is negatively associated with temperature anomalies in the middle domain of the shelf, offshore and southwest of St. Matthew.

Discussion

Ecosystem-based fishery management requires sorting through the influences of environmental drivers and species interactions on the distributions and dynamics of harvested resources. Increasingly, scientists and practitioners are contending with the realities of complex managed ecosystems that require the use of dynamic tools and adaptive management[116]. The complexity introduced by interacting, spatially-structured marine populations can confound even the most scientifically-advanced and well-managed fisheries in the world, such as those in the Bering Sea. Models that can take advantage of spatio-temporal data to uncover drivers of fluctuations in species distributions and abundance over space and time are key ingredients for appropriate management.

We used a spatial dynamic factor model to delineate the major spatial and spatio-temporal patterns in the size-structured distributions of snow crab and Pacific cod in the Eastern Bering Sea. Both species are targets of large, profitable fisheries in one of the most productive marine ecosystems in the world. Previous studies have described how each species seems to respond to environmental variability, specifically bottom temperature[136], [142], and how their distributions may be altered as a result[126], [131]. Moreover, there is ample evidence from stomach content analyses that Pacific cod predation may be an important determinant of snow crab distribution in certain places and times[128], [133], [134]. We sought in this study to integrate these lines of inquiry by

uncovering whether snow crab and Pacific cod have predictable distributions across the EBS, describing coherent patterns in how those distributions have shifted across time, and assessing the places and conditions under which we would expect cod to pose a significant predation risk to snow crab.

Our dynamic species distribution model encompassed five species/size classes that included snow crab predicted to be vulnerable to Pacific cod predation (immature crabs smaller than 58mm CW), and cod of the appropriate size to consume those crabs (cod between 200 and 800mm FL). The model estimated the presence/absence and positive abundance separately for both average spatial distributions and spatio-temporal variability (changes in the distributions through time) through a dynamic factor analysis.

The resulting spatial and spatio-temporal factors reveal cohesive patterns in crab and cod distributions in the EBS. The primary factors for average spatial distributions of both species revealed variation along both the northwest-to-southeast and east-to-west axes of the EBS, and were significantly related to temperature and depth gradients. In addition, and in agreement with other work[126], [129], the loadings of each class on to these spatial factors reveal that cod and crab ordinate in opposite ways to those environmental gradients. While snow crab are primarily associated with the colder, more northerly sections of the middle and outer domains of the EBS, Pacific cod occur towards the southeast and Bristol Bay regions. The estimated spatio-temporal factor loadings suggest further that cod and crab may respond to interannual environmental fluctuations in opposite ways. Although the spatio-temporal factors themselves did not seem to be strongly related to near-bottom temperature anomalies, this finding implies that a suite of environmental drivers (including but not limited to temperature) determine the conditions under which to expect greater overlap between the distributions of snow crab and Pacific cod. The intuition from the combined spatial and spatio-temporal factor

analysis is that there is a spatial push-and-pull dynamic between the distributions of the two species, driven by the environment: in years and locations where cod extends from its average distribution, we would expect a corresponding contraction in the snow crab distribution, and vice versa.

The center-of-gravity and spatial abundance analyses allowed us to explore more specifically how cod and crab distributions have shifted over time. The model recovered major events that are known to have occurred in these two stocks, especially the severe contraction of snow crab distribution to the far north of the EBS from the mid-1990s to the mid-2000s, and the contraction of cod to the southeast in recent years. These fluctuations correspond broadly with trends in estimated abundance from official stock assessments[127], [143]. Currently, the snow crab population is below its biological fishery reference points, and the Pacific cod stock is close to being overfished and recently observed one of the smallest recruitment events in the time series.

Together, the available lines of evidence suggest that when environmental conditions are optimal for crab, they are sub-optimal for Pacific cod. Our observation of large fluctuations (on the order of hundreds of km) in the distribution centers of the two species over time implies—though does not prove—that the two species respond on large scales to the environment, and that interaction between the two species may be important only in specific places and times. This is contrary to our original expectation to find clear, significant negative covariance between cod and crab that would be suggestive of an important interaction. Others have stressed the importance of Pacific cod predation as a primary determinant of snow crab natural mortality[133] and documented fluctuations in cod predation that track crab recruitment pulses, but in general have found no overall strong correlations between Pacific cod and crab abundance[134]. We confirmed this lack of a strong non-spatial correlation across the entire study area. However, when

we segregrated the data by location, we found spatially-explicit negative correlations in cod and crab abundance in some locations along the coastal and southern middle-depth domains of the EBS. We found that these apparent interactions may be linked to interannual near-bottom temperature anomalies: in warm years, cod abundance shifts to the north and may increase predation mortality for snow crab in the far northern part of the middle domain. Hence, cod predation seems to be a spatially-constrained driver of snow crab dynamics, but in years with positive temperature anomalies, the spatial footprint of cod predation risk could expand towards the centroid of snow crab abundance. This finding contextualizes and extends the hypothesis originally stated by Orensanz et al. (2004) that Pacific cod may "chop off" the southern distribution of snow crab in the EBS.

Although the findings of the study suggest a substantial degree of nuance in the interannual spatial distribution shifts of Pacific cod and snow crab, they nevertheless provide important insights for management. Our findings support the hypothesis that it is interannual environmental shifts, not predation *per se* that drives changes in snow crab distributions. The distribution shifts in snow crab can happen rapidly, and it is important for managers to be able to predict these shifts to make better estimations of overall abundance in the stock. Our analysis indicates that to make these predictions, it is more important to focus on predicting changes in bottom-up environmental forcings rather than top-down predation. Near-bottom temperature changes drive changes in the distributions of both species, which in turn drive spatial patterns of predation.

Extensions of our work could use a process-based model to account for movement and better characterize cod predation risk. The most important finding from this study is that temperature and predation likely interact in complex ways as combined drivers to affect crab distribution at specific places in specific years. Although we have delineated

interpretable spatial patterns in this species-environment interaction, we cannot definitively state the absolute effect of Pacific cod on snow crab in the EBS. Nevertheless, we can confidently propose that temperature is a strong driver of distribution, with predation becoming increasingly important only when environmental conditions are right. An interesting future area of study would be to investigate bottom-up control of snow crab prey on Pacific cod productivity (i.e., the inverse of the predation effect on snow crab investigated here). Given that both fisheries are currently experiencing low abundance, it is important to consider bi-directional effects of the species interaction and its implications for fishery rebuilding.

Given the significant patterns associated with temperature found in our study, it is clear that future climate change in the Bering Sea will alter species distributions in the region and determine the future potential for interactions between Pacific cod and snow crab. Joint dynamic species distribution models similar to ours can be used to forecast distribution change while potentially accounting for interactions and the directional influences of climate change[144]. Moving forward with adaptive, ecosystem-based fishery management will require this type of model to understand and predict how the distribution and abundance of valuable managed resources may change in response to both climate and predation.

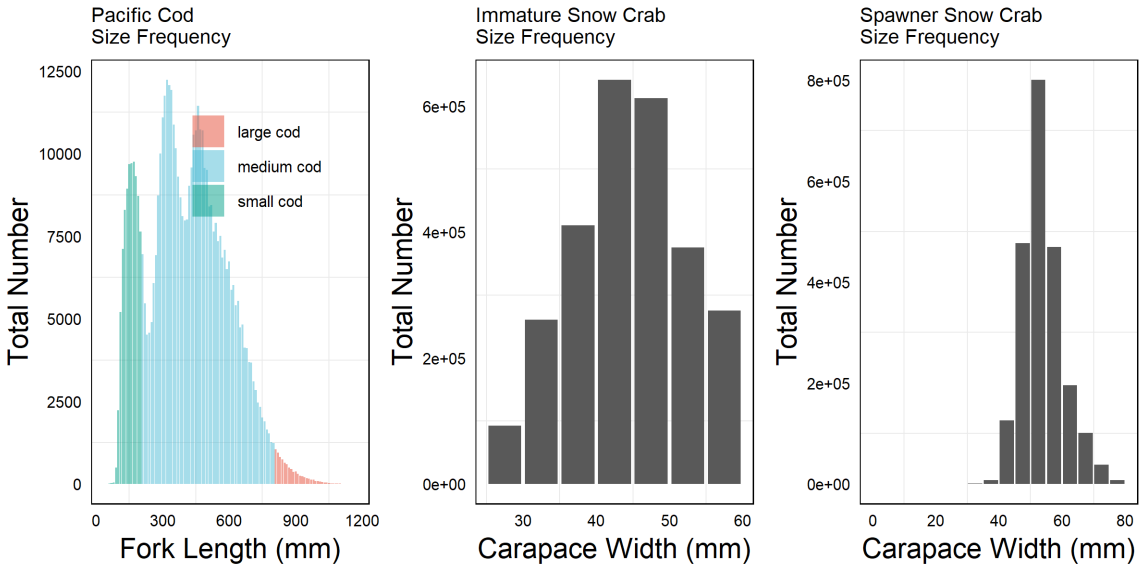

Figure 3.8: Size-frequency distributions for the five classes included in the model, including all observations (n=103,550 observations)

Supplementary Information

Size-frequency

Maps of spatial and spatio-temporal factors

Predicted density

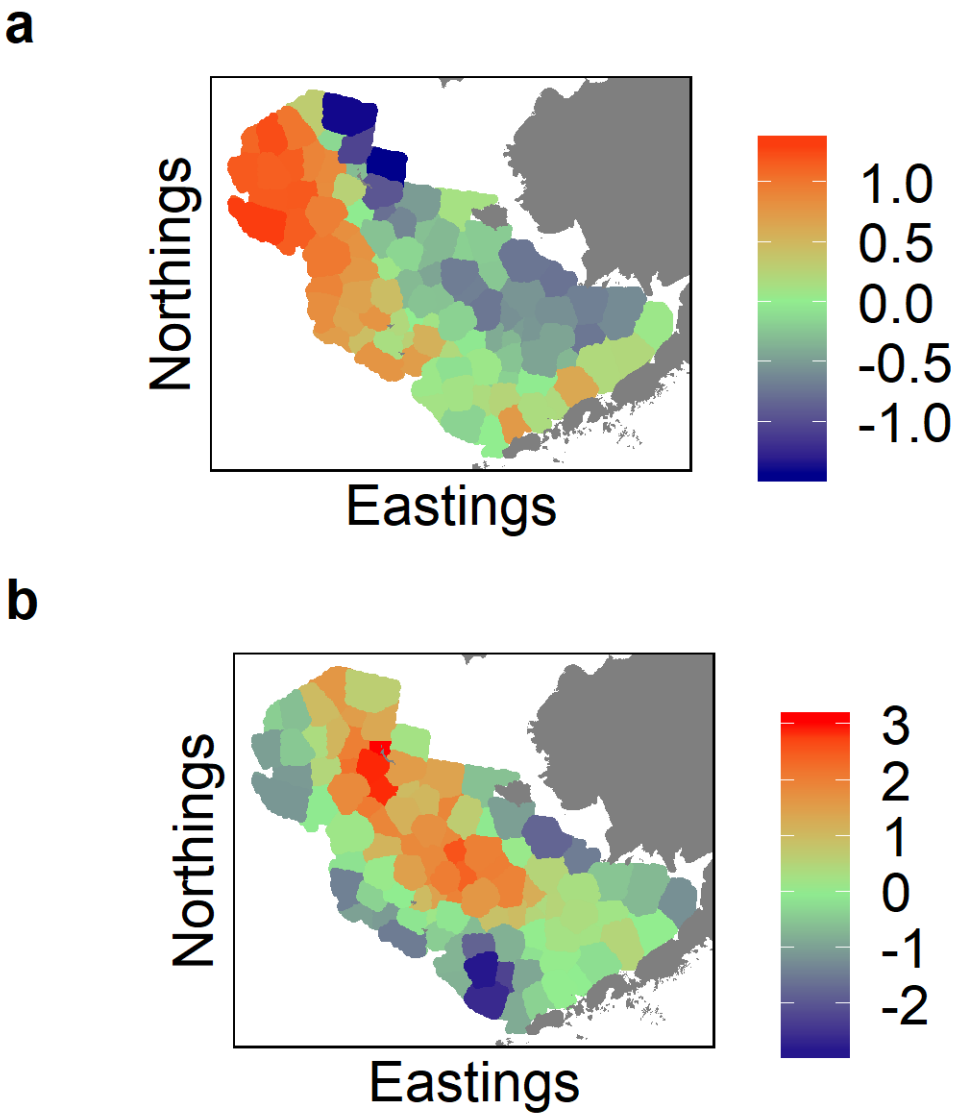

Figure 3.9: The third spatial factor for average encounter rate (a) and positive abundance (b). Warmer colors represent positive values of the factor, while cool colors represent negative values.

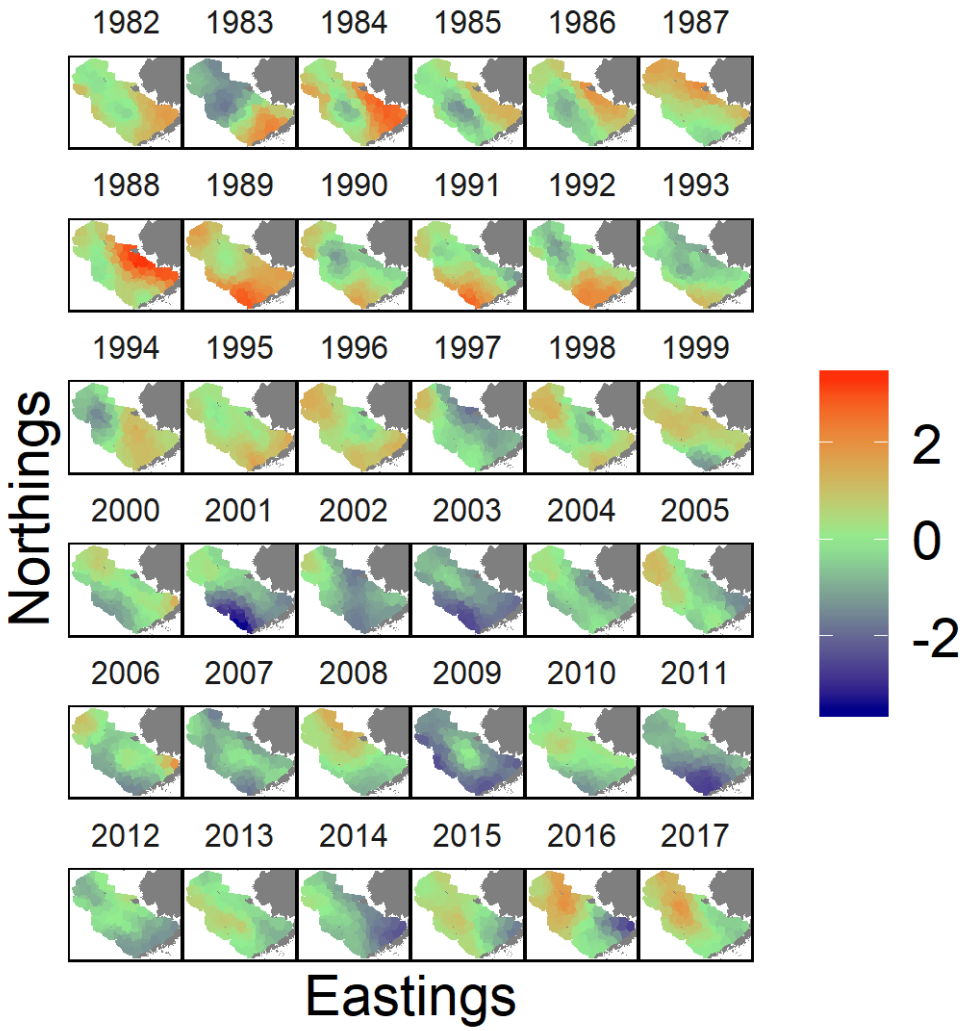

Figure 3.10: Values of the second spatio-temporal factor for encounter probability in each year in the study. Warmer colors represent positive values of the factor, while cooler colors represent negative values.

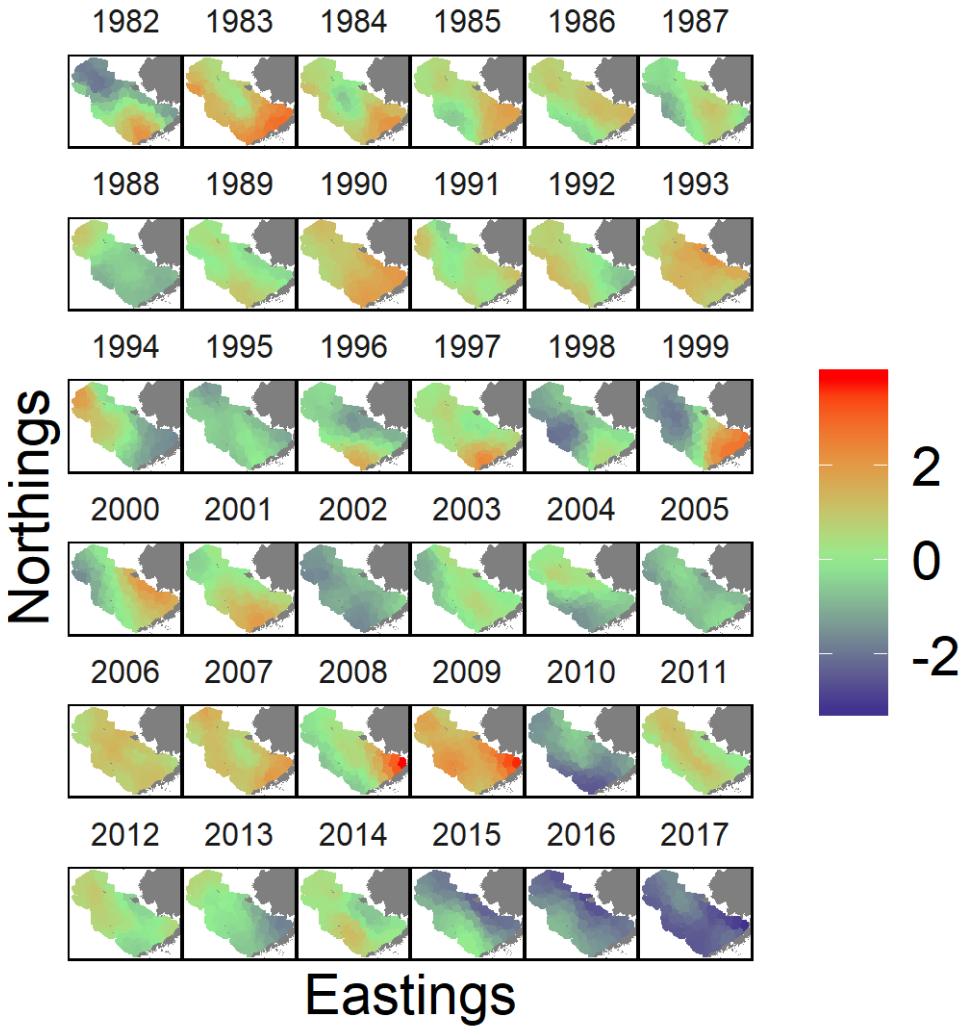

Figure 3.11: Values of the third spatio-temporal factor for encounter probability in each year in the study. Warmer colors represent positive values of the factor, while cooler colors represent negative values.

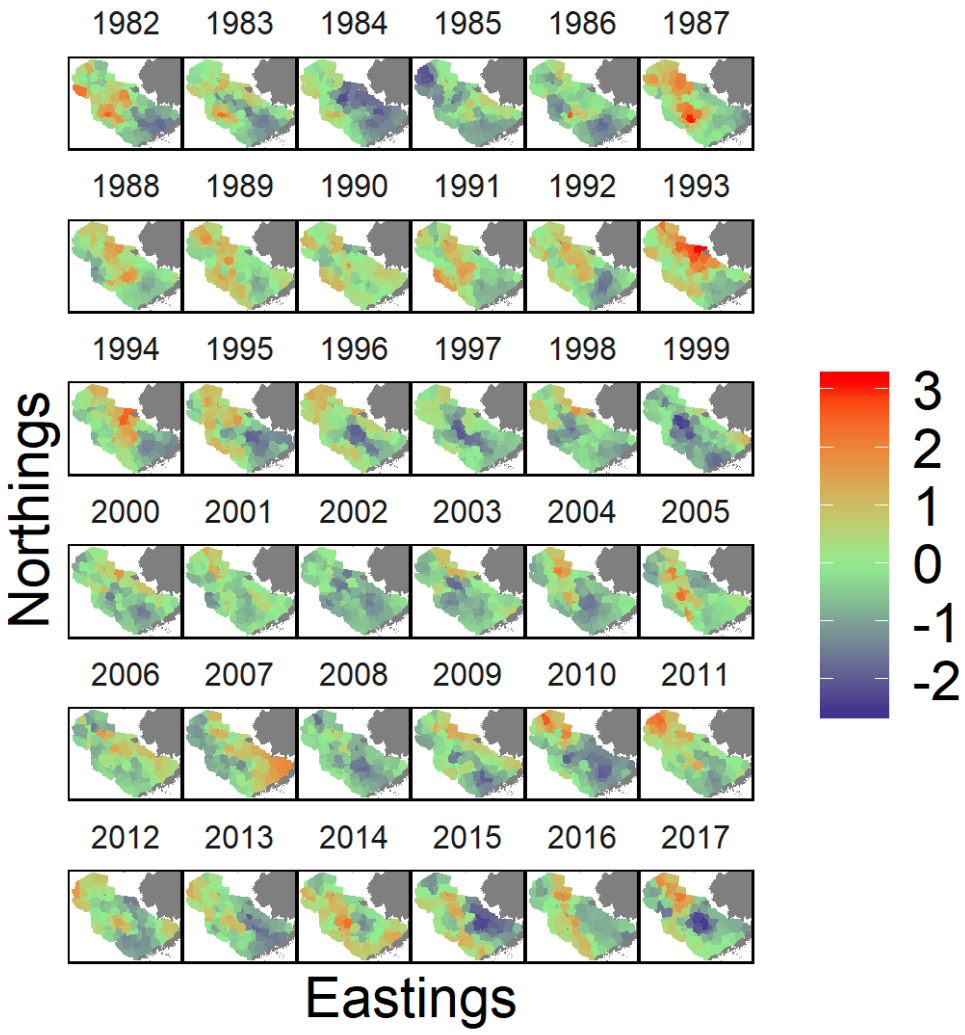

Figure 3.12: Values of the first spatio-temporal factor for positive abundance in each year in the study. Warmer colors represent positive values of the factor, while cooler colors represent negative values.

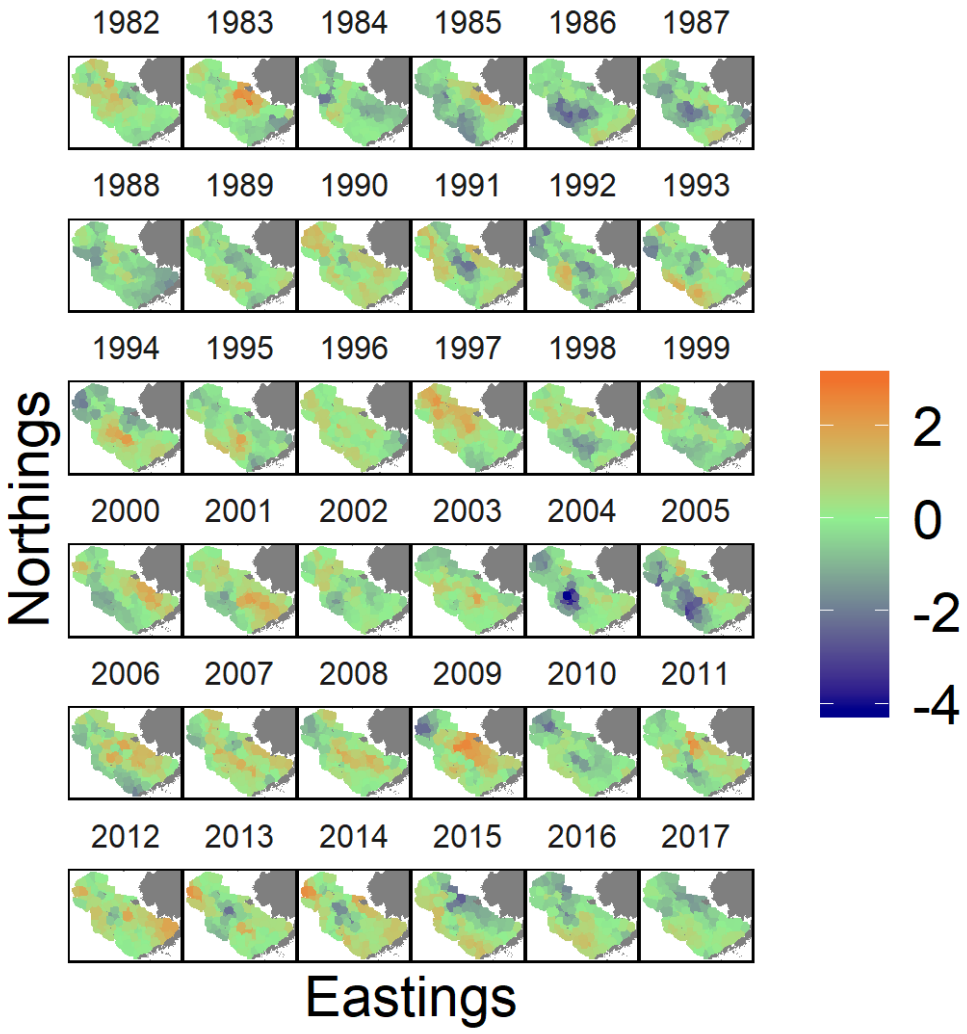

Figure 3.13: Values of the second spatio-temporal factor for positive abundance in each year in the study. Warmer colors represent positive values of the factor, while cooler colors represent negative values.

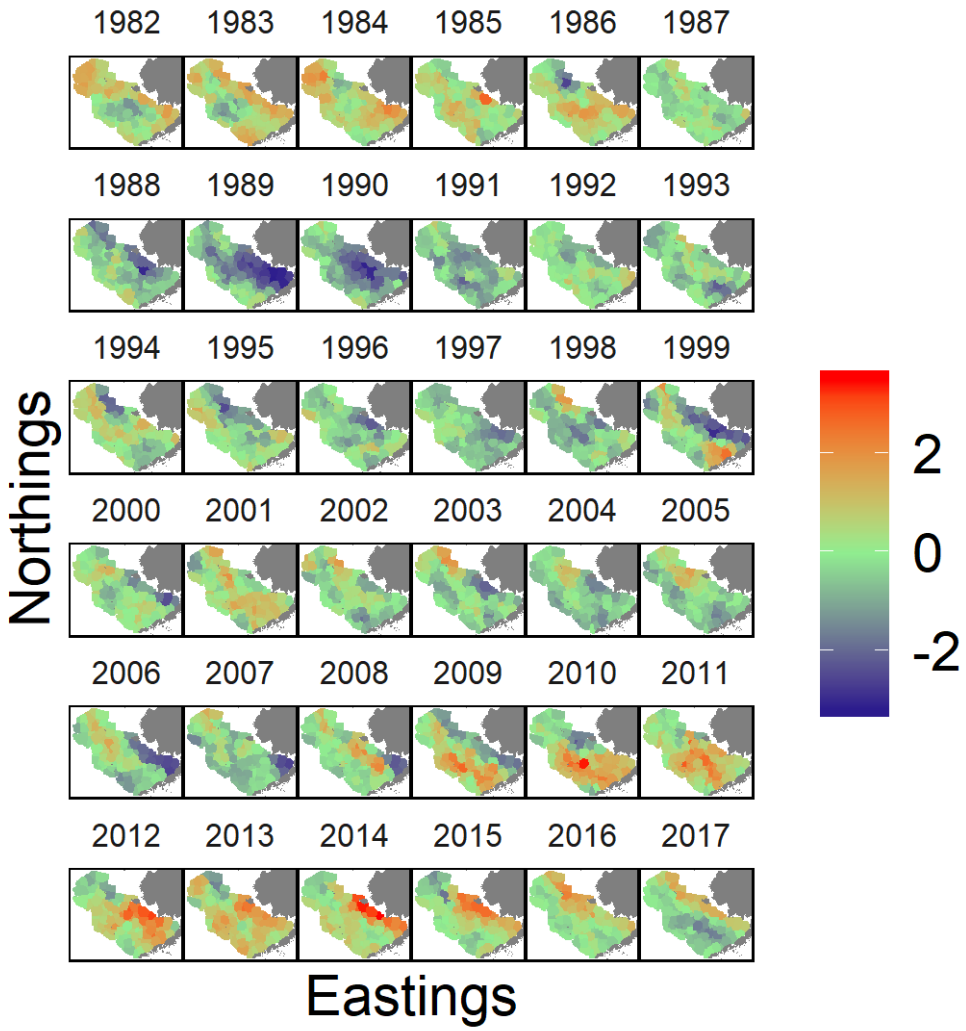

Figure 3.14: Values of the third spatio-temporal factor for positive abundance in each year in the study. Warmer colors represent positive values of the factor, while cooler colors represent negative values.

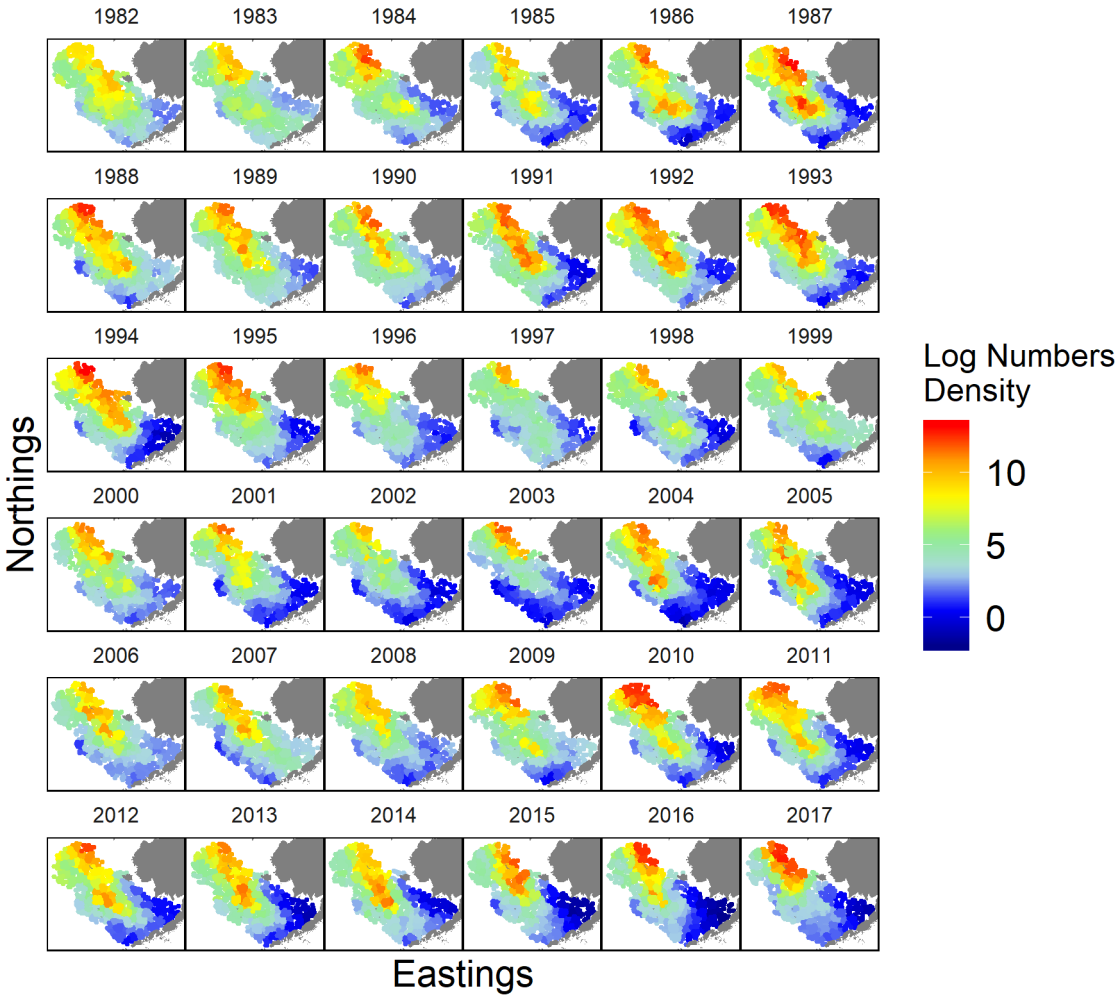

Figure 3.15: Predicted log-abundance of immature snow crab across the EBS in each year in the study

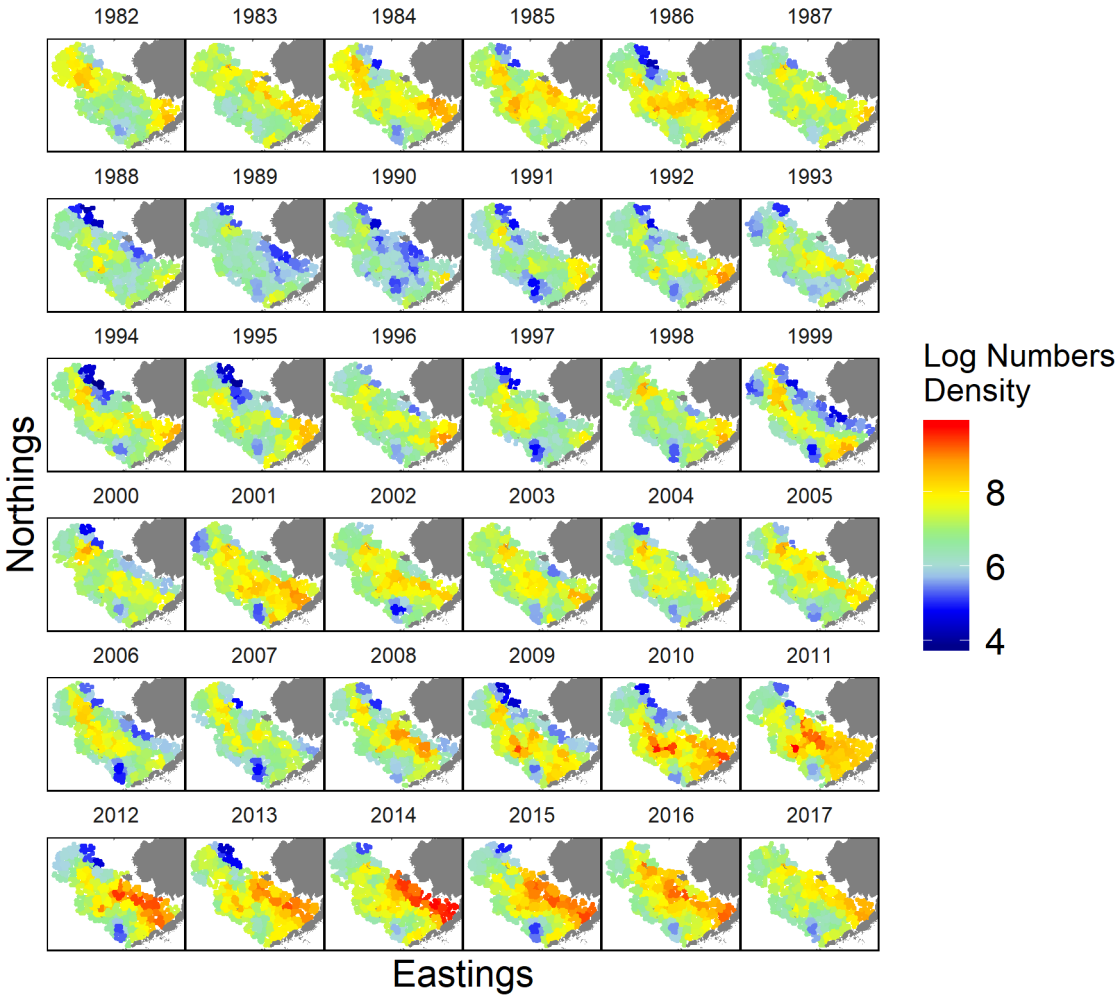

Figure 3.16: Predicted log-abundance of medium-sized Pacific cod across the EBS in each year in the study

Bibliography

[1] J. H. Connell, "Diversity in Tropical Rain Forests and Coral Reefs," *Science*, vol. 199, no. 4335, pp. 1302–1310, 1978 [Online]. Available: http://arxiv.org/abs//links.jstor.org/sici?sici=0036-8075%7B/%%7D2819780324%7B/%%7D293%7B/%%7D3A199%7B/%%7D3A4335%7B/%%7D3C1302%7B/%%7D3ADITRFA%7B/%%7D3E2.0.CO%7B/%%7D3B2-2

[2] K. B. Suttle, M. A. Thomsen, and M. E. Power, "Species Interactions Reverse Grassland Responses to Changing Climate," *Science*, vol. 315, pp. 640–642, 2007.

[3] D. Tilman, "The ecological consequences of changes in biodiversity: a search for general principles," *Ecology*, vol. 80, no. 5, pp. 1455–1474, 1999.

[4] E. L. Berlow, "Strong effects of weak interactions in ecological communities," *Nature*, vol. 398, no. 6725, pp. 330–334, 1999 [Online]. Available: http://apps.webofknowledge.com/full%7B/_%7Drecord.do?product=UA%7B/&%7Dsearch%7B/_%7Dmode=GeneralSearch%7B/&%7Dqid=9%7B/&%7DSID=N1CnMrck8cpHDkGPJYV%7B/&%7Dpage=1%7B/&%7Ddoc=4%7B/&%7DcacheurlFromRightClick=no

[5] W. O. Odadi, M. K. Karachi, S. A. Abdulrazak, and T. P. Young, "African wild ungulates compete with or facilitate cattle depending on season," *Science*, vol. 333, no. November, pp. 1753–1755, 2011.

References

[6] S. C. Pennings and B. R. Silliman, "Linking Biogeography and Community Ecology : Latitudinal Variation in Plant-Herbivore Interaction Strength," *Ecology*, vol. 86, no. 9, pp. 2310–2319, 2005.

[7] B. A. Menge, E. L. Berlow, C. A. Blanchette, S. A. Navarrete, and B. Yamada, "The Keystone Species Concept : Variation in Interaction Strength in a Rocky Intertidal Habitat," vol. 64, no. 3, pp. 249–286, 1994.

[8] S. A. Chamberlain, J. L. Bronstein, and J. A. Rudgers, "How context dependent are species interactions?" *Ecology Letters*, vol. 17, no. 7, pp. 881–890, 2014.

[9] K. J. Vaughn and T. P. Young, "Contingent Conclusions: Year of Initiation Influences Ecological Field Experiments, but Temporal Replication is Rare," *Restoration Ecology*, vol. 18, no. SUPPL. 1, pp. 59–64, 2010.

[10] M. Lima, S. K. M. Ernest, J. H. Brown, A. Belgrano, and N. C. Stenseth, "Chihuahuan Desert Kangaroo Rats: Nonlinear Effects of Population Dynamics, Competition, and Rainfall," *Ecology*, vol. 89, no. 9, pp. 2594–2603, 2008 [Online]. Available: http://doi.wiley.com/10.1890/07-1246.1

[11] C. Holzapfel and B. E. Mahall, "Bidirectional Facilitation and Interference between Shrubs and Annuals in the Mojave Desert," *Ecology*, vol. 80, no. 5, pp. 1747–1761, 1999.

[12] J. H. Daskin and R. A. Alford, "Context-dependent symbioses and their potential roles in wildlife diseases," *Proceedings of the Royal Society B: Biological Sciences*, vol. 279, no. 1733, pp. 1457–1465, 2012.

[13] P. W. Glynn, "Coral reef bleaching: Facts, hypotheses and implications," *Global Change Biology*, vol. 2, no. 6, pp. 495–509, 1996.

[14] J. D. White, O. Sarnelle, and S. K. Hamilton, "Unexpected population response to increasing temperature in the context of a strong species interaction," *Ecological Applications*, 2017.

[15] E. J. Provost *et al.*, "Climate-driven disparities among ecological interactions threaten kelp forest persistence," *Global Change Biology*, vol. 23, no. 1, pp. 353–361, 2017 [Online]. Available: http://arxiv.org/abs/3320

[16] E. R. Deyle, R. M. May, S. B. Munch, and G. Sugihara, "Tracking and forecasting ecosystem interactions in real time," *Proceedings of the Royal Society B: Biological Sciences*, vol. 283, no. 1822, p. 20152258, 2016 [Online]. Available: http://rspb.royalsocietypublishing.org/content/283/1822/20152258.abstract

[17] E. R. Deyle, M. Fogarty, C.-h. Hsieh, L. Kaufman, A. D. Maccall, and S. B. Munch, "Predicting climate effects on Pacific sardine," *Proceedings of the National Academy of Sciences of the United States of America*, vol. 110, no. 16, pp. 6430–6435, 2013 [Online]. Available: http://arxiv.org/abs/arXiv:1408.1149

[18] C.-W. Chang, M. Ushio, and C.-h. Hsieh, "Empirical dynamic modeling for beginners," *Ecological Research*, pp. 1–12, 2017.

[19] H. Ye, E. R. Deyle, L. J. Gilarranz, and G. Sugihara, "Distinguishing time-delayed causal interactions using convergent cross mapping." *Scientific reports*, vol. 5, p. 14750, 2015 [Online]. Available: http://www.nature.com/srep/2015/151005/srep14750/full/srep14750.html

[20] M. S. Foster and D. R. Schiel, "Ecology of giant kelp forests in California: a community profile," *United States Fish and Wildlife Service Biological Report*, vol. 85, pp. 1–152, 1985 [Online]. Available: http://www.osti.gov/energycitations/product.biblio.jsp?osti%7B/_%7Did=5129110

[21] M. H. Graham, J. A. Vásquez, and A. H. Buschmann, "Global Ecology of the Giant Kelp Macrocystis : From Ecotypes To Ecosystems," *Oceanography and Marine Biology*, vol. 45, pp. 39–88, 2007 [Online]. Available: http://scholar.google.com/scholar?hl=en%7B/&%7DbtnG=Search%7B/&%7Dq=intitle:Global+ecology+of+the+giant+kelp+Macrocystis:+from+ecotypes+to+ecosystems.%7B/#%7D0

[22] H. Teagle, S. J. Hawkins, P. J. Moore, and D. A. Smale, "The role of kelp species as biogenic habitat formers in coastal marine ecosystems," *Journal of Experimental Marine Biology and Ecology*, vol. 492, pp. 81–98, 2017 [Online]. Available: http://dx.doi.org/10.1016/j.jembe.2017.01.017

[23] J. A. Estes and J. F. Palmisano, "Sea otters: their role in structuring nearshore communities." vol. 185. pp. 1058–1060, 1974.

[24] M. H. Graham, C. Harrold, S. Lisin, K. Light, J. M. Watanabe, and M. S. Foster, "Population dynamics of giant kelp Macrocystis pyrifera along a wave exposure gradient," *Marine Ecology Progress Series*, vol. 148, pp. 269–279, 1997 [Online]. Available: https://www.infona.pl//resource/bwmeta1.element.elsevier-09f84310-eaaa-3364-8379-aea24b4f775b

[25] R. G. Kvitek, P. J. Iampietro, and C. E. Bowlby, "Sea Otters and Benthic Prey Communities : a Direct Test of the Sea Otter As Keystone Predator in Washington State," *Marine Mammal Science*, vol. 14, no. October, pp. 895–902, 1998.

[26] M. S. Foster and D. R. Schiel, "Loss of predators and the collapse of southern California kelp forests (?): Alternatives, explanations and generalizations," *Journal of Experimental Marine Biology and Ecology*, vol. 393, nos. 1-2, pp. 59–70, 2010 [Online]. Available: http://dx.doi.org/10.1016/j.jembe.2010.07.002

[27] D. C. Reed, A. Rassweiler, M. H. Carr, K. C. Cavanaugh, D. P. Malone, and D. A.

Siegel, "Wave disturbance overwhelms top-down and bottom-up control of primary production in California kelp forests," *Ecology*, vol. 92, no. 11, pp. 2108–2116, 2011.

[28] D. Reed, L. Washburn, A. Rassweiler, R. Miller, T. Bell, and S. Harrer, "Extreme warming challenges sentinel status of kelp forests as indicators of climate change," *Nature Communications*, vol. 7, no. May, p. 13757, 2016 [Online]. Available: http://www.nature.com/doifinder/10.1038/ncomms13757

[29] P. E. Parnell, E. F. Miller, C. E. Lennert-Cody, P. K. Dayton, M. L. Carter, and T. D. Stebbins, "The response of giant kelp (Macrocystis pyrifera) in southern California to low-frequency climate forcing," *Limnology and Oceanography*, vol. 55, no. 6, pp. 2686–2702, 2010 [Online]. Available: http://www.aslo.info/lo/toc/vol%7B/_%7D55/issue%7B/_%7D6/2686.pdf

[30] J. E. Byrnes, D. C. Reed, B. J. Cardinale, K. C. Cavanaugh, S. J. Holbrook, and R. J. Schmitt, "Climate-driven increases in storm frequency simplify kelp forest food webs," *Global Change Biology*, vol. 17, no. 8, pp. 2513–2524, 2011.

[31] T. W. Bell, K. C. Cavanaugh, D. C. Reed, and D. A. Siegel, "Geographical variability in the controls of giant kelp biomass dynamics," *Journal of Biogeography*, vol. 42, no. 10, pp. 2010–2021, 2015.

[32] M. A. Young *et al.*, "Environmental controls on spatial patterns in the long-term persistence of giant kelp in central California," *Ecology*, vol. 86, no. 1, pp. 45–60, 2015 [Online]. Available: http://www.esajournals.org/doi/abs/10.1890/15-0267.1

[33] M. C. Kenner *et al.*, "A multi-decade time series of kelp forest community structure at San Nicolas Island, California (USA)," *Ecology*, vol. 94, no. 11, pp. 2654–2654, 2013 [Online]. Available: http://www.esajournals.org/doi/abs/10.1890/13-0561R.1

[34] G. Sugihara *et al.*, "Detecting causality in complex ecosystems," *Science*, vol. 338, no. 6106, pp. 496–500, 2012 [Online]. Available: http://www.ncbi.nlm.nih.gov/pubmed/22997134

[35] G. Sugihara, "Nonlinear forecasting for the classification of natural time series," *Philosophical Transcations of the Royal Society of London Series A-Mathematical Physical and Engineering Sciences*, vol. 348, pp. 477–495, 1994.

[36] M. S. Foster, "Organization of macroalgal assemblages in the Northeast Pacific: the assumption of homogeneity and the illusion of generality," *Hydrobiologia*, vol. 192, no. 1, pp. 21–33, 1990.

[37] P. Dayton, "Toward an understanding of resilience and the potential effects of enrichments to the benthos at McMurdo Sound, Antarctica." p. 96, 1972.

[38] P. K. Dayton, V. Currie, T. Gerrodette, B. D. Keller, R. Rosenthal, and D. Ven Tresca, "Patch dynamics and stability of some California USA kelp communities," *Ecological Monographs*, vol. 54, no. 3, pp. 253–290, 1984.

[39] P. K. Dayton, M. J. Tegner, P. B. Edwards, and K. L. Riser, "Temporal and spatial scales of kelp demography: the role of oceanographic climate," *Ecological Monographs*, vol. 69, no. 2, pp. 219–250, 1999.

[40] D. C. Reed and M. S. Foster, "The effects of canopy shadings on algal recruitment and growth in a giant kelp forest," *Ecology*, vol. 65, no. 3, pp. 937–948, 1984.

[41] S. D. Ling *et al.*, "Global regime shift dynamics of catastrophic sea urchin overgrazing," *Phil. Trans. R. Soc. B*, vol. 370, p. 20130269, 2014 [Online]. Available: http://arxiv.org/abs/2309

[42] C. Harrold and D. C. Reed, "Food Availability , Sea Urchin Grazing , and Kelp

Forest Community Structure," *Ecology*, vol. 66, no. 4, pp. 1160–1169, 1985.

[43] R. C. Zimmerman and J. N. Kremer, "Episodic nutrient supply to a kelp forest ecosystem in Southern California," *Journal of Marine Research*, vol. 42, no. 3, pp. 591–604, 1984.

[44] K. Wolter and M. S. Timlin, "El Niño/Southern Oscillation behaviour since 1871 as diagnosed in an extended multivariate ENSO index (MEI.ext)," *International Journal of Climatology*, vol. 31, no. 7, pp. 1074–1087, 2011.

[45] N. J. Mantua and S. R. Hare, "The Pacific Decadal Oscillation," vol. 58. pp. 35–44, 2002.

[46] E. Di Lorenzo *et al.*, "North Pacific Gyre Oscillation links ocean climate and ecosystem change," *Geophysical Research Letters*, vol. 35, no. 8, pp. 2–7, 2008.

[47] C.-h. Hsieh, C. Anderson, and G. Sugihara, "Extending nonlinear analysis to short ecological time series." *The American naturalist*, vol. 171, no. 1, pp. 71–80, 2008 [Online]. Available: http://www.jstor.org/stable/10.1086/524202

[48] A. T. Clark *et al.*, "Spatial convergent cross mapping to detect causal relationships from short time series," *Ecology*, vol. 96, no. 5, pp. 1174–1181, 2015.

[49] W. C. O'Reilly, C. B. Olfe, J. Thomas, R. J. Seymour, and R. T. Guza, "The California coastal wave monitoring and prediction system," *Coastal Engineering*, vol. 116, pp. 118–132, 2016 [Online]. Available: http://dx.doi.org/10.1016/j.coastaleng.2016.06.005

[50] F. Takens, "Detecting strange attractors in turbulence," in *Symposium on dynamical systems and turbulence*, vol. 898, D. A. Rand and L. S. Young, Eds. Berlin: Springer-Verlag, 1981, pp. 366–381 [Online]. Available: http://arxiv.org/abs/arXiv:1011.

1669v3

[51] R Core Team, "R: A Language and Environment for Statistical Computing." R Foundation for Statistical Computing, Vienna, Austria, 2018 [Online]. Available: https://www.r-project.org/

[52] H. Ye *et al.*, "rEDM: Applications of Empirical Dynamic Modeling from Time Series." 2018 [Online]. Available: https://github.com/ha0ye/rEDM

[53] T. W. Bell, J. G. Allen, K. C. Cavanaugh, and D. A. Siegel, "Three decades of variability in California's giant kelp forests from the Landsat satellites," *Remote Sensing of Environment*, no. June, pp. 0–1, 2018 [Online]. Available: https://doi.org/10.1016/j.rse.2018.06.039

[54] S. Bennett *et al.*, "Canopy interactions and physical stress gradients in subtidal communities," *Ecology Letters*, vol. 18, no. 7, pp. 677–686, 2015 [Online]. Available: http://arxiv.org/abs/1208

[55] L. G. Harris, A. W. Ebeling, D. R. Laur, and R. J. Rowley, "Community Recovery after Storm Damage : A Case of Facilitation in Primary Succession," *Science*, vol. 224, no. 4655, pp. 1336–1338, 1984.

[56] K. K. Arkema, D. C. Reed, and S. C. Schroeter, "Direct and indirect effects of giant kelp determine benthic community structure and dynamics," *Ecology*, vol. 90, no. 11, pp. 3126–3137, 2009.

[57] K. M. Benes and R. C. Carpenter, "Kelp canopy facilitates understory algal assemblage via competitive release during early stages of secondary succession," *Ecology*, vol. 96, no. 1, pp. 241–251, 2015.

[58] E. Baraza, R. Zamora, and J. A. Hódar, "Conditional outcomes in plant-herbivore

interactions: Neighbours matter," *Oikos*, vol. 113, no. 1, pp. 148–156, 2006.

[59] M. J. Tegner, P. K. Dayton, P. B. Edwards, and K. L. Riser, "Large-scale , low-frequency oceanographic effects on kelp forest succession: a tale of two cohorts," *Marine Ecology Progress Series*, vol. 146, pp. 117–134, 1997.

[60] J. Rocha, J. Yletyinen, R. Biggs, T. Blenckner, and G. Peterson, "Marine regime shifts: drivers and impacts on ecosystems services," *Philosophical Transactions of the Royal Society B: Biological Sciences*, vol. 370, no. 1659, pp. 20130273–20130273, 2014 [Online]. Available: http://rstb.royalsocietypublishing.org/content/370/1659/20130273

[61] H. Ye *et al.*, "Equation-free mechanistic ecosystem forecasting using empirical dynamic modeling," *Proceedings of the National Academy of Sciences*, vol. 112, no. 13, pp. E1569–E1576, 2015 [Online]. Available: http://www.pnas.org/content/early/2015/02/26/1417063112.abstract%7B/%%7D5Cnhttp://www.pnas.org/lookup/doi/10.1073/pnas.1503154112

[62] J. A. McGowan *et al.*, "Predicting coastal algal blooms in southern California," *Ecology*, vol. 98, pp. 1419–1433, 2017.

[63] R. Dirzo, H. S. Young, M. Galetti, G. Ceballos, N. J. B. Isaac, and B. Collen, "Defaunation in the Antrhopocene," *Science*, vol. 401, no. 6195, pp. 401–406, 2014.

[64] D. J. McCauley, M. L. Pinsky, S. R. Palumbi, J. A. Estes, F. H. Joyce, and R. R. Warner, "Marine defaunation: Animal loss in the global ocean," *Science*, vol. 347, no. 6219, pp. 1255641–1255641, 2015 [Online]. Available: http://www.sciencemag.org/cgi/doi/10.1126/science.1255641

[65] H. K. Lotze, M. Coll, A. M. Magera, C. Ward-Paige, and L. Airoldi, "Recovery of

marine animal populations and ecosystems," *Trends in Ecology and Evolution*, vol. 26, no. 11, pp. 595–605, 2011 [Online]. Available: http://dx.doi.org/10.1016/j.tree.2011.07.008

[66] F. Sergio *et al.*, "Top Predators as Conservation Tools: Ecological Rationale, Assumptions, and Efficacy," *Annual Review of Ecology, Evolution, and Systematics*, vol. 39, no. 1, pp. 1–19, 2008.

[67] K. N. Marshall, A. C. Stier, J. F. Samhouri, R. P. Kelly, and E. J. Ward, "Conservation Challenges of Predator Recovery," *Conservation Letters*, vol. 9, no. 1, pp. 70–78, 2016.

[68] A. C. Stier *et al.*, "Ecosystem context and historical contingency in apex predator recoveries," *Science Advances*, vol. 2, no. 5, p. e1501769, 2016.

[69] C. S. Szuwalski, M. G. Burgess, C. Costello, and S. D. Gaines, "High fishery catches through trophic cascades in China," *Proceedings of the National Academy of Sciences*, vol. 114, no. 4, pp. 717–721, 2017.

[70] P. M. Cury *et al.*, "Global seabird response to forage fish depletion- one-third for the birds," *Science*, vol. 334, pp. 1703–1706, 2011 [Online]. Available: http://www.ncbi.nlm.nih.gov/pubmed/21350126

[71] B. J. Bergstrom, L. C. Arias, A. D. Davidson, A. W. Ferguson, L. A. Randa, and S. R. Sheffield, "License to Kill: Reforming Federal Wildlife Control to Restore Biodiversity and Ecosystem Function," *Conservation Letters*, vol. 7, no. 2, pp. 131–142, 2014.

[72] T. B. Muhly and M. Musiani, "Livestock depredation by wolves and the ranching economy in the Northwestern U.S." *Ecological Economics*, vol. 68, nos. 8-9, pp. 2439–2450, 2009.

[73] S. Guénette, S. J. Heymans, V. Christensen, and A. W. Trites, "Ecosystem models show combined effects of fishing, predation, competition, and ocean productivity on Steller sea lions (Eumetopias jubatus) in Alaska," *Canadian Journal of Fisheries and Aquatic Sciences*, vol. 63, no. 11, pp. 2495–2517, 2006 [Online]. Available: http://www.nrcresearchpress.com/doi/abs/10.1139/f06-136

[74] P. Yodzis, "Local trophodynamics and the interaction of marine mammals and fisheries in the Benguela ecosystem," *Journal of Animal Ecology*, vol. 67, no. 4, pp. 635–658, 1998 [Online]. Available: http://doi.wiley.com/10.1046/j.1365-2656.1998.00224.x

[75] P. Yodzis, "Must top predators be culled for the sake of fisheries?" *Trends in Ecology and Evolution*, vol. 16, no. 2, pp. 78–84, 2001.

[76] T. C. Cook, K. James, and M. Bearzi, "Angler perceptions of California sea lion (Zalophus californianus) depredation and marine policy in Southern California," *Marine Policy*, vol. 51, pp. 573–583, 2015 [Online]. Available: http://dx.doi.org/10.1016/j.marpol.2014.09.020

[77] M. L. Riedman and J. a. Estes, "The Sea Otter (Enhydra lutris): Behavior , Ecology , and Natural History," *Biological Report*, vol. 90, no. September, pp. 1–136, 1990.

[78] J. A. Estes, M. L. Riedman, M. M. Staedler, M. T. Tinker, and B. E. Lyon, "Individual variation in prey selection by sea otters: Patterns, causes and implications," *Journal of Animal Ecology*, vol. 72, no. 1, pp. 144–155, 2003.

[79] H. C. Bryant, "Sea otters near Point Sur," *California Fish and Game*, vol. 1, pp. 134–135, 1915.

[80] K. D. Lafferty and M. T. Tinker, "Sea otters are recolonizing southern California in fits and starts," *Ecosphere*, vol. 5, no. 5, pp. 1–11, 2014.

[81] S. Kato and S. C. Schroeter, "Biology of the Red Sea Urchin , Strongylocentrotus franciscanus , and Its Fishery in California," *Marine Fisheries Review*, vol. 47, no. 7, pp. 1–20, 1985.

[82] P. E. Kalvass and J. M. Hendrix, "The California Red Sea Urchin, Strongylocentrotus franciscanus, Fishery: Catch, Effort, and Management Trends," *Marine Fisheries Review*, vol. 59, no. 2, pp. 1–17, 1997 [Online]. Available: http://aquaticcommons.org/9820/

[83] J. A. Estes and G. R. VanBlaricom, "Sea otters and shellfisheries," 1985.

[84] S. Fanshawe, G. R. Vanblaricom, and A. A. Shelly, "Restored top carnivores as detriments to the performance of marine protected areas intended for fishery sustainability: a case study with red abalones and sea otters," *Conservation Biology*, vol. 17, no. 1, pp. 273–283, 2003.

[85] N. L. Andrew *et al.*, "Status and management of world sea urchin fisheries," vol. 40. pp. 343–425, 2002.

[86] B. Hatfield, "The translocation of sea otters to San Nicolas Island: an update," *Proceedings of the 6th California Islands Symposium*, pp. 473–475, 2005 [Online]. Available: http://www.mednscience.org/sites/default/files/products/Hatfield%7B/_%7DTranslocation%7B/_%7DSea%7B/_%7DOtters%7B/_%7DSan%7B/_%7DNicholas%7B/_%7DIsland.pdf

[87] M. T. Tinker, D. F. Doak, and J. A. Estes, "Using Demography and Movement Behavior to Predict Range Expansion of the Southern Sea Otter," *Ecological Applica-*

tions, vol. 18, no. 7, pp. 1781–1794, 2008.

[88] U.S. Fish and Wildlife Service, "Final supplemental environmental impact statement on the translocation of southern sea otters, Volume 1." Ventura Fish; Wildlife Office, Ventura, California, p. 348, 2012.

[89] M. N. Maunder and A. E. Punt, "Standardizing catch and effort data: A review of recent approaches," *Fisheries Research*, vol. 70, nos. 2-3 SPEC. ISS., pp. 141–159, 2004 [Online]. Available: http://arxiv.org/abs/1115

[90] M. T. Tinker and B. B. Hatfield, "California sea otter (Enhydra lutris nereis) census results, spring 2017," U.S. Geological Suvey Data Series 1067, 2017.

[91] J. A. Estes and R. J. Jameson, "A Double-Survey Estimate for Sighting Probability of Sea Otters in California," *Journal of Wildlife Management*, vol. 52, no. 1, pp. 70–76, 1988.

[92] M. T. Tinker, D. P. Costa, J. A. Estes, and N. Wieringa, "Individual dietary specialization and dive behaviour in the California sea otter: Using archival time-depth data to detect alternative foraging strategies," *Deep-Sea Research Part II: Topical Studies in Oceanography*, vol. 54, nos. 3-4, pp. 330–342, 2007.

[93] G. B. Bentall, "Morphological and Behavioral Correlates of Population Status in the Southern Sea Otter, Enhydra Lutris Nereis: a Comparative Study Between Central California and San Nicolas Island," Master's thesis, University of California, Santa Cruz, 2005.

[94] R. S. Ostfeld, "Foraging Strategies and Prey Switching in the California Sea Otter," *Oecologia*, vol. 53, no. 2, pp. 170–178, 1982.

[95] J. J. Pella and P. K. Tomlinson, "A generalized stock production model," *Bull.*

Inter-Am. Trop. Tuna Com, vol. 13, pp. 421–458, 1969.

[96] L. W. Botsford, A. Campbell, and R. Miller, "Biological reference points in the management of North American sea urchin fisheries," *Canadian Journal of Fisheries and Aquatic Sciences*, vol. 61, no. 8, pp. 1325–1337, 2004.

[97] A. E. Punt and C. Szuwalski, "How well can FMSYand BMSYbe estimated using empirical measures of surplus production?" *Fisheries Research*, vols. 134-136, pp. 113–124, 2012.

[98] L. C. Yeates, T. M. Williams, and T. L. Fink, "Diving and foraging energetics of the smallest marine mammal, the sea otter (Enhydra lutris)," *Journal of Experimental Biology*, vol. 210, no. 11, pp. 1960–1970, 2007 [Online]. Available: http://jeb.biologists.org/cgi/doi/10.1242/jeb.02767

[99] A. B. Hollowed, J. N. Ianelli, and P. a. Livingston, "Including predation mortality in stock assessments: a case study for Gulf of Alaska walleye pollock," *ICES Journal of Marine Science*, vol. 57, pp. 279–293, 2000 [Online]. Available: http://icesjms.oxfordjournals.org/content/57/2/279.abstract%7B/%%7D5Cnhttp://icesjms.oxfordjournals.org/content/57/2/279.full.pdf

[100] N. T. Shears, D. J. Kushner, S. L. Katz, and S. D. Gaines, "Reconciling conflict between the direct and indirect effects of marine reserve protection," *Environmental Conservation*, vol. 39, no. 3, pp. 225–236, 2012 [Online]. Available: http://www.journals.cambridge.org/abstract%7B/_%7DS0376892912000082

[101] B. Carpenter *et al.*, "Stan : A Probabilistic Programming Language," *Journal of Statisical Software*, vol. 76, no. 1, 2017.

[102] M. J. Betancourt and M. Girolami, "Hamiltonian Monte Carlo for Hierarchical

Models," *Current trends in Bayesian methodology with applications*, vol. 79, p. 30, 2015 [Online]. Available: http://arxiv.org/abs/1312.0906

[103] A. Vehtari, A. Gelman, and J. Gabry, "Practical Bayesian model evaluation using leave-one-out cross-validation and WAIC," *Statistics and Computing*, vol. 27, no. 5, pp. 1413–1432, 2017.

[104] M. T. Tinker, G. Bentall, and J. a Estes, "Food limitation leads to behavioral diversification and dietary specialization in sea otters." *Proceedings of the National Academy of Sciences of the United States of America*, vol. 105, no. 2, pp. 560–565, 2008.

[105] U.S. Fish and Wildlife Service, "Final supplemental environmental impact statement on the translocation of southern sea otters, Volume 2." Ventura Fish; Wildlife Office, Ventura, California, 2012.

[106] K. M. Cammen, D. B. Rasher, and R. S. Steneck, "Predator recovery, shifting baselines, and the adaptive management challenges they create," *Ecosphere*, vol. 10, no. 2, 2019.

[107] A. S. Guerra, "Wolves of the Sea: Managing human-wildlife conflict in an increasingly tense ocean," *Marine Policy*, vol. 99, no. November 2018, pp. 369–373, 2018.

[108] J. A. Vucetich, D. W. Smith, and D. R. Stahler, "Influence of harvest, climate and wolf predation on Yellowstone elk, 1961-2004," *Oikos*, vol. 111, no. 2, pp. 259–270, 2005.

[109] L. Morissette, V. Christensen, and D. Pauly, "Marine Mammal Impacts in Exploited Ecosystems: Would Large Scale Culling Benefit Fisheries?" *PLoS ONE*, vol. 7, no. 9, 2012.

[110] E. T. Mezquida, S. J. Slater, and C. W. Benkman, "Sage-Grouse and Indirect Interactions : Potential Implications of Coyote Control on Sage- Grouse Populations," *The Condor*, vol. 108, no. 4, pp. 747–759, 2006.

[111] A. Sih, P. Crowley, M. McPeek, J. Petranka, and K. Strohmeier, "Predation, Competition, and Prey Communities: A Review of Field Experiments," *Annual Review of Ecology and Systematics*, vol. 16, no. 1, pp. 269–311, 1985.

[112] G. J. Wright, R. O. Peterson, D. W. Smith, and T. O. Lemke, "Selection of Northern Yellowstone Elk by Gray Wolves and Hunters," *Journal of Wildlife Management*, vol. 70, no. 4, pp. 1070–1078, 2006.

[113] J. Jurado-Molina, J. S. Palleiro-Nayar, and N. L. Gutiérrez, "Developing a Bayesian framework for stock assessment and decision analysis of the red sea urchin fishery in Baja California , Mexico Desarrollo de un marco Bayesiano para la valoración del stock y el análisis de decisión de la pesquería del erizo rojo en," *Ciencias Marinas*, vol. 35, no. 2, pp. 183–193, 2009.

[114] A. Gelman, H. S. Stern, J. B. Carlin, D. B. Dunson, A. Vehtari, and D. B. Rubin, *Bayesian data analysis*. Chapman; Hall/CRC, 2013.

[115] E. K. Pikitch *et al.*, "Ecosystem-Based Fishery Management," *Science*, vol. 300, no. July, pp. 2003–2003, 2004 [Online]. Available: http://www.sciencemag.org/content/307/5716/1725.short

[116] M. Fogarty, "The art of ecosystem-based fishery management," *Canadian Journal of Fisheries and Aquatic Sciences*, vol. 71, no. November 2013, pp. 479–490, 2014.

[117] T. J. Pitcher, D. Kalikoski, K. Short, D. Varkey, and G. Pramod, "An evaluation of progress in implementing ecosystem-based management of fisheries in 33 countries,"

Marine Policy, vol. 33, no. 2, pp. 223–232, 2009.

[118] A. Orio, U. Bergström, A. B. Florin, A. Lehmann, I. Šics, and M. Casini, "Spatial contraction of demersal fish populations in a large marine ecosystem," *Journal of Biogeography*, no. December 2018, pp. 633–645, 2019.

[119] A. B. Hollowed *et al.*, "Are multispecies models an improvement on single-species models for measuring fishing impacts on marine ecosystems?" *ICES Journal of Marine Science: Journal du Conseil*, vol. 57, no. 3, pp. 707–719, 2000 [Online]. Available: http://icesjms.oxfordjournals.org/content/57/3/707.abstract

[120] D. P. Swain and R. K. Mohn, " Forage fish and the factors governing recovery of Atlantic cod (Gadus morhua) on the eastern Scotian Shelf," *Canadian Journal of Fisheries and Aquatic Sciences*, vol. 69, no. 6, pp. 997–1001, 2012.

[121] J. Pagel and F. M. Schurr, "Forecasting species ranges by statistical estimation of ecological niches and spatial population dynamics," *Global Ecology and Biogeography*, vol. 21, no. 2, pp. 293–304, 2012.

[122] C. S. Szuwalski, K. A. Vert-Pre, A. E. Punt, T. A. Branch, and R. Hilborn, "Examining common assumptions about recruitment: A meta-analysis of recruitment dynamics for worldwide marine fisheries," *Fish and Fisheries*, vol. 16, no. 4, pp. 633–648, 2015.

[123] A. Kempf, G. Huse, G. Dingsør, J. Floeter, and A. Temming, "The importance of overlap – predicting North Sea cod recovery with a multi species fisheries assessment model," *ICES Journal of Marine Science*, vol. 67, pp. 1989–1997, 2010.

[124] K. T. Frank, B. Petrie, W. C. Leggett, and D. G. Boyce, "Large scale, synchronous variability of marine fish populations driven by commercial exploitation," *Proceedings*

of the National Academy of Sciences, vol. 113, no. 29, pp. 8248–8253, 2016.

[125] D. P. Swain, H. P. Benoît, M. O. Hammill, and J. A. Sulikowski, "Risk of extinction of a unique skate population due to predation by a recovering marine mammal," *Ecological Applications*, p. e01921, 2019 [Online]. Available: https://onlinelibrary.wiley.com/doi/abs/10.1002/eap.1921

[126] C. Parada, D. A. Armstrong, B. Ernst, S. Hinckley, and J. M. Orensanz, "Spatial dynamics of snow crab (chionoecetes opilio) in the eastern bering sea-putting together the pieces of the puzzle," *Bulletin of Marine Science*, vol. 86, no. 2, pp. 413–437, 2010.

[127] C. Szuwalski, "A stock assessment for eastern Bering Sea snow crab," North Pacific Fishery Management Council, Anchorage, AK, September, 2018 [Online]. Available: https://www.npfmc.org/wp-content/PDFdocuments/resources/SAFE/CrabSAFE/2018/1-EBSsnow%7B/_%7DSAFE%7B/_%7D2018.pdf

[128] J. Zheng and G. H. Kruse, "Recruitment variation of eastern Bering Sea crabs: Climate-forcing or top-down effects?" *Progress in Oceanography*, vol. 68, nos. 2-4, pp. 184–204, 2006.

[129] J. L. Orensanz, B. Ernst, D. A. Armstrong, P. J. Stabeno, and P. Livingston, "Contraction of the geographic range of distribution of snow crab (Chionoecetes Opilio) in the Eastern Bering Sea : an environmental ratchet ?" *CalCOFI Reports*, vol. 45, pp. 65–79, 2004.

[130] T. Wyllie-Echeverria and W. S. Wooster, "Year-to-year variations in Bering Sea ice cover and some consequences for fish distributions," *Fisheries Oceanography*, vol. 7, no. 2, pp. 159–170, 1998.

[131] B. Ernst, J. (. Orensanz, and D. A. Armstrong, "Spatial dynamics of female snow crab (Chionoecetes opilio) in the eastern Bering Sea," *Canadian Journal of Fisheries and Aquatic Sciences*, vol. 62, no. 11, p. 2673, 2005 [Online]. Available: http://www.nrcresearchpress.com/doi/10.1139/f05-197

[132] B. Ernst, D. A. Armstrong, J. Burgos, and J. (. Orensanz, "Life history schedule and periodic recruitment of female snow crab (Chionoecetes opilio) in the eastern Bering Sea," *Canadian Journal of Fisheries and Aquatic Sciences*, vol. 69, pp. 532–550, 2012.

[133] P. A. Livingston, "Interannual trends in Pacific cod, Gadus macrocephalus, predation on three commercially important crab species in the eastern Bering Sea," *Fishery Bulletin*, vol. 87, no. 4, pp. 807–827, 1989.

[134] J. Burgos, B. Ernst, D. Armstrong, and J. M. Orensanz, "Fluctuations in range and abundance of snow crab (Chionoecetes opilio) from the eastern bering sea: What role for pacific cod (Gadus macrocephalus) predation?" *Bulletin of Marine Science*, vol. 89, no. 1, pp. 57–81, 2013.

[135] D. Chabot, B. Sainte-Marie, K. Briand, and J. M. Hanson, "Atlantic cod and snow crab predator-prey size relationship in the Gulf of St. Lawrence, Canada," *Marine Ecology Progress Series*, vol. 363, pp. 227–240, 2008.

[136] T. P. Hurst, J. H. Moss, and J. A. Miller, "Distributional patterns of 0-group Pacific cod (Gadus macrocephalus) in the eastern Bering SEas under variable recruitment and thermal conditions," *ICES Journal of Marine Science*, vol. 69, no. 2, pp. 163–174, 2012.

[137] J. T. Thorson *et al.*, "Joint dynamic species distribution models: a tool for community ordination and spatio-temporal monitoring," *Global Ecology and Biogeography*, no. August, 2016 [Online]. Available: http://doi.wiley.com/10.1111/geb.12464

[138] J. T. Thorson, "Guidance for decisions using the Vector Autoregressive Spatio-Temporal (VAST) package in stock, ecosystem, habitat and climate assessments," *Fisheries Research*, vol. 210, no. July 2018, pp. 143–161, 2019 [Online]. Available: https://doi.org/10.1016/j.fishres.2018.10.013

[139] F. Lindgren, H. Rue, and J. Lindstrom, "An explicit link between Gaussian fields and Gaussian Markov random fields: the stochastic partial differential equation approach," *Journal of the Royal Statistical Society. Series B*, vol. 73, no. 4, pp. 423–498, 2011.

[140] J. B. Illian, S. H. Sørbye, and H. Rue, "A toolbox for fitting complex spatial point process models using integrated nested Laplace approximation (INLA)," *Annals of Applied Statistics*, vol. 6, no. 4, pp. 1499–1530, 2012.

[141] K. Kristensen, A. Nielsen, C. W. Berg, H. Skaug, and B. Bell, "TMB: Automatic Differentiation and Laplace Approximation," 2015 [Online]. Available: http://arxiv.org/abs/1509.00660%7B/%%7D0Ahttp://dx.doi.org/10.18637/jss.v070.i05

[142] S. Kotwicki and R. R. Lauth, "Detecting temporal trends and environmentally-driven changes in the spatial distribution of bottom fishes and crabs on the eastern Bering Sea shelf," *Deep-Sea Research Part II: Topical Studies in Oceanography*, vol. 94, pp. 231–243, 2013 [Online]. Available: http://dx.doi.org/10.1016/j.dsr2.2013.03.017

[143] G. G. Thompson, "Assessment of the Pacific Cod Stock in the Eastern Bering Sea," North Pacific Fishery Management Council Stock Assessment; Fishery Evaluation, December, 2018.

[144] J. T. Thorson, M. L. Pinsky, and E. J. Ward, "Model-based inference for estimating shifts in species distribution, area occupied and centre of gravity," *Methods in Ecology*

and Evolution, vol. 7, no. 8, pp. 990–1002, 2016.